Studies on Free-Space Optical (FSO) Systems Applying CDMA and OFDM over Fading Environment

フェージング環境下における CDMA/OFDM 方式を適用した自由空間光システムに関する研究

March 2016

Graduate School of Global Information and Telecommunication Studies
Waseda University

Wireless Communication System II

Fan BAI

Waseda University

Doctoral Dissertation

Studies on Free-Space Optical (FSO) System Applying CDMA and OFDM over Fading Environment

January 2016

Graduate School of Global Information and Telecommunication Studies

FAN BAI

Acknowledgements

I would like to express my appreciation and thanks to my supervisor Professor Dr.Takuro Sato, who have assisted me to complete this research. I'd like to appreciate your encouraging my research and for providing a good study environment during the period of my Ph.D course at GITS, Waseda University. Your advice on both study as well as on my future work have been invaluable. I confirm that I will continue to be influence by your rigorous scholarship, forward-looking exercise and teaching in my future life. It is my great honor to study under your supervision.

I would also like to thank my doctoral thesis examination members: Waseda University, Professor Dr.Shigeru Shimamoto, Emeritus Professor Dr.Mitsuji Matsumoto and Professor Dr.Toshitaka Tsuda; University of Electro-Communications, Pro.Dr.Nobuo Nakajima. I am grateful for their willingness to serve as my doctoral thesis reviewer and examiner, and I also want to thank you for your brilliant comments and suggestions to improve this work.

I would especially like to thank many people who provide the expert opinion and sharing their extensive knowledge during my Ph.D course at the GITS, Waseda University. I am very grateful to my past and present dear colleagues including Dr.Peng Liu, Dr.Jiang Liu, Dr.Abdelmoula Bekkali, Dr.Dimitar, Dr.Pham Tien Dat, Mr.Yuwei Su, Mr.Di Zhang, Mr.Tuo Xie, Mr.Dayong, Kou, Mr.Zihuan Li. Many thanks to all the GITS faculty members who helped me during the past years. Here, I am highly indebted to Professor Dr.Huilin Jiang who helped me to achieve successful results in this work. I would also like to thank all my friends in Tokyo, Beijing, Changchun and Sydney.

Special thanks go to my lovely family and my girlfriend for their powerful support over all these years. All my work would not have been possible without their support. This thesis is dedicated to the whole family as a token of my gratitude.

Finally, I would like to thank the China Scholarship Council (CSC) which support me to extend and complete the studies in Japan.

Contents

Acknowledgements i

Contents ii

List of Figures iv

List of Tables vii

Abbreviations viii

Symbols x

1 Introduction 1
- 1.1 Background and Motivation . . . 1
- 1.2 Main Research Contribution . . . 6
- 1.3 Organization of the Thesis . . . 7

2 Fundamentals of FSO Communication Systems 11
- 2.1 Overview of FSO System Model . . . 11
- 2.2 Influence Factors on FSO system . . . 17
  - 2.2.1 Channel Attenuation . . . 18
  - 2.2.2 Turbulence Effect . . . 20
- 2.3 Atmospheric Turbulence Statistical Models . . . 23
  - 2.3.1 Log-normal Turbulence Model . . . 24
  - 2.3.2 Gamma-Gamma Turbulence Model . . . 25
- 2.4 Turbulence Mitigation Techniques . . . 27
  - 2.4.1 Spatial Diversity Techniques . . . 27
  - 2.4.2 Robust Modulation Schemes . . . 29
  - 2.4.3 Coherent Detection . . . 32

3 OFDM-Based RoFSO Systems with Spatial Diversity over Correlated Log-normal Fading Channels 34
- 3.1 Introduction . . . 34

3.2 Turbulence Model 38
3.2.1 Channel Correlation in Turbulent FSO Links with Diversity Reception 38
3.2.2 Correlated Log-normal Turbulence Model 42
3.3 Performance Analysis of Proposed System 44
3.3.1 Proposed System Model 44
3.3.2 Signal-to-Noise-Ratio and Bit-Error-Ratio 47
3.3.3 Analysis of Outage Probability 49
3.4 Numerical Results and Discussions 50
3.5 Conclusion 57

4 PolSK-Based Direct Detection OCDMA Systems Through Turbulent FSO Links 58
4.1 Introduction 58
4.2 Analysis of PolSK Modulated OCDMA Systems Over Turbulent FSO Links 63
4.2.1 System Model 63
4.2.2 Signal-to-Noise-Ratio and Bit-Error Ratio Analysis 70
4.2.3 Outage Probability Analysis 73
4.3 Numerical Results and Discussions 74
4.4 Conclusion 81

5 PolSK-Based OCDMA Systems with Heterodyne Detection over Turbulent FSO Links 82
5.1 Introduction 82
5.2 Performance Analysis of Heterodyne Detection PolSK-OCDMA FSO Systems 84
5.2.1 System Model 84
5.2.2 Signal-to-Noise-Ratio and Bit-Error Ratio Analysis 90
5.2.3 Outage Probability Analysis 92
5.3 Numerical Results and Discussions 92
5.4 Conclusion 97

6 Conclusion 98
6.1 Summary of Thesis 98
6.2 Future Works 100

Bibliography 101

List of Figures

1.1 Outlines of research contributions and road map. 10

2.1 Trends in both wired and wireless communication technologies. . . . 13
2.2 The block diagram of conventional FSO system with (a) internal modulation, (b) external modulation. 15
2.3 Scintillation index versus refraction structure index C_n^2 with wavelength $\lambda = 850nm, 1550nm$ for a range of turbulence regimes. 22
2.4 The probability density function of Log-normal under weak, moderate and strong turbulence regimes. 24
2.5 Gamma-Gamma distribution under varying degrees of turbulence strength. 25
2.6 The block diagram of modulation issues. 29
2.7 The block diagram of a typical coherent receiver of FSO system. . . 32

3.1 The typical MSM RoFSO system configuration. 36
3.2 A dual diversity reception based optics link over turbulent channel. *by F.BAI, performance analysis of RoFSO lnks with diversity reception for transmission of OFDM signals under correlated log-normal fading channels. Journal of ICT standardization [75].* 39
3.3 Irradiance intensity under correlated log-normal distribution with different values of channel correlation coefficient. 43
3.4 OFDM modulation based FSO system with spatial diversity in the presence of turbulence effect. 45
3.5 Channel correlation coefficient ρ_{12} against separation distance d_{12} and scintillation index for variation of turbulence strength regimes. 51
3.6 Average BER versus electrical SNR of proposed system with both of MRC and EGC combining schemes over turbulence channel. *by F.BAI, performance analysis of RoFSO lnks with diversity reception for transmission of OFDM signals under correlated log-normal fading channels. Journal of ICT standardization [25,75].* 52
3.7 Average BER versus electrical SNR of proposed system over turbulence channel under different modulation schemes. *by F.BAI, performance analysis of RoFSO lnks with diversity reception for transmission of OFDM signals under correlated log-normal fading channels. Journal of ICT standardization [25,75].* 53

3.8 Link performance comparison of a turbulent OFDM-based FSO link under ternary reception, dual diversity reception and single reception conditions. *by F.BAI, performance analysis of RoFSO lnks with diversity reception for transmission of OFDM signals under correlated log-normal fading channels. Journal of ICT standardization [25,75].* 55
3.9 Performance of dual diversity reception with MRC combining scheme in term of outage probability. *by F.BAI, performance analysis of RoFSO lnks with diversity reception for transmission of OFDM signals under correlated log-normal fading channels. Journal of ICT standardization [25,75].* 56

4.1 The electrical field vector of linear polarization light (a), circle polarization light (b) and elliptical polarization light (c). E: electric field, H: magnetic field 59
4.2 Conventional CDMA signals over turbulent RoFSO link. 62
4.3 PolSK modulated OCDMA systems over turbulent FSO links. *by F.BAI, performance analysis of polarization modulated direct-detection optical CDMA systems over turbulent FSO links modeled by the gamma-gamma distribution, MDPI, Photonics [69].* 63
4.4 Block diagram of the proposed system transceiver structure. *by F.BAI, performance analysis of polarization modulated direct-detection optical CDMA systems over turbulent FSO links modeled by the gamma-gamma distribution MDPI, Photonics [69].* 67
4.5 Performance comparison between the PolSK- and OOK-based OCDMA systems over turbulence channel. *by F.BAI, performance analysis of polarization modulated direct-detection optical CDMA systems over turbulent FSO links modeled by the gamma-gamma distribution, MDPI, Photonics [69].* 76
4.6 BER performance against received optical cross the whole turbulence regimes, $K = 1$, $K = 25$ and $K = 45$. *by F.BAI, performance analysis of polarization modulated direct-detection optical CDMA systems over turbulent FSO links modeled by the gamma-gamma distribution, MDPI, Photonics[69].* 77
4.7 Average BER performance versus the number of active users K with different prime number p in the presence of turbulence. *by F.BAI, performance analysis of polarization modulated direct-detection optical CDMA systems over turbulent FSO links modeled by the gamma-gamma distribution, MDPI, Photonics[69].* 78
4.8 Outage probability P_{out} against received optical power, when SNR_{th} = (10 dB, 20 dB), $K = 1$ in the presence of turbulence. *by F.BAI, performance analysis of polarization modulated direct-detection optical CDMA systems over turbulent FSO links modeled by the gamma-gamma distribution, MDPI, Photonics [69].* 79

4.9 Average BER performance versus the number of active users K with different prime number p in the presence of turbulence. *by F.BAI, performance analysis of polarization modulated direct-detection optical CDMA systems over turbulent FSO links modeled by the gamma-gamma distribution, MDPI, Photonics [69].* 80

5.1 Heterodyne detection PolSK-OCDMA FSO link. *by F.BAI, performance analysis of heterodyne-detected OCDMA systems using PolSK modulation over a free-space optical turbulence channel, MDPI, Electronics[91].* 85

5.2 Average BER versus SNR in both of OOK- and PolSK-based OCDMA-FSO link, when $K = 1$. *by F.BAI, performance analysis of heterodyne-detected OCDMA systems using PolSK modulation over a free-space optical turbulence channel, MDPI, Electronics [91].* 93

5.3 Average BER versus variation of number of users when $P_R = -20$ dBm in the presence of turbulence, (**a**) Heterodyne detection; (**b**) direct detection. *by F.BAI, performance analysis of heterodyne-detected OCDMA systems using PolSK modulation over a free-space optical turbulence channel, MDPI, Electronics [91].* 94

5.4 Variation of the outage probability against number of users, when P_R=-20dBm under turbulence channel. *by F.BAI, performance analysis of heterodyne-detected OCDMA systems using PolSK modulation over a free-space optical turbulence channel, MDPI, Electronics [91].* 95

List of Tables

2.1 Comparison between internal modulation and external modulation. 16
2.2 Comparison between IM/DD and coherent. 31

3.1 Numerical Parameters. *by F.BAI, performance analysis of RoFSO lnks with diversity reception for transmission of OFDM signals under correlated log-normal fading channels. Journal of ICT standardization [25,75].* 50

4.1 Numerical parameters. *by F.BAI, performance analysis of polarization modulated direct-detection optical CDMA systems over turbulent FSO links modeled by the gamma-gamma distribution, MDPI, Photonics [69].* 74

5.1 Comparison between homodyne detection and heterodyne detection. 83
5.2 Numerical parameters. *by F.BAI, performance analysis of heterodyne-detected OCDMA systems using PolSK modulation over a free-space optical turbulence channel, MDPI, Electronics [91].* 92

Abbreviations

OWC	**O**ptical **W**reless **C**ommunication
FSO	**F**ree **S**pace **O**ptical
UWB	**U**ltra **W**ide **B**and
AM	**A**mplitude **M**odulation
FM	**F**requency **M**odulation
AWGN	**A**dditive **W**hite **G**ussian **N**oise
BER	**B**it **E**rror **R**atio
CDMA	**C**ode **D**ivision **M**ultiple **A**ccess
OFDM	**O**rthogonal **F**requency **D**ivision **M**ultiplexing
E/O	**E**lectrical **O**ptical
EDFA	**E**rbium **D**oped **F**iber **A**mplifier
RoF	**R**adio **O**ver **F**iber
IM/DD	**I**ntensity **M**odulation **D**irect **D**etection
LD	**L**aser **D**iode
PD	**P**hoto **D**etector
MAI	**M**ultiple **A**ccess **I**nterference
OMI	**O**ptical **M**odulation **I**ndex
PDF	**P**robability **D**ensity **F**unction
RF	**R**adio **F**requency
RIN	**R**elative **I**ntensity **N**oise
SIM	**S**ubcarrier **I**ntensity **M**odulation
MSM	**M**ultiple **S**ubcarrier **M**odulation

PolSK	**P**olarization **S**hift **K**eying
SI	**S**cintillation **I**ndex
AA	**A**perture **A**veraging
MPC	**M**odified **P**rime **C**ode
SNR	**S**ignal **T**o **N**oise **R**atio
OOK	**O**n **O**ff **K**eying
SOP	**S**tate **O**f **P**olarization
IF	**I**ntermediate **F**requency
PAPR	**P**eak **T**o **A**verage **P**ower **R**atio
LO	**L**ocal **O**scillator
LTE	**L**ong **T**erm **E**volution
CSI	**C**hannel **S**tate **I**nformation
MRC	**M**aximum **R**atio **C**ombining
EGC	**E**qual **G**ain **C**ombining
OP	**O**utage **P**robability
PC	**P**olarization **C**ontroller
PBS	**P**olarization **B**eam **S**plliter
PBC	**P**olarization **B**eam **C**ombiner
BPF	**B**and **P**ass **F**ilter
MF	**M**atched **F**ilter
LPF	**L**ow **P**ass **F**ilter

Symbols

L	Transmission distance
V	Visibility coefficient
$\alpha_{at}(\lambda)$	Attenuation coefficient
$\alpha_{sc}(\lambda)$	Scattering coefficient
R	Rainfall rate
$\sigma(V)$	Particle size distribution coefficient
n	Refractive index
l_0	Inner scale size
L_0	Outer scale size
D	Aperture diameter
C_n^2	Index of refraction structure
σ_I^2	Scintillation index
I	Optical intensity
k	Number of optical wave
$\sigma_{R.S}^2$	Rytov variance
X	Random variable of the signal current
$K_n(.)$	Modified Bessel function
α	Small-scale
β	Large-scale
$\Re$	Detector responsivity
I_{ph}	Received power by irradiance
m	OMI

ξ_3	Third-order nonlinearity coefficient
ρ_{12}	Channel correlation coefficient
$B_{I,12}$	Spatial covariance function
d_{12}	Space distance between adjacent point
$J_0(.)$	Bessel function of the first kind and zero order
$\Phi_{n.eff}(K)$	Effective atmospheric spectrum
$K_{X.0}$	Low-pass spatial frequency cutoffs
$K_{Y.0}$	High-pass spatial frequency cutoffs
ω_n	Set of orthogonal sub-carriers frequency
T_S	Symbol duration
L_{loss}	Channel loss
$n_{FSO}(t)$	Additive white Gaussian noise
R_D	Detector responsivity
K_B	Boltzmann's constant
T_{abs}	Absolute temperature
F_e	Noise figure
q	Electron charge
B_e	Filter bandwidth
N_s	Number of subcarrier
λ	Operating wavelength
τ_k	Time delay
$\Delta\varphi$	Phase difference
$S_k(t)$	CDMA signal
J	Jones matrix
XOR	Exclusive disjunction operation
K	Number of active users
W	Code weight
F	Code length
p	Prime code parameter
$erfc(.)$	Complementary error function

Chapter 1

Introduction

1.1 Background and Motivation

Nowadays, with the demand on the high-speed and high-quality communication applications such as HDTV, 5G communication and so on, we can observe an explosion in the both of wired and wireless networking traffic [1]. In the field of wired communications, fiber optical has been often applies as the backbone of the data transmission links for its own benefits in long-distance and high-capacity applications. However, with regard to the optical fiber communications, under some special environment conditions such as in disaster area, outlying islands without optical fiber infrastructure, which is difficult to reestablish communication link in a short time or installed with a high-cost condition. Meanwhile, various of broadband wireless technologies are under active research investigation including the IEEE 802.11 based WLAN systems, IEEE 802.16 based WMAN (WiMAX) systems and ultra wide-band (UWB) PAN systems [2]. Further, the typical transmission capacity for optical fiber communications increase from 10 Gps to 40 Gbps in recent years [3]. Unfortunately, there is still no advanced wireless communication systems that support this kind capacity to our best knowledge.

To measure up to the above mentioned challenges in next generation wired/wireless technologies specification, optical wireless communication (OWC) known as free-space optical (FSO) as a promising technology combining the advantages of wired and wireless communication has been proposed for its potential in high data rate, low cost, easier deployment and wide bandwidth on unregulated spectra [4]. Thus, commercial FSO communication systems can be seem as a good candidate for providing an attractive solution to the last mile problem of bridging the gap between the end user and fiber optic backbone networks [5].

Generally, FSO communication technology means that optical beam modulated by using the light emitting diodes (LED) is transmitted through the atmosphere channel and detected by the photo-diodes (PD) then converted to electrical signal at the receiver side [6],[7]. According to the different application scenarios, FSO communication technology can be classified into terrestrial optical communication and deep space optical communication, and also can be classified into indoor optical communication and outdoor optical communication [8],[9],[10]. Despite the many benefits in FSO technology, however, different from the optical fiber has been considered as a predictable medium, FSO systems are over the link described by random process model then optical beam will experience the various of channel effects, leading to the degradation of system availability and performance. In the cases of indoor optical communication and deep space optical communication, challenges of reflecting light and space fading I have to face when we considering in the designing to improve the FSO link performance [11],[12],[13]. In this thesis, I investigate several performance characteristics of proposed FSO communication system operating on a terrestrial link.

Therefore, when we considering the case of near ground FSO communication systems (terrestrial link), there are three primary impact factors that can limit the quality of beam propagation, including the absorbtion, scattering and refractive index fluctuation [14],[15]. The phenomenon of absorbtion and scattering collectively defined as the attenuation in the amount of radiation transmitted through

atmospheric turbulence channel. However, the most important problem for the terrestrial FSO link is optical scintillation which is mainly caused by random fluctuation of refractive index due to temperature, pressure, and wind variations along the propagation path [16].

For the short terrestrial FSO links, a significant variation in degree of the received optical power arises by optical scintillation while optical beam propagating through the atmospheric turbulence channel [17]. Several statistical models have been developed to characterize behaviour of variation of irradiance fluctuation (optical scintillation) such as Log-normal and Gamma-Gamma turbulence models [18], [19]. To promote practical design of FSO system, this work will study the impacts of proposed turbulence mitigation method on FSO link performance. Over the years, a number of active researches on overcoming the degradation of FSO link performance due to turbulence induced optical scintillation effects have been proposed [20],[21]. The outline of research contribution and motivation is illustrated in Fig.1.1.

In this thesis, the link performance impairments due to optical scintillation can be mitigated by employing several methods around issues of FSO challenge as shown in Fig.1.1, including the spatial diversity techniques, robust modulation techniques and coherent detection technology. The reduction of optical scintillation associate with increasing the receiver collecting area has been recognized as aperture averaging when the receiver aperture size is large beyond the irradiance correlation width in early radio communication systems [22]. However, aperture averaging may not a optimum solution to reducing the scintillation effects, by reason of its increasing cost in designing of FSO systems [23]. For the spatial diversity techniques, the use of several smaller apertures that being able to achieve the same performance as aperture averaging has been wildly used in the field of FSO systems in recent years [24]. However, the efficiency of spatial diversity techniques for improving the system performance depend on the conditions of channel correlation among the sub-channels [25]. In general, by assuming that sub-channels are independent of each other (uncorrelated case), a number of works have been deep discussed

the performance of FSO link with variation of modulation schemes and receiver combining schemes [25],[26]. In [27], an evaluation of spatial diversity in FSO link has been reported, but there is no complete physical insight into the relationship between the channel correlation and system performance, and no consideration on the comparison with aperture averaging techniques has been investigated to our knowledge. Thus, I proposed a novel model taking numerical simulation to quantify the channel correlation in a diversity reception FSO system in this work.

The on-off keying (OOK) modulation is wildly applied in FSO communication systems cause of ease in implementation and bandwidth efficiency [28]. However, conventionally OOK-FSO system using a fixed threshold detection need to determine the variation of channel characteristics which are highly sensitive to the turbulence fluctuation induced result in increased detection error [29]. Face to the challenges of OOK-FSO system using fixed threshold detection, an investigation of phase shift keying (PSK)/quadrature amplitude modulation (QAM) modulated orthogonal frequency-division multiplexing (OFDM) used as a multi-carrier modulation in turbulent FSO link has been discussed in this research.

Apart from the subcarrier intensity modulation (SIM)-based FSO system, polarization shift keying (PolSK) modulation was proposed as an alternative technique to both envelop- and phase-based in FSO communication systems [30],[31]. For this modulation scheme, the information is encoded as different states of polarization (SOPs) of the laser source by using an external modulator (i.e., Mach-Zender modulator). Fortunately, the SOPs can be maintained, and polarization states are the most stable properties compared with amplitude and phase when optical beam propagating through atmosphere link [32]. Various PolSK-based FSO systems have been proposed and analysis results demonstrate that PolSK scheme offers an improved link performance in terms of peak optical power [33],[34]. In addition, the authors reported for the first experiment performance of optical code-division multiple-access (OCDMA) signal transmitted through FSO links [35], and the use of OCDMA technique as a countermeasure for turbulence mitigation was considered

in [36], taking into account the optical scintillation and multiple access interference (MAI) effects. In order to support multiple users in practical access environment, a new model of combining the OCDMA technology and PolSK modulation has been proposed for its benefits in stable quality of signal and large capacity over turbulence link in this work.

Moreover, receiver detection techniques can be classified into direct detection and coherent detection. Such intensity modulation direct detection (IM/DD) as a mature optical communication technology was wildly applied in FSO links, which performance is independent of carrier phase and the SOP of incoming signal [37]. Otherwise, with the recent development of digital signal processing (DSP), coherent detection technology has drawn a lot of attention in practical optical communication systems from the late 1980s for its ability to achieve the theoretical receiver sensitivity limit [38]. Different from the direct direction, coherent signal is detected from the phase information carried on electric fields. Some previous literatures on coherent detected FSO system can be found in [37],[39]. The analysis results proved that coherent detection offers an improved link performance in terms of error probability and outage probability. To cope with the shortages of direct detected FSO systems, the use coherent detection for providing a significant potential in background noise rejection and detector sensitivity, leading to the turbulence fading reduction has been reported in [40],[38],[37]. The aiming at demonstrating the potential of combined PolSK modulation and coherent detection for combating the degradation of signal quality due to the turbulence fluctuation is key to this proposal. Besides, it should be noted that the term coherent used in this work is different from that used in radio frequency communications. It means that is not necessary to have knowledge of the carrier phase and frequency information in the electrical demodulation processing [41].

1.2 Main Research Contribution

This work focus on the investigation of transmission performance of FSO system using the variation of mitigation techniques for fading through atmospheric turbulence channel with the view to understanding its benefits and limitations. The primary research contribution is aimed at introducing solutions of analyzing and measuring the turbulence-induced fading on the performance in the designing of advanced FSO systems.

In [42], the bit-error-ratio (BER) for direct detection OFDM-FSO system with aperture averaged single receiver has been measured and studied. Different from the previous proposed system model, a theoretical study and numerical results for the transmission performance of OFDM-based RoFSO systems with diversity reception over correlated log-normal turbulence channel are presented and discussed. The error probability and outage probability expressions of the proposed system under turbulence and channel correlation effects have been derived. The system performance of diversity reception scheme has been also compared with aperture averaging (AA) scheme under the same RoFSO link conditions. The analysis of receiver combining schemes including the maximal ratio combining (MRC) and equal gain combining (EGC) is carried out. In this contribution, I pay my attention on the performance metric parameters such as intensity fluctuation and channel correlation for evaluating the quality of OFDM signal transmission through turbulent RoFSO links with diversity reception. Different from the previous literature, this work provides a novel transceiver architecture, which combining the diversity reception and OFDM technique can lead to the substantial link performance improvement in the presence of turbulence, especially in the high demand on transmission capacity.

Another original contribution is provide an analytical modeling to characterize the transmission of optical code-division multiple-access (OCDMA) systems deploying polarization shift keying (PolSK) over FSO links across the weak and strong turbulence regimes. Different from the previous internal modulated CDMA-FSO

system model [36], [43], the combing the external modulated scheme and OCDMA technique has been proposed to bear on consideration in the field of FSO communication systems because of its potential ability on improved received power and multiple users access. Here, an analytical modeling for PolSK-based OCDMA system with direct detection over turbulent FSO link is proposed and discussed. I derived closed-form expressions for the error probability and outage probability in the terms of Meijer-G function, taking into consideration the multiple access interference (MAI) and intensity fluctuation due to turbulence effect on the FSO link modeled by Gamma-Gamma distribution. I demonstrate the advantages of proposed system by performing a comparison with on-off keying (OOK) modulation obtained from an evaluation of performance under the same environment conditions.

Finally, an analytical and mathematical modeling for describing the PolSK-based OCDMA signal transmission through the turbulent FSO link when considering the use of coherent detection as countermeasure for system performance improvement is proposed and discussed. The presented work shows the most significant impact factor that degrade the performance of the proposed system in the presence of turbulence, and also indicates that the proposed approach offers an optimum link performance compared with conventional cases.

1.3 Organization of the Thesis

This thesis consists of six chapters. **Chapter 1** provides an overview of FSO issues, and primary goal as well as the original contribution of this work are also presented. The rest of the thesis is organized as follows

In **Chapter 2**, a review of FSO communication systems including the fundamental theory and its progress in application is presented. The most important influence factors that limit the quality of data transmission such as channel attenuation and

intensity fluctuation is introduced. Then, statistical models for describing the intensity fluctuation in varying degrees of turbulence strength are presented. Various of mitigation methods used to overcome the degradation of link performance are outlined.

In **Chapter 3**, an analytical approach is provided to evaluate the performance of OFDM-based RoFSO system with diversity reception over correlated Log-normal turbulence channel, in terms of error probability and outage probability considering the effect of channel correlation and receiver combining schemes. I derived the expressions for OFDM signals bit-error-ratio (BER) and outage probability, taking into consideration both correlation coefficient parameter and optical scintillation. Moreover, a definite major purpose of this chapter is using a performance comparison with aperture averaged single receiver to highlight the benefits of diversity reception for combating the turbulence-induced fading in quality of signal.

Chapter 4 uses the advantages of combining PolSK and OCDMA technology in FSO system with direct detection over 1-km atmospheric turbulence link modeled by Gamma-Gamma distribution. First, detailed of designing in the proposed system architecture is described. Then, the transmission performance of PolSK modulated OCDMA signal over turbulent FSO link is evaluated, in terms of the BER and outage probability. We derived a closed-form expressions of BER and outage probability by Meijer-G function, taking into consideration the multiple access interference, and turbulence-induced optical scintillation is also considered. Further, the efficiency of PolSK modulation in enhancing the performance of OCDMA FSO link across the weak and strong turbulence regimes compared with OOK modulation is obtained from numerical results.

In **Chapter 5**, an analytical modeling is provided to characterize the performance of PolSK-OCDMA systems with heterodyne detection over turbulent FSO link across the whole turbulence regimes. First, a novel transceiver architecture and mathematical modeling for describing the PolSK-based OCDMA signal transmission through

FSO link with heterodyne detection are presented. This work aiming at demonstrate the advantages of coherent detection technique in improving the sensitivity of receiver, and can be used as an useful mitigation method for overcoming the degradation of quality of signal in the presence of turbulence effect.

Finally, the **Chapter 6** provides a conclusion of this thesis and provides some plans for the way of future research.

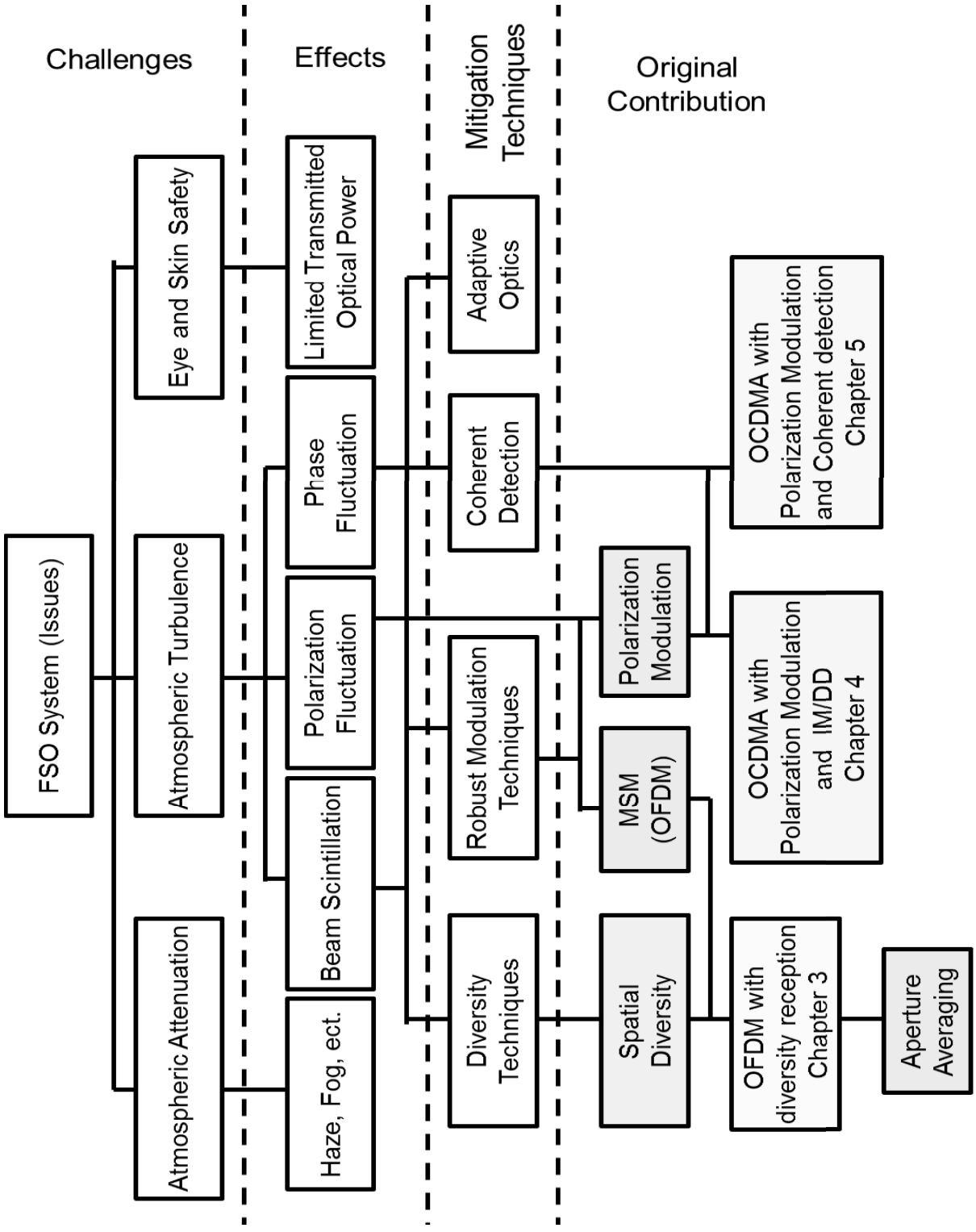

FIGURE 1.1: Outlines of research contributions and road map.

Chapter 2

Fundamentals of FSO Communication Systems

In this chapter, I first give an overview on free-space optical communication systems including the technology development and basic theory. I then present a background knowledge of influence factors on FSO system and provide statistical models for describing the intensity fluctuation in variation of degrees of turbulence strength. Finally, in case of FSO link, some useful solutions in turbulence mitigation such as spatial diversity, robust modulation schemes and coherent detection have been reviewed.

2.1 Overview of FSO System Model

Since the ancient times, optical wireless communication (OWC) has been played an important role in the military situation. In the Zhou dynasty in China as around 700 BC, the beacon towers were built at the top of the mountain to give border alarm to soldiers. The attack message via beacon transmitted through the air and received without a time delay. Method is lighting and extinguishing the fire as

the original binary modulation. However, the limitation of this method was that only predetermined messages can be transmitted, leading to a simplex information content. A famous experiment has been present in the 1880s, Alexander Graham Bell applied and then received the patent of "photo phone", which demonstrates that the basic principle of optical wireless communication: voice sounds can be converted to the telephone signal and transmitted through the free air by a beam of light for a short distance [43]. Moreover, this invention successful proves that OWC technique can be seen as a potential method in the reality communication environment.

Unfortunately, OWC has no became a commercial communication solution in civilian market in the following years. In the same time, as to fiber optics technology has been carried out by Pro.Charles K. Kao in 1960s, we face to an explosive growth in practical optical fiber applications over the past 40 years [44] However, the OWC technology did not "dead" rather than the most of OWC applications were used for defense or aerospace programs to provide high security and fast communication link such as ground-to-ground, ground-to-satellite, etc. From the 1960s, the NASA JPL has made a project to research the optical communication demonstrator (OCD) which provided a valuable reference for the development of free space laser systems [45]. In the 2006s, Japan Aerospace Exploration Agency (JAXA) first successfully tested the communication connection between the low earth orbit satellite and a near-ground station (NICT, Koganei, Tokyo) using laser beams [46]. The fact that OWC becomes an inseparable part of the modem information system based on the way of accumulated experience.

Back to current commercial telecommunication market, OWC known as FSO has got his big chance as to the rapid development of optoelectronic devices. Besides, with the increased requirement on the huge bandwidth and high quality applications for the backbone infrastructure (i.e., optical fiber). It requires an effectively and new assist in enhancing the performance of current networks, which can apply the emerging applications as the second choice to replace old devices without

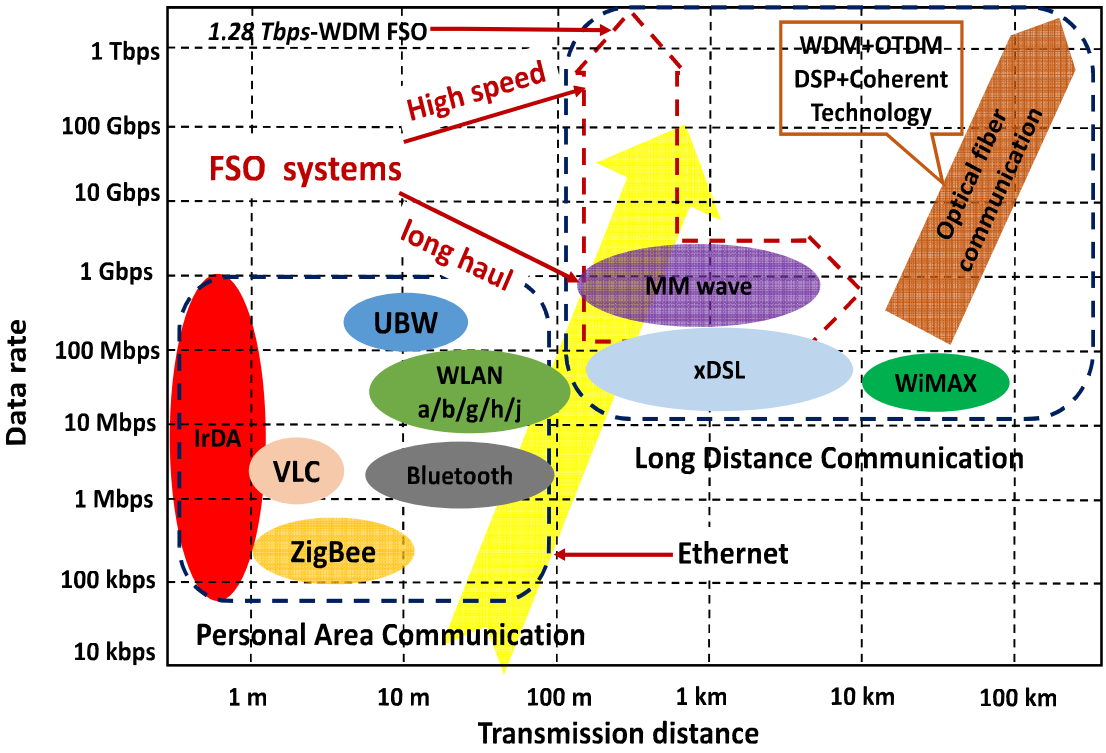

FIGURE 2.1: Trends in both wired and wireless communication technologies.

adding mountains of optical cables. Further, face to a well known challenge "last mile" in the access networks, variation solutions both wired and wireless have been proposed, Fiber To The X (FTTX) within passive optical network (PON) device [47]; radio such as WiFi, WiMax and UWB [48]. At the present time, to copied the success of FSO in the use of military and aerospace, FSO technology in particular the access network have been accepted and reported in the last few years [49]. It is shown that FSO acts as a reliable communication technique with ease deployment of heterogeneous services within the access networks, arising from its intrinsic characteristics in transparent traffic type and data protocol makes it suit for the requirements of existing access network.

The Figure 2.1 shows the trends in both wired and wireless communication technologies. Focus on basic theory of FSO, the signal carried by optical beam and transmitted between the two points (transmitter and receiver) through the unguided channels. In this way, FSO operation requires line-of-sight (LOS), which simply

means that information is successful transfer between the source and destination without any obstacle along the propagation path [50]. Like the optical fiber link, the original signal modulated by the intensity, phase or polarization which imbedded into the optical carrier, and then received by using photo-detector (PD) to convert to the RF signal. However, different from the optical fiber over a guided channel, the FSO link uses collimated optical source and submit through the unguided channel such as air or deep space. In this work, the channel of interest is atmosphere. So, since the FSO link are under the atmospheric turbulence effects, the optical beam will suffer the effects of turbulence-induced channel fading, which impairs the quality of signal. Therefore, in such study around the fading environment influence on FSO link performance becomes necessary.

Currently, FSO communication system is established as an alternative approach for providing the high quality data transmission in particular "last mile" problem of bridging the gap between the end user and backbone construction. These systems can carry full-duplex as well as multiple services data at gigabit-per-second rates combined with existing infrastructures over metropolitan distance [6]. The most significant features of FSO system can be concluded as: FSO system operation window is in a huge frequency range of an optical carrier spans from $10^{12} - 10^{16}$ Hz to 2000 THz data bandwidth, thus, it allows an increased channel bandwidth compared to RF communication systems with lower usable frequency bandwidth; An extremely narrow optical beam has been adopted for the FSO communication with a diffraction limited range between the 0.01 - 0.1 mrad for its potential in spatial isolation from interference; As to the spectrum resource becomes increasingly rare as well as high cost, FSO system operates in a free license spectrum with short and ease in deployment conditions; FSO technology combine the advantages of RF system and optical fiber to be used in a wide range of application areas within a variety of different architectures. It offers an alternative solution for improving the link performance in the maintenance of the existing devices without additional cost [6].

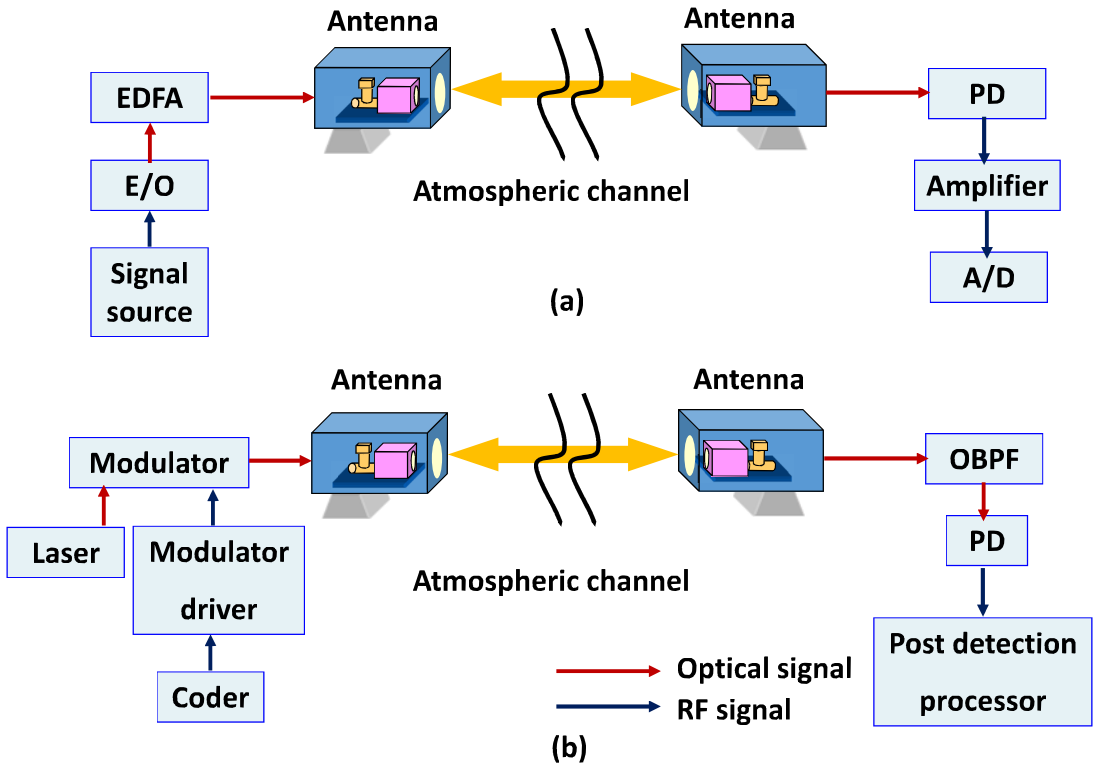

FIGURE 2.2: The block diagram of conventional FSO system with (a) internal modulation, (b) external modulation. OBPF: optical band-pass filter

Facing the complicated fading environment situation that requires an effective designing of FSO system configuration in combating the channel fading. The block diagram of conventional FSO system with intensity modulation/external modulation is shown in Figure 2.2. A conventional FSO system primary consists of three parts with optical transmitter, receiver and atmospheric turbulence channel to provide bi-directional transmission capability. Similar to the optical fiber system, the source RF signal onto the optical carrier which modulated by using the light emitting diode (LED) or laser for the data transmission. The development and application of high quality FSO transmitter depend on the laser intensity and minimum divergence, which correspond to the lens size, power and beam quality [51]. Traditionally, FSO system modulation schemes have two categories as internal modulation and external modulation. The use of internal modulator provides benefits in simplicity and cost effectiveness, while the use of external modulator offers higher data rate and higher quality [52]. However, external modulator has an important problem of nonlinear

TABLE 2.1: Comparison between internal modulation and external modulation.

	Internal modulation	External modulation
Modulation method	Directly by changing the current	Switching between two logical levels occurs within modulator
Advantages	Low cost Simple structure	Increase in both the bit rate and transmission distance
Challenges	Degradation effects on laser line width	Modulation process is complex nonlinear response
Modulator type	Laser diode Light-emitting diode	Mach-Zender interferometer Electroabsorption

response. Further, using characteristics of optical field such as state of polarization that modulated via the optical phase modulator as an external modulation has been discussed in this work. Consequently, the optical signal collected by the receiver lens after a propagation through the turbulence channel, and then converted to the RF signal by the photo-detector (PD) and through the following final demodulation. There has two classes of detection types as IM/DD and coherent detection in practical FSO systems. The more detailed principle of detection schemes introduced in the following sections.

Generally, FSO system configuration also can be divided into two classes depending the operation wavelength window as near 800 nm and near 1500 nm. It is well known the most of optical fiber infrastructures select the operation wavelength on 1550 nm. For better using the existing resources at no addition cost as well as reduction of solar background radiation, operation wavelength window near 1500 nm has been selected for the designing of the FSO optical transceiver. In addition, the optical beam propagates through the turbulence under the channel fading induced degradation of signal quality, which can be compensated by using a high level optical power to enhance the link performance. However, I must confirm the optical power at their respective wavelengths not beyond the safety levels standards. The optical beam power with the wavelengths form $400 - 1400$ nm which can pass the cornea and cause the damage to eye by focused optical beam on the retina. Therefore, the use of near 1550 nm as operation wavelength is out of the range of above mentioned,

leading to the the optical beam power are absorbed by the cornea before arriving the retina. Some of international organizations provide standards on the eye safety issue of optical beam and can be found in [53]. Another reason for selecting the wavelengths at 800 nm and 1550 nm correspond the increased signal power loss caused by atmospheric absorption. A detailed knowledge of channel absorption scheme presented in the following section.

Besides access network applications of FSO communication systems, a number of models of FSO system were utilized in various cases of different areas, such as inter-satellite communication in the space have been realized by European space agency (ESA). In 2013s, the Lunar Laser Communication Demonstration (LLCD) is NASA's first high-rate, two-way, space laser communication demonstration [54]. This project successful demonstrate the communication connection between the ground-based laser component installation and space terminal that will reach lunar orbit can transmit the data rate at 600 Mbps over laser, and transmission distance is over 238 km. Moreover, the use of modified FSO technology for high-speed, low-range underwater applications becomes more popular in the current time [55]. Some detailed analytical model for describing the properties of light while propagating through the underwater have been proposed [56]. It provides solid theoretic foundation for developing the underwater FSO system in the future commercial market.

2.2 Influence Factors on FSO system

In regard to the FSO technology, the fundamental limitation of communication reliability generates from the channel environment which it propagates through atmosphere as an unguided link. The atmospheric interacts with optical beam due to the composition of atmosphere, which corresponds to the aerosols known as molecules and suspended particles. Under this interaction effects that produces a variety of

optical phenomenon including the absorption at specific optical wavelength, scattering and optical scintillation due to the variation of the atmosphere's refractive index under the effect of temperature. Thus, it arises the degradation of the transmission performance, resulting in the power losses, amplitude fluctuation, phase aberration and fluctuation in varying degrees of polarization. Understanding of the effect of atmosphere environment induced channel fading at quality of received signal becomes a primary challenge in FSO issue. This section explains this challenge and introduces the statistical models for describing the intensity fluctuation in variation of turbulence strength.

2.2.1 Channel Attenuation

For the propagation links are over the atmosphere, the light photons and molecules have an interaction process along its path. It means that part of optical power is converted into heat power, and seem as photons' absorption by the molecular constituents. The scattering takes place when there is an effect of scatterers, which can change the propagation path and characteristic of optical beam , then affects to the received optical power. Absorption and scattering presented in the atmosphere is a complex process. It often grouped together defined as attenuation in the amount of the radiation through the atmospheric turbulence channel, resulting in arising the pure power losses experienced by the propagating optical beam.

A well-known mathematical modeling was established for describing the link power budget, including the transmitted power and power losses when optical beam propagating through the atmosphere. For the case of the power losses in the FSO link, it includes the rain and visibility losses due to atmospheric turbulence effect, geometric loss and the pointing loss, and loss caused by the optical device (i.e., lens). Other power degradation at the receiver end which is influence by the data modulation format, various noise include the laser noise, excess noise in the photo-diode and background light.

In the regard to the power loss model with a given transmission distance L, and defined by the Beer's law as [57]

$$\frac{P_R}{P_T} = exp(-\alpha_a(\lambda)L) \tag{2.1}$$

where P_R and P_T are the received and transmitted power, respectively, $\alpha_a(\lambda)$ is attenuation coefficient with the λ being the operating wavelength. With is, the $\alpha_a(\lambda)$ is sum of the absorption coefficient and scattering coefficient, and can be derived as [57]:

$$\alpha_a(\lambda) = \alpha_{at}(\lambda) + \alpha_{sc}(\lambda) \tag{2.2}$$

where $\alpha_{at}(\lambda)$ and $\alpha_{sc}(\lambda)$ denote the attenuation coefficient and scattering coefficient, respectively. As to the absorption mainly rely on the wavelength and operating wavelengths used are based on a weak absorption regime (i.e., 1550nm), scattering can be seems as a dominated influence factor and thus equation becomes: $\alpha_a(\lambda) \approx \alpha_{sc}(\lambda)$. Moreover, the light scattering can be classed as: Rayleigh scattering when scatter is smaller than wavelength; Mie scattering when the wavelength is of the comparable size to the wavelength; non-selective scattering when the scatter is much larger than wavelength. Unlike absorption influence, there is only a directional redistribution of the optical power would generates the reduction of the light wave intensity for a long propagation.

Further, in case of fog particles size is corresponding to the optical beam operation wavelength in FSO communication systems, with this reason, the Mie scattering becomes the dominant scattering processing within the major photo scattering particle of fog. General speaking, the Mie scattering is higher than the rain and snow induced power losses. In the case of rain induced loss can be expressed as [57]:

$$L_r = aLR^b \tag{2.3}$$

where R is the rainfall rate (mm/h), a and b are given according to the location; Then, the $\alpha_{at}(\lambda)$ can be described as a function of visibility $V(km)$ in term of attenuation [57]:

$$L_v = \left\{ \left[13L \left(\left(\lambda \times 10^9 \right) / \left(500 \right) \right)^{-\sigma(V)} \right] / V \right\} \tag{2.4}$$

where $\sigma(V)$ is the particle size distribution coefficient, defined with Kim's model as [57]:

$$\sigma(V) \begin{cases} 1.6 & V > 50km \\ 1.3 & 6km < V < 50km \\ 0.16V + 0.34 & 1km < V < 6km \\ V - 0.5 & 0.5km < V < 1km \\ 0 & V < 0.5km \end{cases} \tag{2.5}$$

2.2.2 Turbulence Effect

Since the optical beam transmited through the atmospheric turbulence link, it will experience the variation effects of environment conditions referred to as both absorption and scattering by the atmospheric particles. However, the most significant channel effects to the optical link performance are general caused by the turbulence induced phenomenon of temperature inhomogeneities that leads to an interaction between light wave and turbulent medium, resulting in random phase and amplitude fluctuations (optical scintillation) of the propagating beam which results in the FSO link reliability at a poor level as to the received signal quality degradation. Generally, atmospheric turbulence can be categorized in regimes depending on the magnitude of index of refraction variation and inhomogeneities [58]. The turbulence induced the random fluctuation of the refractive index n products a random variations in atmospheric temperature form point to point that describing the changes are as a function of atmospheric pressure, altitude and wind speed. The refractive

index n within turbulence air temperature can be described as [57]:

$$n = 1 + 77.6(1 + 7.52 \times 10^{-3}\lambda^{-2})\frac{p_p}{T_a} \times 10^{-6} \tag{2.6}$$

where p_p is turbulence air pressure. Moreover, the turbulence air can be seem that acts as refractive prisms with a range of scale size and refractive indices, which sizes from the inner scale size l_0 to the outer scale of turbulence L_0. It induces a substantial changes in both the pointing (i.e., beam wander, beam spreading) and intensity (optical scintillation) when optical beam propagating through the FSO links. In the case of the beam wander effect caused by large scale, however, when the aperture diameter D is beyond the $\sqrt{L\lambda/2\pi}$ known as Fresnel zone which provides a potential compensation to diffraction effect and leading to be assumed as insignificant [57]. For this reason, the use of he aperture averaging (AA) has been proposed. It provides an advantage in improving the link performance in the presence of turbulence. The aperture averaging scheme acts a special form of spatial diversity, and discussed in this work.

However, when taking into account the turbulence effect, an important parameter for measuring the variation in refractive index fluctuation is the index of refraction structure C_n^2 proposed by Kolmogorov, which determines the relationship between the operating wavelength, altitude and turbulence air temperature. A wildly common accepted model to describe the C_n^2 is Hufnagel-Valley model, and is derived as [57]:

$$\begin{aligned} C_n^2(h) = {} & 0.00594(v_w/27)^2(10^{-5}h)^{10}exp(-h/1000) \\ & + 2.7 \times 10^{-16}exp(-h/1500) + A_n exp(-h/100) \end{aligned} \tag{2.7}$$

where h and v_w are the altitude (meter) and wind-speed (m/s), respectively, and A_n is taken as the nominal value of the $C_n^2(h = 0)$ within the zero altitude. In general, the C_n^2 is assumed to be a constant to define the range of turbulence strength regime, from the $10^{-13}m^{-2/3}$ to the $10^{-17}m^{-2/3}$ for the weak and strong turbulence regime,

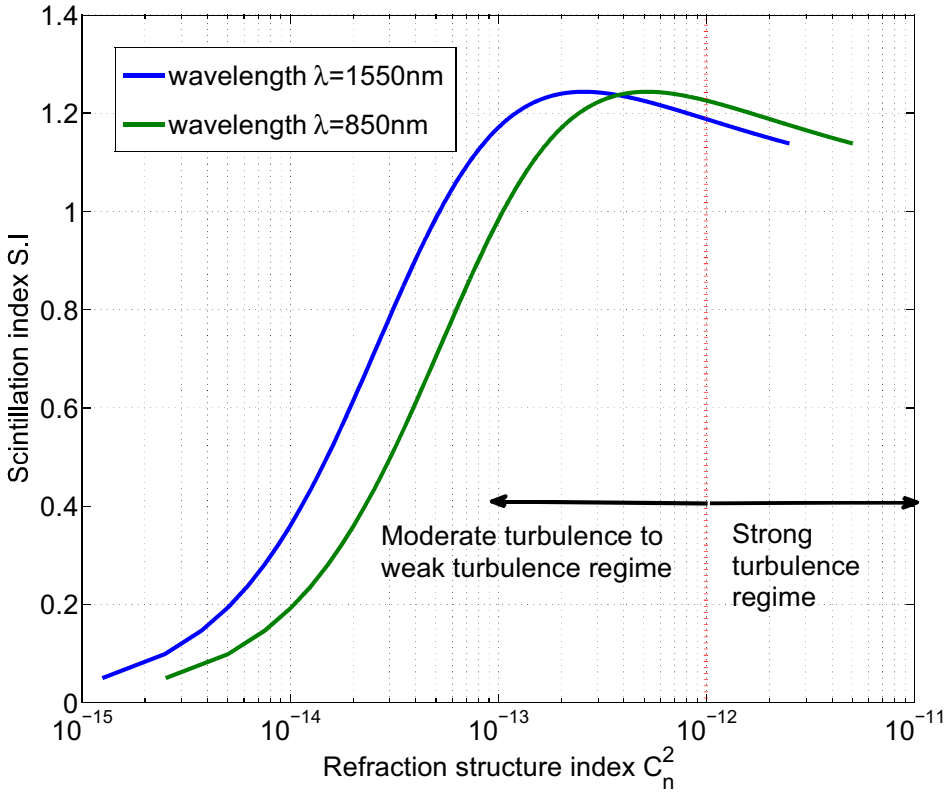

FIGURE 2.3: Scintillation index versus refraction structure index C_n^2 with wavelength $\lambda = 850nm, 1550nm$ for a range of turbulence regimes.

respectively, $10^{-15}m^{-2/3}$ with being a average value for turbulence level [59].

Apart from the index of refraction structure for turbulence measurement, the normalized variance of light intensity σ_I^2 known as optical scintillation which characterizes the strength of intensity fluctuation, and given a statistical description for the light intensity as following [57]

$$\sigma_I^2 = \frac{\langle I^2 \rangle - \langle I \rangle^2}{\langle I \rangle^2} \tag{2.8}$$

where I is optical intensity, and the symbol $\langle . \rangle$ denote the average over scintillation. For the case of log-amplitude variance and defined for spherical wave model is derived as [57]:

$$\sigma_A^2 = 0.124 C_n^2 k^{7/6} L^{11/6} \tag{2.9}$$

where $k = 2\pi/\lambda$ is the number of optical wave. In the weak turbulence regime, the normalized variance of intensity referred as scintillation index S is linear proportional to the Rytov variance and can be expressed as [57]:

$$\sigma_I^2 = exp(\sigma_{lnI}^2) - 1 \approx 4\sigma_A^2 \tag{2.10}$$

and a functional relation between the scintillation index and Rytov variance in the region of weak turbulence for the spherical wave thus given by [57]

$$\sigma_I^2(weak) = \sigma_{R.S}^2 = 0.5C_n^2 k^{7/6} L^{11/6} \tag{2.11}$$

where $\sigma_{R.S}^2$ denotes the Rytov variance for the spherical wave model. It would note that Rytov variance is path distance-, wavelength- and index of refraction structure-dependent parameter for defining the turbulence regimes. In order to describe the statistical properties of turbulence-induced variation of intensity fluctuation, several mathematical models have been introduced, which include the log-normal, the Gamma-Gamma corresponding to the weak, weak-to-strong turbulence regimes, respectively. I will discuss these models in the next section.

2.3 Atmospheric Turbulence Statistical Models

The optical scintillation caused by atmospheric turbulence is a significant impairment factor which can generates the intensity fluctuation in the received optical beam, leading to the degradation of signal quality and increases the error probability in the link performance. The various mathematical models have been proposed to provide statistical description of intensity fluctuation in varying degrees of turbulence strength. Comprehending of the statistical distribution of the intensity in the presence of turbulence is an important way to predict the reliability of FSO link operating in such fading environment.

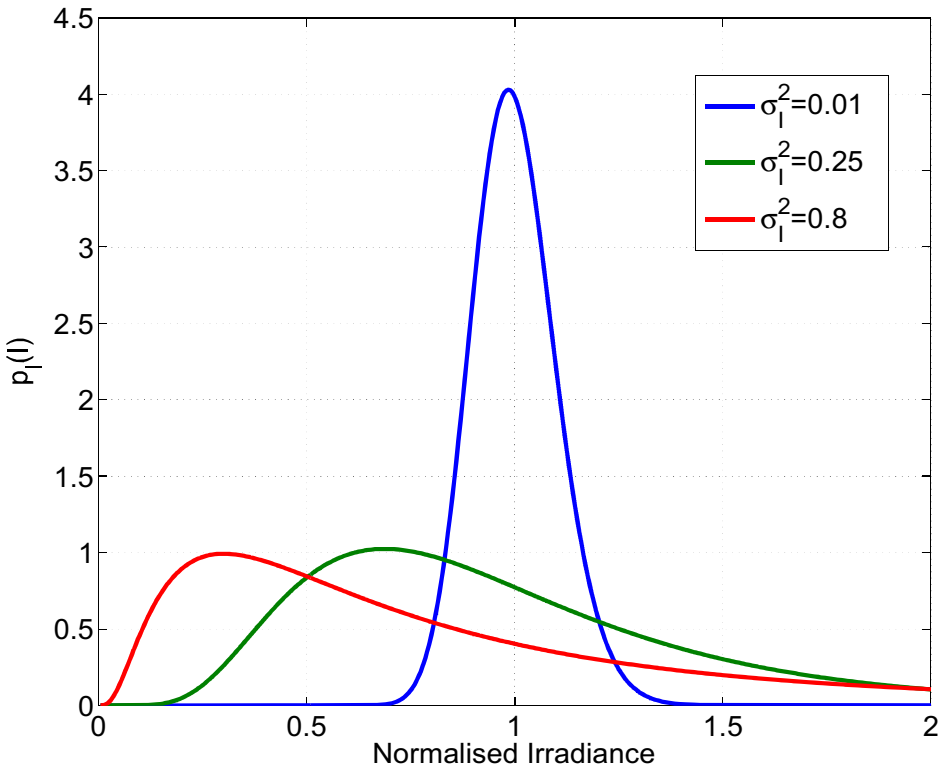

FIGURE 2.4: The probability density function of Log-normal under weak, moderate and strong turbulence regimes.

2.3.1 Log-normal Turbulence Model

Following the above mentioned on scintillation index and Rytov variance, when the optical beam propagating through the weak turbulence regime, the statistical of intensity fluctuation obtained from the experiment and representation for a log-normal distribution is given by [57]:

$$p_I(I) = \frac{1}{\sqrt{2\pi}\sigma_I}\frac{1}{I}exp\left(-\frac{ln\frac{I}{\langle I\rangle} + \sigma_I^2/2}{2\sigma_I^2}\right) \tag{2.12}$$

The Fig.2.4 plots a probability density function of log-normal. In general, log-normal turbulence distribution is based on the Rytov approximation. However, this model can predict for the weak turbulence within a small scintillation index, $\sigma_A^2 < 0.3$. Unfortunately, the log-normal turbulence model is only valid in this range

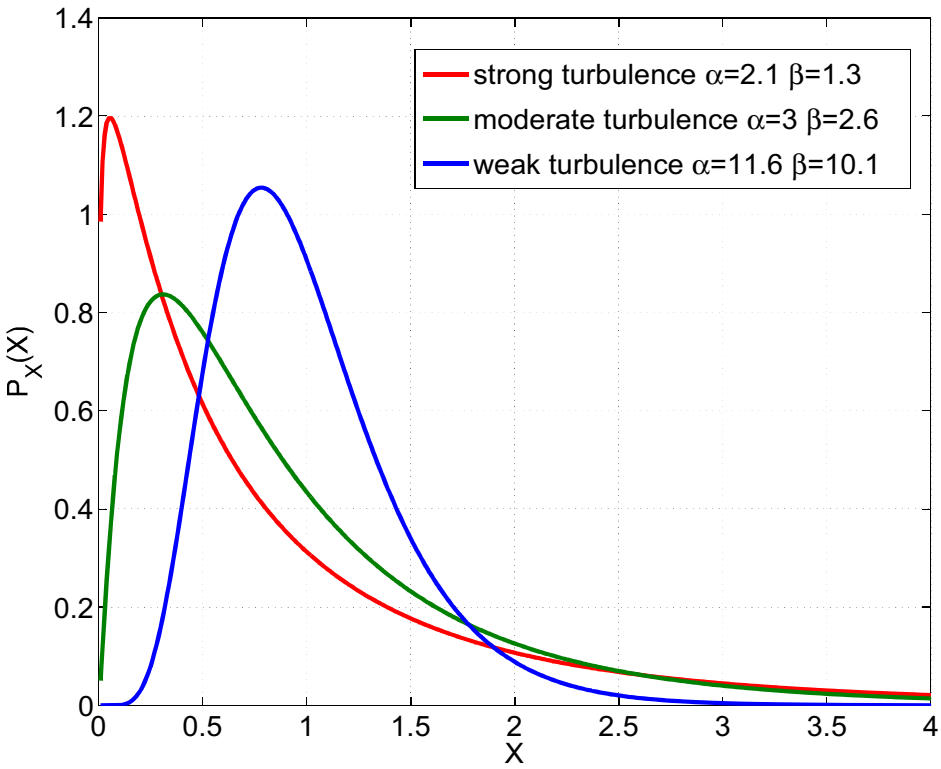

FIGURE 2.5: Gamma-Gamma distribution under varying degrees of turbulence strength.

caused by a single scattering. Otherwise, this assumption will becomes invalid due to a combination of path distance and index of refraction structure rising under the multiple scattering situation. Thus, it requires a model can be used to cover a wider turbulence regime.

2.3.2 Gamma-Gamma Turbulence Model

A common turbulence model has been consider to be suitable for describing the channel fading from weak to strong turbulence regimes, known as Gamma-Gamma distribution has been proposed by Andrew *et al.* This assumption provide a s-tatistical description for processing where optical beam propagating through the atmospheric turbulence is assumed to comprise small scale (scattering) and large

scale (refraction) effects. The Gamma-Gamma turbulence model describes both small-scale and large-scale atmospheric fluctuations and factorizes the irradiance as the product of two independent random processes, each having a Gamma PDF and defined as [57]:

$$f_X(X)_{G-G} = \frac{2(\alpha\beta)^{\frac{\alpha+\beta}{2}}}{\Gamma(\alpha)\Gamma(\beta)}(X)^{\frac{\alpha+\beta}{2}-1}K_{\alpha-\beta}(2\sqrt{\alpha\beta X}), X > 0 \tag{2.13}$$

where $X = I/\langle I\rangle$; I is a random variable of the signal current, $\Gamma(.)$ is the Gamma function, and $K_n(.)$ denotes a modified Bessel function of the second kind of order n, the parameters α and β represented the small-scale and large-scale irradiance fluctuation and defined for the spherical wave with aperture averaging (AA) as [57]:

$$\alpha = \left\{ exp\left[\frac{0.49\sigma^2}{(1+0.18d^2+0.56\sigma^{12/5})^{-7/6}} \right] - 1 \right\}^{-1} \tag{2.14}$$

$$\beta = \left\{ exp\left[\frac{0.51\sigma^2\left(1+0.69\sigma^{12/5}\right)^{-5/6}}{(1+0.9d^2+0.62d^2\sigma^{12/5})} \right] - 1 \right\}^{-1} \tag{2.15}$$

where $\sigma^2 = 0.5w^{7/6}C_n^2L^{11/6}$ denotes the Rytov variance, and $d = \sqrt{wD^2/4L}$, D is the aperture diameter, $w = 2\pi/\lambda$ is wave number and λ is operating wavelength, C_n^2 denotes the turbulence structure index of the refraction constant and L is transmission distance. The Fig.2.5 plots a probability density function of Gamma-Gamma across the whole turbulence regime. The scintillation index SI in term of Gamma function is given by [57]:

$$SI = 1/\alpha + 1/\beta + 1/\alpha\beta \tag{2.16}$$

when the $\beta = 1$, this assumption is viewed as K-distribution model.

2.4 Turbulence Mitigation Techniques

To design the free-space optical communication systems for achieving a reliable link performance, considering and selecting an efficient solution of mitigating the turbulence effects is important. In order to avoid turbulence effect associated with signal fading, a number of researchers proposed various methods from a different perspective, including spatial diversity techniques, robust modulation schemes and coherent detection within high receiver sensitivity. In this section, some useful turbulence mitigation methods and related fundamentals for later proposals will be introduced.

2.4.1 Spatial Diversity Techniques

Traditionally, single-input single-output (SISO) link configuration has been wildly development and used in the field of FSO communication system, however, the link performance is at a poor level especially in the strong turbulence regime [60]. The use of aperture averaging (AA) as the first option can be used to provide a compensation to turbulence-induced signal fading, which lies in their inherent reduction of intensity fluctuation by increasing the receiver aperture size [36],[61]. In the case of aperture averaging, the receiver aperture size required to be much larger than the correlation length of atmospheric turbulence, $D \gg d_0$. I should note the correlation length as $d_0 \approx \sqrt{\lambda L}$. By this way, this method can offers an improved link performance under the whole turbulence regime. But on the contrary, the receiver can be defined as "point aperture" when the aperture size approximates to zero, $D = 0$. Further, a number of experimental results demonstrate that some limitations to overcome the scintillation effects by aperture averaging technique [36],[22]. At the same time, as increasing the aperture size brings the increasing capacity, it also brings the reduction of data rate. In application situation, it also need consider the cost of practical aperture lens in spite of increasing aperture size to reduce the intensity fluctuation effectively. Furthermore, the aperture averaging

offers a turbulence mitigation way to achieve a optimum link performance which only generates at a given range.

Face to above mentioned challenges, spatial diversity as a mature technology in the field of wireless communication, has been proposed by using the multiple apertures at the receiver (single-input multiple-output, SIMO) or transmitter (multiple-input single-output, MISO) or combination (MIMO), which is regard as another alternative to overcome the turbulence-induced signal fading [62]. In the usual situation, the aperture averaging can be viewed as a simple form of spatial diversity techniques where $D \gg d_0$. Differently, spatial diversity techniques offer an enhanced link performance where possible to satisfy the condition as $D < d_0$. The spatial diversity based FSO link has been first proposed in [63]. It is demonstrate that spatial diversity provide an useful way to combat signal fading and reduction of temporary blockages. However, with the diversity reception, to maximize diversity reception gain, any adjacent receivers must be sufficiently far apart as independent case due to the channel correlation considered as an impairment factor to link performance improvement. Thus, it is important to take into account the relation between the sub-channel correlation among the each adjacent receiver and performance over turbulence link. Considering the comparing system between the FSO receiver aperture size with the single large aperture (AA) as much as the several smaller apertures (spatial diversity) also can be used to determine the advantages of diversity reception in scintillation compensation and resistance to complete blockage. Apart form the channel correlation parameter, an optimum combining techniques are also important to improve the FSO link performance. The diversity reception combining schemes generally consist of maximum ratio combining (MRC), equal gain combining (EGC) and selection combining (SEC). The MRC can provide an optimum combining performance, but implementation is with an inherent complexities, which is highly sensitive to channel estimation error. EGC is inefficient for system with branches having acutely low SNR conditions [25].

Certainly, there still exists some challenges of spatial diversity approach that can

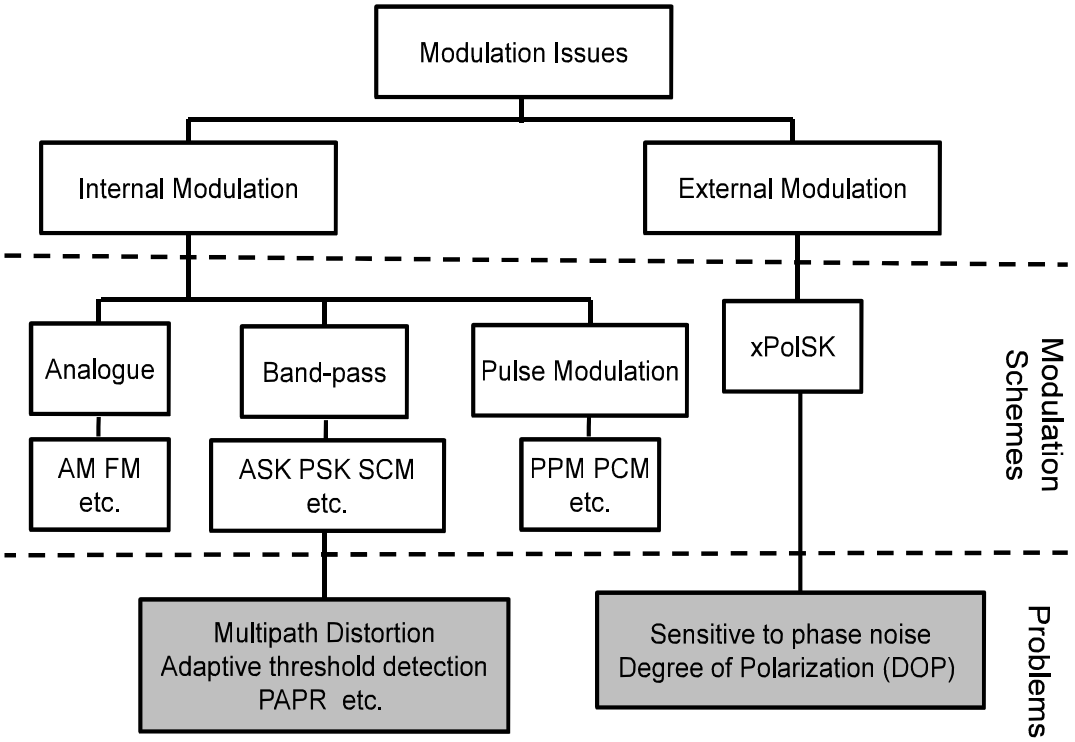

FIGURE 2.6: The block diagram of modulation issues.

be concluded as follow: adding the complexity of system configuration within the tracking subsystem; the more complicated coupling technology for multiple optical beams onto diversity reception, resulting in increasing the overall system cost and decreasing the reliability of link performance.

2.4.2 Robust Modulation Schemes

Currently, intensity modulation direct detection (IM/DD) scheme has been wildly utilized in both of outdoor and indoor FSO applications. Under the atmospheric turbulence conditions, especially in high turbulence strength level, it would be to pump more optical power at the optical source and focus more power onto small detected areas. Nevertheless, I have to consider the limitation of eye safety standard associated with range of optical power. Further, below the 2.5 Gbps data rates, the intensity modulated FSO system has been wildly adopted as a internal modulation;

beyond the 2.5 Gbps; external modulation is normally adopted. Meanwhile, the on-off keying (OOK) is often known as a dominant modulation scheme employed in IM/DD FSO system because of ease in implementation and bandwidth efficient. However, the OOK modulated optical carrier is highly sensitive to intensity fluctuation, thus, an adaptive threshold detection technology is required to achieve performance improvement, which adds to the complexity of receiver configuration [64]. Another common useful IM/DD based issue is subcarrier intensity modulation (SIM) which already has the successful experience in the field of RF communication applications such as 4G. The reason for bringing the SIM into the FSO system which is reason to its the benefit in increased the capacity by accommodating multiple users on different sub-carriers [65],[66]. It provides a choice to avoid the adaptive threshold requirement in OOK-based FSO link. In the SIM scheme, RF subcarrier signal first modulated with the user data, which is then used to modulate the intensity of the continuous lightwave from the laser diode (LD) generating, resulting in transmitted optical power that could proportional to the original RF modulated signal. In addition, a DC bias added to undertake that the signal amplitude is positive. These properties lead to a poor power efficiency while the increased transmitted optical power correspond to DC bias increasing. Moreover, I also need to consider the possibility of signal distortion caused by the inherent laser nonlinearity in this issue. A general function of received signal after the photo-detector in the absence of turbulence can be always described as

$$i(t) = \underbrace{I_{ph}}_{\text{DC}} + \underbrace{I_{ph} m S(t)}_{\text{desired data}} + \underbrace{I_{ph} \xi_3 (S(t))^3}_{\text{IMD}} + n(t) \tag{2.17}$$

where I_{ph} is the received photocurrent, m denotes the OMI, and ξ_3 is the third-order nonlinearity coefficient.

Orthogonal frequency division multiplexing (OFDM) known as a special case of multiple subcarrier modulation (MSM), which is used to intensity modulated optical carrier signal after the RF pre-modulated on different sub-carriers. In [42],

TABLE 2.2: Comparison between IM/DD and coherent.

	IM/DD	Coherent
Problem	Quantum limit of detection	Sensitive to phase noise
Characteristic	Proportion to transmitted field amplitude	intermediate frequency (IF)
Modulation method		I and Q or PolSK
Detection method	Direct detection	Heterodyne/Homodyne

a transmission performance of OFDM based FSO link in the presence of turbulence has been evaluated and discussed. The analysis results prove that proposed system performance sensitive to the turbulence, and choosing an optimal optical modulation index (OMI) can enhance the overall quality of link transmission. Unfortunately, a particular challenge for OFDM with IM/DD, where arises the high peak-to-average-ratio (PAPR) caused by accommodating large number of users. Thus, several methods have been proposed for the power reduction in MSM scheme.

Different from the IM-based FSO system as mentioned above, various polarization shift keying (PolSK) schemes have been applied in FSO systems, where information is encoded as different state of polarization (SOP) by using external phase modulator. Both theoretical analysis and experimental results demonstrate that polarization sate is much more stable compared to amplitude and phase in the case of an optical beam propagation. The optical wave depolarization can be neglected in a turbulent channel as discussion in [67]. The binary PolSK modulation scheme offers an improved link performance in term of the peak optical power by about 3 dB compared to ASK with the OOK format has been reported in [68],[69]. Finally, the Fig.2.6 shows the block diagram of modulation issues. Both of the SIM-(internal modulation) and PolSK-(external modulation) based FSO system will be introduced in the following chapters.

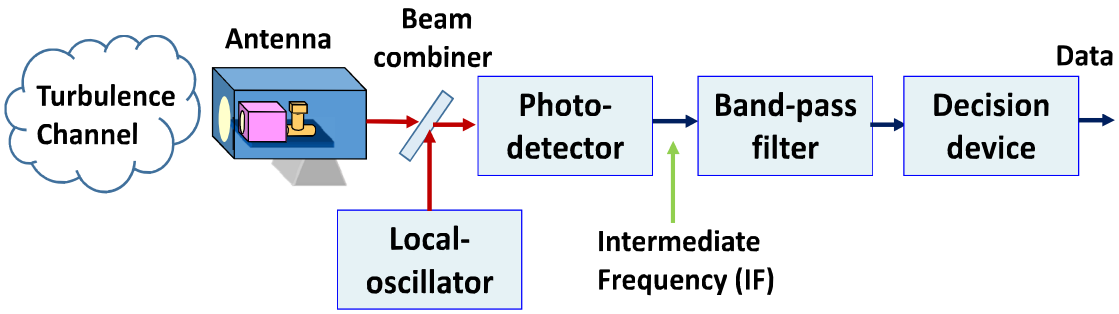

FIGURE 2.7: The block diagram of a typical coherent receiver of FSO system.

2.4.3 Coherent Detection

Although IM/DD has been wildly employed in FSO communication systems, which has inherent advantages in ease of implementation, independent of phase and SOP of incoming signal in real systems. But, the received signal information is only associated with the intensity of the transmitted field, which is randomly fluctuating in the real FSO systems. This leads to the performance loss with undesirable error floor, which is more sever under the strong turbulence regime. Unlike IM/DD scheme, with the coherent receiver, the information of optical beam can be restored by amplitude, phase and state of polarization. It offers an improved frequency selectivity, better background noise rejection and increased detector sensitivity, especially in potential ability of reduction of signal faded. The block diagram of a typical coherent receiver of FSO system as shown in Fig.2.7. A local oscillator (LO) is used to combine the incoming optical signal, however, it does not have to the same frequency as the incoming information. Thus, two variants of coherent detection generated as heterodyne and homodyne, which depends on whether the intermediate frequency (IF) is zero. Therefore, I provide a general mathematical modeling for describing the coherent detection processing, and then the mixed optical power (LO and signal) incident on the photo-detector can be expressed as:

$$P_R(t) = P_s + P_{LO} + 2\sqrt{P_s P_{LO}} cos((\omega_s - \omega_{LO})t + \varphi_s + \varphi_r - \varphi_{LO}) \tag{2.18}$$

where P_s and P_{LO} are received optical power and LO power, respectively. I would

note that the intermediate frequency as $\omega_{IF} = \omega_s - \omega_{LO}$, and φ_s, φ_r and φ_{LO} are encoded phase information, overall phase noise including the transmitter phase noise and phase noise due to turbulence channel, and LO phase noise, respectively. Obviously, the phase and SOP of incoming optical signal have became the significant influence factors to coherent detection link performance. In order to solve this problem, a variants configuration of coherent detection have been proposed such as by using the square-law demodulation in [70], however, resulting in more complicated and high cost than IM/DD system. In general, the heterodyne detection can offer the features compared with direct detection as: a LO with a sufficient power achieves the shot-noise limited receiver sensitivity. This is due to the signal gain offered by the LO; Compared with DD system, the receiver sensitivity can be improved by using the phase detection (polarization states), a heterodyne receiver only selects the polarization components of the received optical signal that match the polarization of the LO and rejects the others; heterodyne detection with efficient LO provides an excellent background noise rejection and channel fading compensation over direct detection.

Chapter 3

OFDM-Based RoFSO Systems with Spatial Diversity over Correlated Log-normal Fading Channels

3.1 Introduction

Nowadays, there has an increasing requirement on the high data rate and high-quality applications for the communication devices, we have to face to an important problem for explosion in the network traffic. The commercial FSO systems can be viewed as a good candidate for supporting the heterogeneous services in the real access networks, as to its ability on the high-speed and high-security over un-license spectra. Further, combining the advantages of radio communication and laser beam, which are similar to radio-over-fiber (RoF) [71], has been proposed to transmit the RF signal but excluding the fiber medium referred as radio-over free space optics (RoFSO). It provides a cost effective and high-capacity solution to connect the wireless services and optical fiber construction. As to the practical standards, the

first ITU-T recommendation in the area of G.640 for FSO application has been published [72].

It is well known that the main impairment factor is atmospheric turbulence, results in irradiance fluctuation of the received optical signal. This effect referred as the optical scintillation, which general cause the degradation of signal quality. Spatial diversity technique as an attractive approach with its inherent property in compensating to turbulence induced signal fading has been considered in FSO communication systems. Thus, spatial diversity plays an important role in turbulence mitigation methods. However, in this way, the most efficient diversity technology depends on the conditions of multiple uncorrelated sub-channels. Based on the fact that any two adjacent antennas must be far apart as an independent case, thus, correlation coefficient $\rho_{12} = 0$. Further, to determine the channel correlation which will generates among the sub-channels, is important to achieves a reliable link performance. Several studies on spatial diversity in FSO system with various modulation and receiver combining schemes under independent case have been discussed in [73].

OFDM known as a special case of multiple sub-carriers modulation (MSM) is wildly accepted to wireless communication that divides the spectrum into a number of equally spaced sub-channels and carrying a portion of a users information on each channel. OFDM/OFDMA technologies, which are the air interface for the Long Term Evolution (LTE) as well as one of important broadband applications by using the RoF techniques [74]. OFDM technologies have also been applied on several high-speed digital communication standards such as HDTV broadcasting (i.e., DVB-T) and IEEE 802.16. As to the MSM-based RoFSO system, the RF signal mapped into multiple sub-carriers and converted to the optical signals by using the intensity modulation direct detection (IM/DD), and then transmitted through the turbulent channel [42]. At the receiver end, the received optical signal is converted to the electrical signal by using the photo-detector (PD). As Fig.3.1 shows the typical multiple sub-carriers modulation RoFSO system configuration [25],[75].

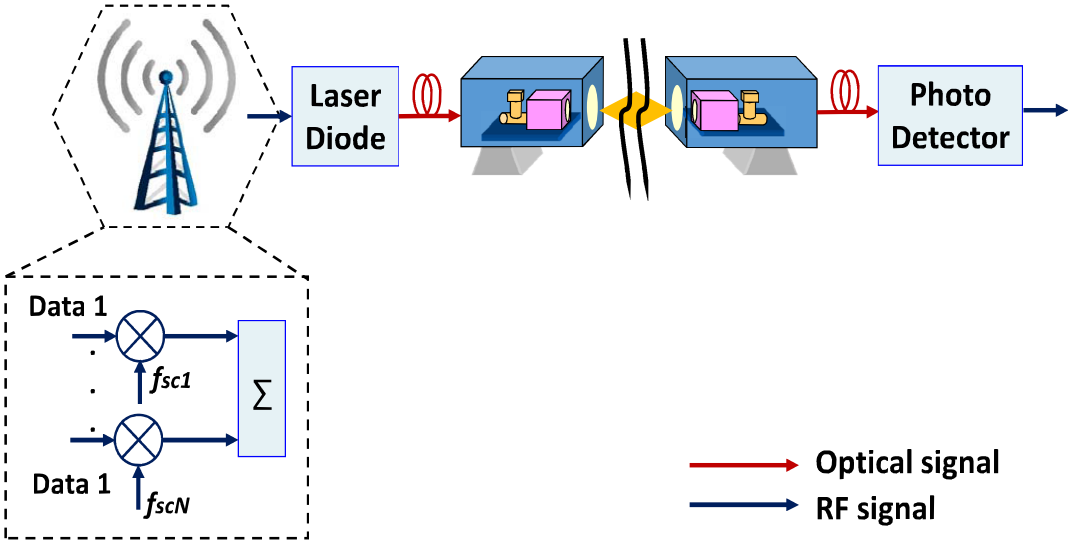

FIGURE 3.1: The typical MSM RoFSO system configuration.

Since the FSO system is modeled as the diversity reception scheme in the presence of the turbulence. In order to investigate the benefits of this proposal, different signal replicas combining schemes have been proposed and discussed in [76], which are based on the availability of channel state information (CSI). An efficient diversity scheme is required to improve the link performance considering the spatially independent and correlation channels. The diversity reception scheme consists of three primary linear combining techniques: maximum ratio combining (MRC) provides an optimum linear combining performance, resulting in a maximum-likehood receiver configuration. However, implementation complexity is an inherent property in this method, and system is extremely sensitive to channel estimation error. The MRC scheme in the term of average signal-to-noise-ratio (SNR) over the statistics of the turbulence distribution can be described as [63]:

$$\langle SNR_{MRC}(X)\rangle = \int_0^\infty \frac{1}{N}\left(\sum_{n=1}^{N} SNR_n(X)\right) P_X(X)dX \tag{3.1}$$

where N denotes the total number of the reception, the $SNR_n(X)$ is SNR of the nth reception, and $P_X(X)$ denotes the probability density function (PDF) for describing the variation of turbulence strength. In the regard to the equal gain combining

(EGC) scheme which as an efficient technique for reducing the system implementation complexity has been proposed when an accurate estimation of the received optical signal is difficult in MRC scheme. In general, the EGC scheme in the term of average SNR with weighting factors as a constant (unity), therefore, is given by [63]:

$$\langle SNR_{EGC}(X)\rangle = \int_0^{\infty} \frac{1}{N^2}\left(\sum_{n=1}^{N}\sqrt{SNR_n(X)}\right)^2 P_X(X)dX \tag{3.2}$$

In this chapter, I proposed a novel OFDM-based RoFSO system with spatial diversity reception over correlated log-normal turbulence distribution channel. The final goal of this chapter is to analyze and explore the potential of proposed system for deploying in practical high-performance high-speed transmission. First, I investigate the effect of turbulence and changed channel correlation on link performance, in terms of averaging BER and outage probability (OP). An analytical modeling for investigating the proposed system taking into consideration the diversity combining schemes and number of diversity reception has been established. Moreover, I give a comparison between the diversity receiver scheme and aperture averaging (AA) under the same link conditions. In this analysis, the use of spatial diversity configuration employing the OFDM modulation can be seem as a countermeasure for combating the turbulence-induced signal fading and enhancing the FSO link performance in the case of the real operation environment. In addition, this theoretical study will providing a guideline to optimized construct the actual system designing by applying an optimum transmission performance, especially for the areas where connect between the wireless services and optical fiber construction. I should mentioned that the work of this chapter is reference to my previous paper, which published on [25], [75].

3.2 Turbulence Model

3.2.1 Channel Correlation in Turbulent FSO Links with Diversity Reception

In this subsection, I look back the theories used to present the expressions for describing the channel correlation parameter among the diversity receiver over turbulent channel. Further, a mathematical modeling for the joint probability density function (PDF) which represents two log-normal random variables (RVs) of the irradiance intensity in the presence of turbulence has been presented.

As well known, the most serious problem that affect the quality of optical signal when propagating through atmosphere are caused by variation of the refractive index as earlier mentioned. In fact, it is important to consider this phenomenon which can arises the irradiance intensity fluctuation to the received signal, leading to an increasing in the error probability level in proposed system. Irradiance intensity fluctuation induced signal faded that depends on the size of the receive aperture, a number of literatures proposed to compensate the power fading by increasing the size of aperture beyond the correlation length as aperture averaging (AA) solution. In the normal, aperture averaging scheme can be seem as a special form of spatial diversity schemes.

In this proposal, a spatial domain technique can be used to model a novel RoFSO system and employ the two apertures to collect OFDM signal at different positions. This model has been limited in the plane-wave applications. Consider a dual diversity reception based optics link as shown in Fig.3.2 [25],[75]. The L denotes the propagation distance, and P_1 and P_2 represent the center point of receiver aperture. Then, the ρ_{12} can be described as the channel correlation coefficient between the two component receiver apertures, $1th$ receiver aperture and $2th$ receiver aperture,

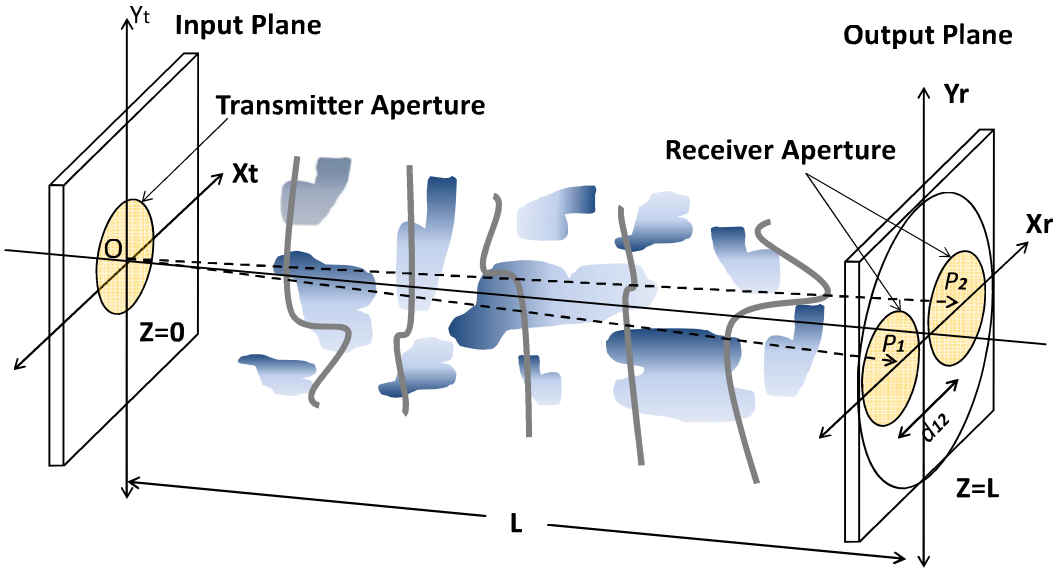

FIGURE 3.2: A dual diversity reception based optics link over turbulent channel. *by F.BAI, performance analysis of RoFSO lnks with diversity reception for transmission of OFDM signals under correlated log-normal fading channels. Journal of ICT standardization [75].*

respectively. Thus, the channel correlation coefficient is given by [76], [75], [25],

$$\rho_{12}\left(d_{12}, D\right) = \frac{B_{I,12}(I_1, I_2, d_{12}, D)}{\sqrt{\sigma_1^2 \sigma_2^2}} \tag{3.3}$$

where d_{12} denotes the separation distance between the center-to-center point in the adjacent aperture plane (P_1, P_2), D denotes the aperture diameter. $B_{I,12}$ and σ_j^2 (j=1,2) are the spatial covariance function of the irradiance and scintillation index of the jth diversity receiver, respectively. For purpose of further analysis on the link performance, I prefer to introduce the light irradiance spatial covariance function as follow [25], [75]:

$$B_{I,12}(I_1, I_2, d_{12}, D) = \frac{\langle I_1 I_2 \rangle}{\langle I_1 \rangle \langle I_2 \rangle} - 1 \tag{3.4}$$

and the irradiance spatial covariance function is a more general statistic model with its special case when the space distance between adjacent point, $d_{12} = 0$, known as

scintillation index can be described as [25], [75]:

$$B_{I,ij}(I_i, I_j, 0, D) = \sigma^2_{i=j}(D) = \frac{\left\langle I^2_{i=j} \right\rangle}{\left\langle I_{i=j} \right\rangle^2} - 1 \tag{3.5}$$

where I denotes the collected irradiance intensity by the single receiver aperture, the symbol $\langle . \rangle$ with being the average over scintillation.

Conventionally, two points on-axis log-amplitude fluctuation covariance function in terms of the log-amplitude X and log-amplitude variance σ^2_X based on extended Rytov theory, thus, is defined by [57]

$$\begin{aligned} B_{X,12}(r_1, r_2, L) =& \left\langle (X_1 X_2)^2 \right\rangle - \left\langle (X_1 X_2) \right\rangle^2 \\ =& \frac{1}{2} Re \left[E_2(r_1, r_2, L) + E_3(r_1, r_2, L) \right] \end{aligned} \tag{3.6}$$

where $r_{i,j}$ is the transverse vector, $Re(.)$ denotes the real part of function. E_2 and E_3 are two second-order statistical moments, and when optical beam at output plane, $r_i = r_j = 0$, can be expressed as [57]:

$$\begin{aligned} E_2(0, 0, L) =& 4\pi^2 k^2 L \int_0^1 \int_0^\infty K \Phi_{n.eff}(K) \\ & exp\left(-\frac{K^2 D^2}{16} \right) J_0(K d_{12}) dK d\xi \end{aligned} \tag{3.7}$$

and

$$\begin{aligned} E_3(0, 0, L) =& -4\pi^2 k^2 L \int_0^1 \int_0^\infty K \Phi_{n.eff}(K) \\ & exp\left(-\frac{K^2 D^2}{16} - i\frac{L\xi}{k} \right) J_0(K d_{12}) dK d\xi \end{aligned} \tag{3.8}$$

where $k = 2\pi/\lambda$ denotes the number of optical wave, $\xi = 1 - z/L$, L represents the propagation distance, and $J_0(.)$ is Bessel function of the first kind and zero order. Further, the covariance function is valid under all turbulence regimes when effective atmospheric spectrum $\Phi_{n.eff}(K)$ has been used. The effective atmospheric spectrum $\Phi_{n.eff}(K)$ under neglecting the inner-scale and outer-scale conditions can

be derived as [57]:

$$\Phi_{n.eff}(K) = 0.033C_n^2K^{-11/3}\left[exp(-\frac{K^2}{K_{X.0}^2}) + \frac{K^{11/3}}{(K^2+K_{Y.0}^2)^{11/6}}\right] \tag{3.9}$$

with

$$K_{X.0}^2 = \frac{k}{L}\frac{2.61}{1+1.1\sigma_R^2} \tag{3.10}$$

and

$$K_{Y.0}^2 = \frac{3k}{L}(1+0.69\sigma_R^{12/5}) \tag{3.11}$$

where $K_{X.0}$ and $K_{Y.0}$ represent the low-pass and high-pass spatial frequency cutoffs, respectively. It is noted that low-pass spatial frequency cutoff $K_{X.0}$ is related to the diffraction effects caused by turbulence cells smaller than the spatial coherence radius, and high-pass spatial frequency cutoff $K_{Y.0}$ denotes the deflection effects of turbulence larger than the scattering disk. From the previous literatures, the arising of channel correlation is mainly on the reflection effects. The parameter σ_R^2 denotes the Rytov variance. The parameter C_n^2 is known as index of refraction structure and assumed to be a constant to define the range of turbulence strength.

Considering the log-amplitude variance is sufficiently small, and making the transverse vector with $r_i = r_j = 0$ for the on-axis values at output plane, thus, the scintillation index can be modified as follow [57]:

$$B_{I,i=j}(I_{i=j}, I_{i=j}, 0, D) = \sigma_{i=j}^2(D) = exp\left[4B_{X,1=2}(0,0,L)\right] - 1 \tag{3.12}$$

According to the relationship between the irradiance spatial covariance and log-amplitude covariance as shown in equation 3.12. Further, bring the equation 3.7,

3.8 and 3.9 into the equation 3.4, thus, I can obtain

$$\begin{aligned} B_{I,12}(I_1, I_2, d_{12}, D) =& exp\left\{2Re\left[E_2(0,0,L) + E_3(0,0,L)\right]\right\} - 1 \\ =& exp\left\{8\pi^2 k^2 L \int_0^1 \int_0^\infty \Phi_{n.eff}(K) exp(-\frac{K^2 D^2}{16}) \right. \\ & \left. \times J_0(K d_{12}) \left[1 - cos\left(\frac{LK^2\xi}{k}\right)\right] dK d\xi \right\} - 1 \end{aligned} \tag{3.13}$$

Finally, as the mentioned above, the scintillation index parameter σ^2 defined where $d_{12} = 0$ in equation 3.13. Then, the channel correlation coefficient ρ_{12} obtained from the equation 3.13 and 3.3.

3.2.2 Correlated Log-normal Turbulence Model

Theory basis to the FSO system operating under the atmospheric turbulence condition can be established on a mathematical modeling by the probability density function of randomly irradiance intensity that describes the system's behavior across the different turbulence regimes [59]. In this subsection, I first give a review of correlated log-normal turbulence model to represent the combining faded of irradiance intensity. It provides an useful way to determine the effect of channel correlation on the link performance under turbulence condition. Based on previous literatures, probability density function (PDF) of irradiance intensity fading in term of log-normal distribution for single receiver is given by [25], [75]

$$f_I(I) = \frac{1}{2I} \frac{1}{(2\pi\sigma_X^2)^{1/2}} exp\left\{-\frac{(ln(I) - ln(I_0))^2}{8\sigma_X^2}\right\} \tag{3.14}$$

where I_0 being with the irradiance intensity without turbulence effects, $I = I_0 exp(2X - 2\langle X \rangle)$. Hence, in the case of spatial diversity scheme where signal transmitted/-collected by multiple transceivers, a general spatial correlation matrix M is used to model the channel correlation among the transceivers, thus, can be described as

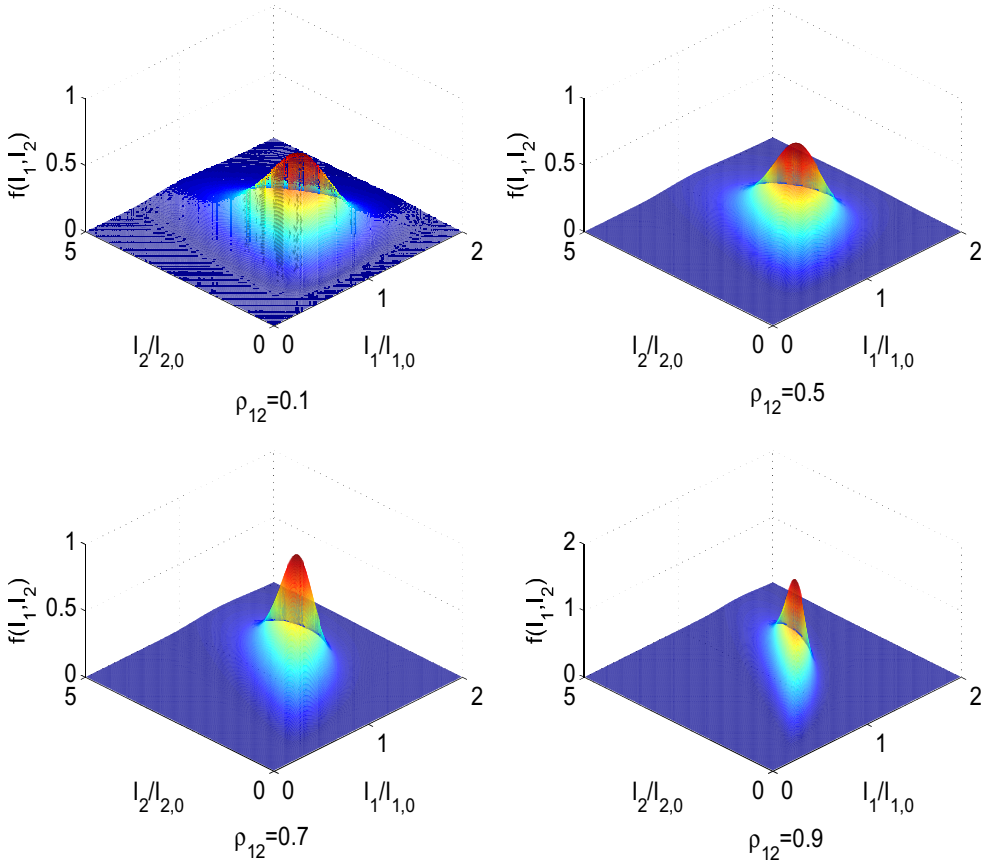

FIGURE 3.3: Irradiance intensity under correlated log-normal distribution with different values of channel correlation coefficient.

[63]:

$$M = \begin{bmatrix} m_{11}(d_{11}) & m_{12}(d_{12}) & \cdots & m_{1n}(d_{1n}) \\ m_{21}(d_{21}) & m_{22}(d_{22}) & \cdots & m_{2n}(d_{2n}) \\ \vdots & \vdots & \ddots & \vdots \\ m_{n1}(d_{n1}) & m_{n2}(d_{n2}) & \cdots & m_{nn}(d_{nn}) \end{bmatrix}_{n \times n} \tag{3.15}$$

where d_{nn} with being the separation space between the two component transceivers. It should note that $m(d) = B_X$ is log-amplitude spatial covariance function. Further, the spatial covariance matrix can be expressed as:

$$N = \sigma_x^2 M \tag{3.16}$$

where σ_x^2 is variance of irradiance intensity with turbulence effect. This math model also can be expanded to the spatial diversity at both multiple transmitters and receivers condition such as MIMO scheme.

To define the turbulence-induced channel fading in term of scintillation by diversity reception, a correlated joint turbulence distribution of the irradiance intensity by log-normal modeling is derived as follow:

$$\begin{aligned} f_{I_1,I_2}(I_1,I_2) =& \frac{1}{4I_1I_2}\frac{1}{2\pi\sigma_{X_1}\sigma_{X_2}\sqrt{1-\rho_{12}^2}} \\ & \times exp\left\{-\frac{1}{8(1-\rho_{12}^2)}\left[\frac{(lnI_1-lnI_{1,0})^2}{\sigma_{X_1}^2}+\frac{(lnI_2-lnI_{2,0})^2}{\sigma_{X_2}^2}\right.\right. \\ & \left.\left.-2\rho_{12}\frac{(lnI_1-lnI_{1,0})(lnI_2-lnI_{2,0})}{\sigma_{X_1}\sigma_{X_2}}\right]\right\} \end{aligned} \tag{3.17}$$

where $I_{1,0}$ and $I_{2,0}$ are the collected irradiance intensity by the $1th$ receiver aperture and $2th$ receiver aperture without turbulence condition. The figure 3.3 shows the irradiance intensity over correlated log-normal distribution [25],[75].

3.3 Performance Analysis of Proposed System

3.3.1 Proposed System Model

Following, I focus on building an math model able to characterize the OFDM signal propagation through a turbulent FSO link employing IM/DD by dual diversity reception in this subsection. I presented the expressions of the SNR, BER and outage probability, taking into consideration the scintillation effect, and both of MRC and EGC combining schemes. As the shown in figure 3.4, a novel FSO configuration is considered where the OFDM signal was propagated via single aperture and collected by dual apertures over turbulence channel modeled by joint correlated log-normal distribution [25],[75].

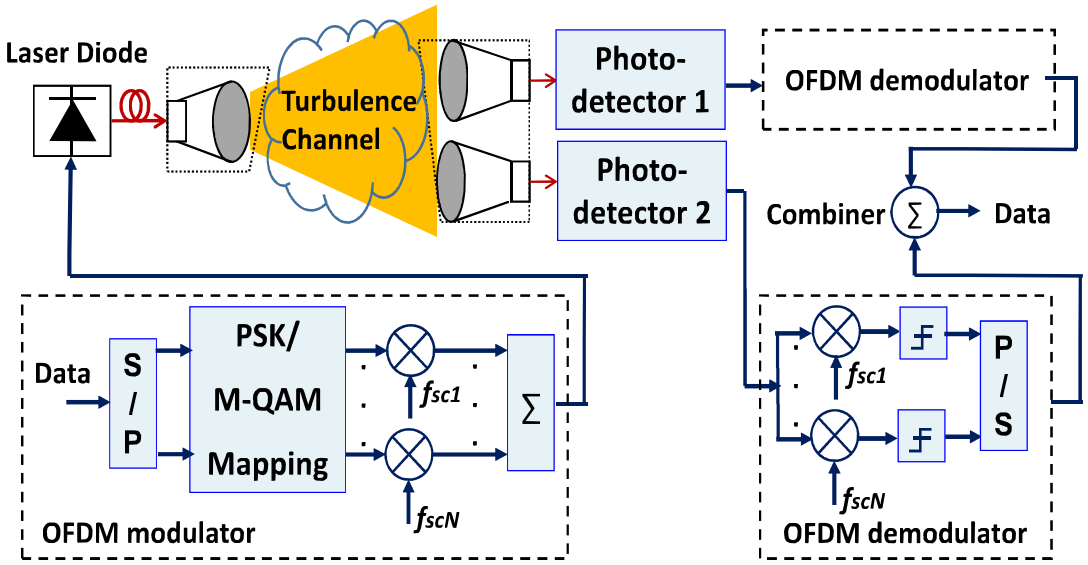

FIGURE 3.4: OFDM modulation based FSO system with spatial diversity in the presence of turbulence effect.

OFDM technology as a special form of multiple sub-carrier modulation where its each subcarrier is orthogonal to the other sub-carriers and separated by the correlation technique at the receiver side. It offers advantages in improved transmission data rate and distortion reduction of signal quality. However, such as high peak-average-power-ratio (PAPR) caused by large number of subcarrier is acts an particularly crucial in IM/DD OFDM systems. In this proposed system, the each low rate RF signal modulated by using the PSK or QAM modulation and then combined on high frequency carrier. Thus, the OFDM signal for number of N_s sub-carriers, after up-conversion can be expressed as [42],[25], [75]

$$S_{OFDM}(t) = \sum_{n-0}^{N_s-1} X_n exp\left\{j(\omega_n + 2\pi f_c)t\right\}, 0 \leq t < T_s \tag{3.18}$$

where ω_n and T_S are the set of orthogonal sub-carriers frequency and OFDM symbol duration, respectively. $X_n = a_n + jb_n$ is complex data symbol in the nth subcarrier, with a_n and b_n are the in-phase and quadrature modulation symbols. The first raw data is mapped according to different types of modulation techniques (PSK/QAM). Each symbol X_n is amplitude modulated on orthogonal sub-carriers [25],[75]. The

signal $S_{OFDM}(t)$ is then used to modulate the optical intensity by using the laser diode (LD) and converted to the optical signal. It should note that inter-modulation distortion (IMD) has been neglected in this work. Then, the transmitted optical power is given by

$$P(t) = P_t \left(1 + \sum_{n=0}^{N-1} m_n S_{OFDM}(t)\right) \tag{3.19}$$

where P_t and m_n are the average transmitted optical power and modulation index on per sub-carrier, respectively.

Considering the main influence factors, including the channel attenuation and scintillation in the field of FSO link, thus, the received optical power after photo-detectors can be described as [25], [75]:

$$P_{r.FSO}(t) = P(t) L_{loss} X + n_{FSO}(t) \tag{3.20}$$

where L_{loss} includes the sum of path losses due to attenuation, geometrical loss and pointing error. The $n_{FSO}(t)$ quantifies the additive white Gaussian noise (AWGN), and the variation of the irradiance intensity X that associate to the log-normal distribution, including the X_1 and X_2 for each sub-channel.

Then, the received optical signal converted to the electrical signal by each photo-detector (PD), hence, the FSO noise can be filtered after passing the PDs. Moreover, the each sub-channel passes through the electrical filter and OFDM demodulator. Assuming the total photo current at output of the combiner in the presence of turbulence is given [25], [75]

$$i(t, I_1, I_2, X) = I_{ph}(I_1, I_2) \left(1 + \sum_{n=0}^{N-1} m_n S_{OFDM,1,2}(t)\right) + n_{opt,1,2}(t) \tag{3.21}$$

where $I_{ph} = R_D P_t L_{loss} X$ is DC of the received photo current which depends on received irradiance intensity and has the same statistic to X, including the I_1 and

I_2 received by each receiver aperture, R_D is detector responsivity. It note that the optical modulation index (OMI) per sub-carrier is given as

$$m_n = \frac{m_{total}}{\sqrt{N}}, n = 0, 1, ..N-1 \tag{3.22}$$

In this RoFSO link, the total noise parameter $n_{opt}(t)$ is the sum of thermal noise, shot noise and relative intensity noise, respectively, is modeled as Gaussian white random process with zero mean and variance $\sigma_N^2 = N_0/2$. Then, the total noise power can be described as [25], [75]

$$N_0(I_1, I_2) = \frac{4K_B T_{abs} F_e}{R_L} + 2qI_{ph}(I_1, I_2) + (RIN)I_{ph}^2(I_1, I_2) \tag{3.23}$$

where K_B and T_{abs} are the Boltzmann's constant and absolute temperature, respectively, F_e denotes the noise figure, RIN with being the relative intensity noise, R_L is the load resistor od photo-detector, and q is the electron charge.

3.3.2 Signal-to-Noise-Ratio and Bit-Error-Ratio

In this subsection, a comparison between the MRC and EGC combining scheme obtained from the performance evaluation of proposed system has been discussed, in terms of BER and SNR. In the regard to the MRC combining scheme, the instantaneous electrical signal-to-noise-ratio (SNR) in the presence of turbulence can be expressed as

$$\gamma_{MRC}(I_1, I_2, X_1^2, X_2^2) = \sum_{j=1}^{2} \gamma_j(X_j^2)/2 \tag{3.24}$$

and with EGC combining scheme by dual diversity reception is derived as

$$\gamma_{EGC}(I_1, I_2, X_1^2, X_2^2) = \left(\sqrt{\gamma_1(X_1^2)} + \sqrt{\gamma_2(X_2^2)}\right)^2 /4 \tag{3.25}$$

where γ_j denotes the SNR of the jth receiver aperture within turbulence effect. In the case of both of MRC and EGC combining scheme in term of electrical SNR for the proposed system, thus, can be derived as follow

$$\gamma_{MRC}(X_1^2, X_2^2) = \frac{m_n^2(I_{ph.1}^2(I_1, X_1) + I_{ph.2}^2(I_2, X_2))}{2N_0(I_1, I_2)B_e} \tag{3.26}$$

and

$$\gamma_{EGC}(X_1^2, X_2^2) = \left[\frac{\sqrt{m_n^2 I_{ph.1}^2(I_1, X_1)} + \sqrt{m_n^2 I_{ph.2}^2(I_2, X_2)}}{2\sqrt{N_0(I_1, I_2)B_e}}\right]^2 \tag{3.27}$$

where $I_{ph.j}$ is the DC current part that related to the I_j with the same statistics model as X_j, B_e denotes the electrical filter bandwidth.

Hence, when considering the M-QAM is used to modulate the original RF signal in the case of OFDM modulator where sub-channel collected irradiance intensity I_1, I_2 following a joint correlated log-normal distribution, taking into account the channel correlation with representation of log-amplitude fluctuation by parameter X, thus, the equation 3.17 can be modified as follow

$$\begin{aligned} f_{X_1,X_2}(X_1, X_2) =& \frac{1}{2\pi\sigma_{X_1}\sigma_{X_2}\sqrt{1-\rho_{12}^2}} \\ & \times exp\left\{-\frac{1}{2\left(1-\rho_{12}^2\right)}\left[\frac{(X_1 - \langle X_1\rangle)^2}{\sigma_{X_1}^2} + \frac{(X_2 - \langle X_2\rangle)^2}{\sigma_{X_2}^2}\right.\right. \\ & \left.\left. -2\rho_{12}\frac{(X_1 - \langle X_1\rangle)(X_2 - \langle X_2\rangle)}{\sigma_{X_1}\sigma_{X_2}}\right]\right\} \end{aligned} \tag{3.28}$$

Further, the BER_{total} for the M-QAM based OFDM signal, where $M = 2^n$ and n is an even number, under the turbulence effect is derived as [25], [75]

$$BER_{total}(X_1^2, X_2^2) = \frac{2(1-\sqrt{M}^{-1})}{log_2^M} erfc\left(\sqrt{\frac{3\gamma_{total}(X_1^2, X_2^2)}{2(M-1)}}\right) \tag{3.29}$$

where $erfc(.)$ denotes the complementary error function as

$$erfc(x) = \frac{1}{\sqrt{x}} \int_{x}^{\infty} e^{-y^2} dy \tag{3.30}$$

Finally, the total average BER_{total} for the received signal over correlated log-normal distribution can be obtained from

$$\langle BER_{total} \rangle = \int_{0}^{\infty} \int_{0}^{\infty} f_{X_1,X_2}(X_1, X_2) BER_{total}(X_1^2, X_2^2) dX_1 dX_2 \tag{3.31}$$

where $f_{X_1,X_2}(X_1, X_2)$ denotes the probability density function as above mentioned for describing the variation of signal fading.

3.3.3 Analysis of Outage Probability

The outage probability as an useful performance metric has been commonly used in evaluation of fading channel. It is defined as the probability that instantaneous SNR (γ_{total}) falls below a specific threshold SNR (γ_{th}), where represents a value of the SNR above which quality of link is satisfactory. It provides an alternative way to evaluate the signal f larly under the scintillation effect condition. The outage probability for a given threshold SNR (γ_{th}) can be described as [69],[75]:

$$P_{out}(\gamma_{th}) = P\left[\gamma_{total} < \gamma_{th}\right] \tag{3.32}$$

The outage probability by the MRC combining scheme is derived as

$$P_{out}(\gamma_{th}) = \int_{0}^{\gamma_{th}} \int_{0}^{\gamma_{th}-\gamma_2} f(\gamma_1, \gamma_2) d\gamma_1 d\gamma_2 \tag{3.33}$$

where $f(\gamma_1, \gamma_2)$ denotes the function of SNR follow the correlated log-normal distribution model.

TABLE 3.1: Numerical Parameters. *by F.BAI, performance analysis of RoFSO lnks with diversity reception for transmission of OFDM signals under correlated log-normal fading channels. Journal of ICT standardization [25,75].*

Operation wavelength λ	1550nm
Relative intensity noise RIN	-130dB/Hz
Photo detector load resistor R_L	50Ω
Absolute temperature T_{abs}	300K
Propagation distance L	2000m
Electron charge	1.602×10^{19}
Noise figure F_e	2dB
Filter bandwidth B_e	2GHz
Number of subcarrier N_s	256
Optical modulation index m_n	0.01
Responsivity of detector R_D	0.8A/W

3.4 Numerical Results and Discussions

Following, the characters evaluation results of OFDM-based FSO Link with spatial diversity over correlated log-normal distribution obtained from the simulation by MATLAB. The related evaluation parameters used in this work are shown in Tabel 3.1.

Ever since the property of channel correlation coefficient has been investigate in several works [75], I would to remark the important points that will be useful while analyzing the link performance to follow. Figure 3.5 shows the channel correlation coefficient ρ_{12} as a function of separation distance under variation turbulence regimes represented by σ_R^2, and aperture size with being a fixed value $D = 2cm$. From the graph, it shows that the ρ_{12} decreases with increasing separation distance d_{12}, and the curves go cross a zero point where the channel correlation length ρ_c is defined as, $\rho_{12}(\rho_c) = 0$ under the changed turbulence strength σ_R^2. In general, the channel correlation length ρ_c acts an important parameter which is useful way of making a quick judicial decision on whether channel correlations exist among component antennas. The obtained result also shows the when the two sub-channels are overlapped, they must be perfectly correlated. In general, two sub-channels are as an independent case of each other when the d_{12} is larger than channel correlation

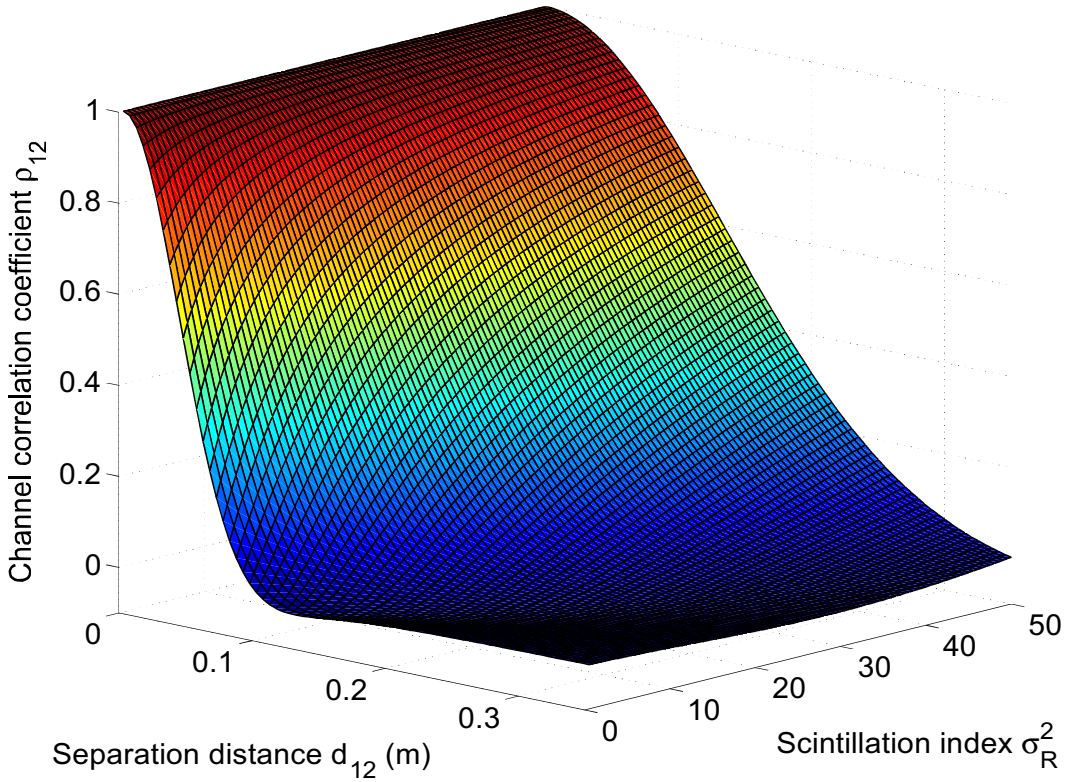

FIGURE 3.5: Channel correlation coefficient ρ_{12} against separation distance d_{12} and scintillation index for variation of turbulence strength regimes.

length ρ_c, and channel correlation is also affected by variance of turbulence strength. Moreover, considering the aperture averaging (AA) scheme based the previous literatures in [36], the point aperture is defined as $D < \sqrt{L\lambda}$. Thus, the point aperture size D is approximate to $2cm$ in this analysis. The effect of AA ($D \gg \sqrt{\lambda L}$) on the system performance will be discussed in following result.

In Fig.3.6, a link performance comparison between the EGC and MRC combining schemes with different channel correlation coefficient, $\rho_{12} = (0.9, 0.1)$, respectively [25],[75]. It is observed that performance of receiver with EGC combiner is close to the receiver with MRC combiner when link under the only two reception components and within same channel correlation coefficient condition. The result also shown that there is a 2dB difference between the ρ_{12}=0.1 and ρ_{12}=0.9 at BER=10^{-6}. It should note that the receiver aperture size is $D = 2cm$ which acts point aperture

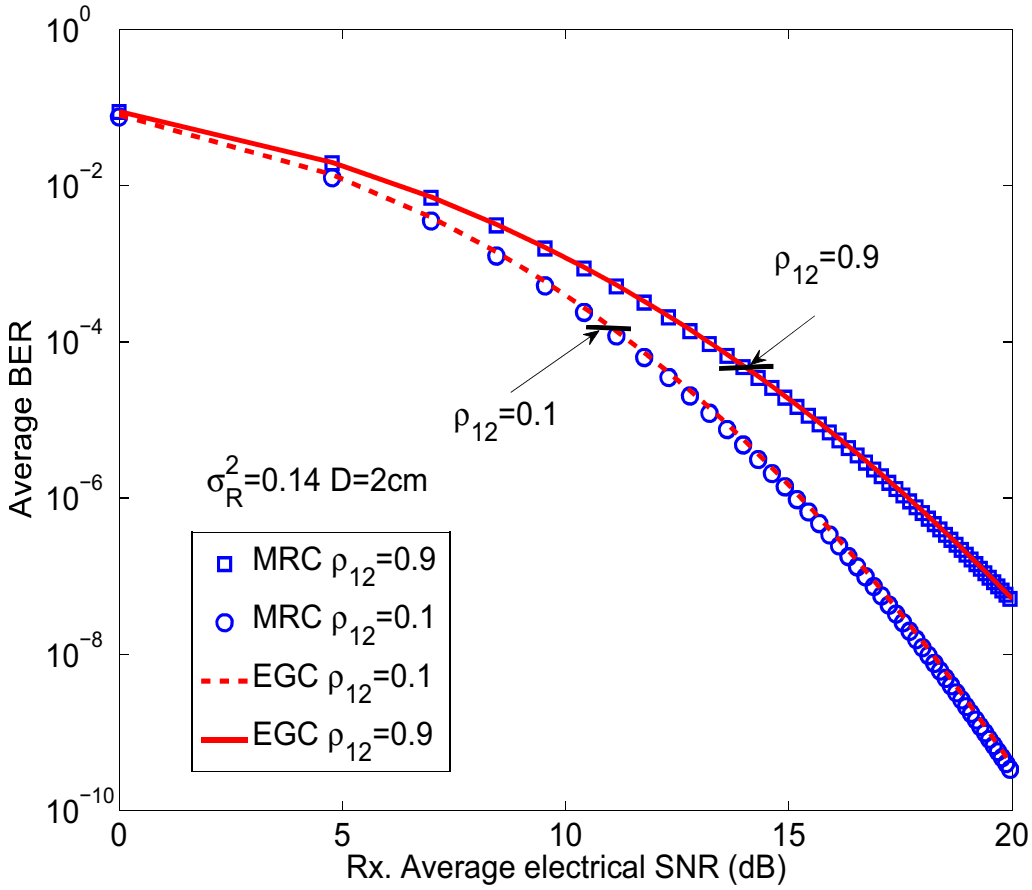

FIGURE 3.6: Average BER versus electrical SNR of proposed system with both of MRC and EGC combining schemes over turbulence channel. *by F.BAI, performance analysis of RoFSO lnks with diversity reception for transmission of OFDM signals under correlated log-normal fading channels. Journal of ICT standardization [25,75].*

scheme, and Rytov variance with being $\sigma_R^2 = 0.14$ defined as weak turbulence regime. In uncorrelated channel, $\rho_{12}(\rho_c) = 0$, each receiver aperture deployment far apart, and separation distance beyond to the channel correlation length ρ_c. Thus, the transmission performance can be seen as under an independent condition without sub-channel interference. This point of view is also in contract I typically see in RF wireless communication [77], where only the uncorrelated channel has a lower data error level, leading to a potential ability on the reduction of signal fading. The obtained result demonstrates that efficient separation between the apertures is crucial to achieve the promised improvement of system from independent dual

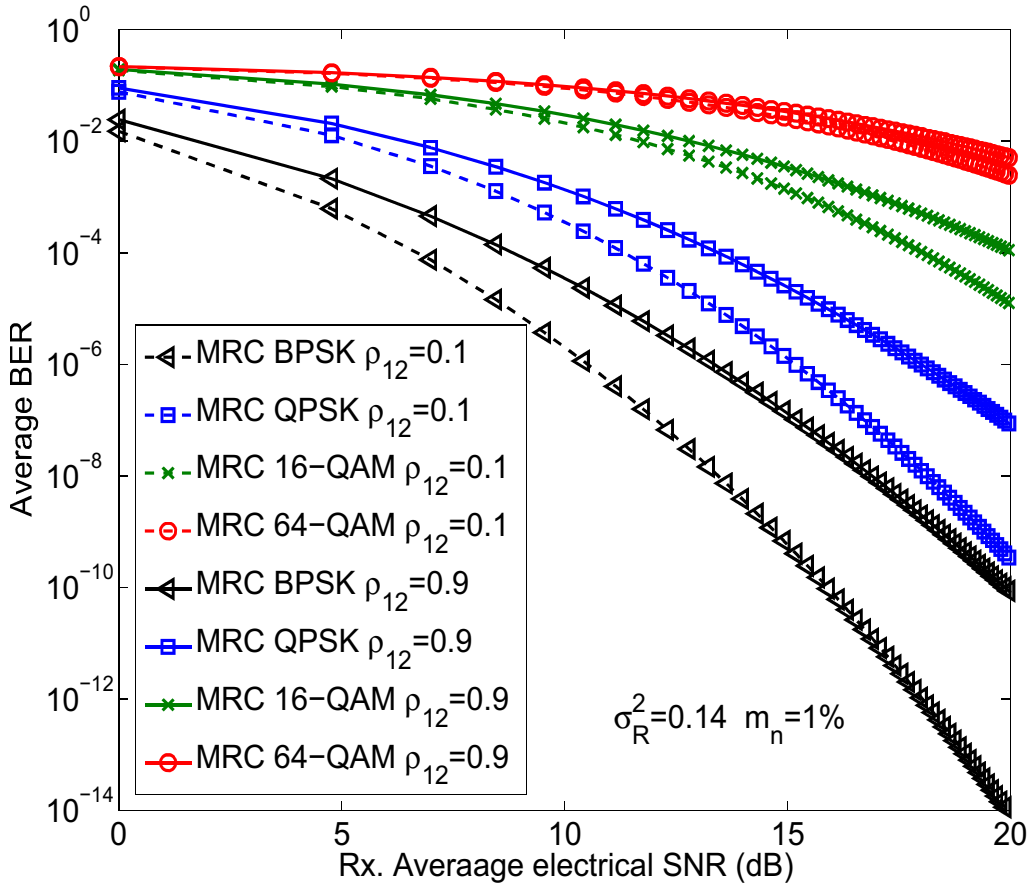

FIGURE 3.7: Average BER versus electrical SNR of proposed system over turbulence channel under different modulation schemes. *by F.BAI, performance analysis of RoFSO lnks with diversity reception for transmission of OFDM signals under correlated log-normal fading channels. Journal of ICT standardization [25,75].*

diversity reception (channel correlation coefficient ρ_{12} approximate to zero, i.e. $\rho_{12} = 0.1$). In fact, they are also highly sensitive to the turbulence due to the required precision in accurate constellation scaling in the following signal processing.

In Fig.3.7, the figure plots the average BER versus the average electrical SNR for different modulation types, such as BPSK, QPSK, 16-QAM, 64-QAM, respectively, and considering the MRC combining scheme with correlation coefficient $\rho_{12} = 0.1$ as a independent case and $\rho_{12} = 0.9$ over weak turbulence channel, $\sigma_R^2 = 0.14$ with the point receiver aperture size $D = 2cm$ [25],[75]. The proposed FSO link performance

is degraded as well as the correlation coefficient is high. However, as to the average BER=10^{-10}, the BPSK with correlation coefficient $\rho_{12} = 0.1$ outperforms BPSK with correlation coefficient $\rho_{12} = 0.9$ by approximately 5dB. These results indicate the importance of channel correlation and also demonstrate the effect of correlation on system performance. For instance, the effect of modulation on the average BER in clearly apparent. For the average SNR=14dB, the average BER increases from 10^{-9} to $10^{-1.5}$ for QPSK and 64-QAM with same correlation coefficient $\rho_{12} = 0.1$, respectively. Actually, the average error probability of spatial diversity OFDM-FSO system with larger constellation size requires higher received optical power to accurately discriminate among the transmitted information.

To highlight the performance enhancement by using diversity reception, I have shown in Fig.3.8 the system performance with ternary, dual and single reception (AA) in weak turbulence regime $\sigma_R^2 = 0.14$, and using MRC scheme for two different channel correlation coefficient $\rho_{12} = (0, 0.9)$, respectively [25],[75]. In this analysis, the effect of aperture averaging on system performance have been considered, i.e. $D = 4cm$ for single reception. It should be noted that the collected area of single aperture is approximately equal to the sum of the diversity apertures area in this case. Before expressing the analysis content, I first derive the function of electrical SNR within MRC combiner, based on previous mentioned on equation 3.24, and is given

$$\gamma_{MRC}(I_1, I_2, I_3, X_1^2, X_2^2, X_3^2) = \sum_{j=1}^{3} \gamma_j(X_j^2) \tag{3.34}$$

and average BER over scintillation is derived as

$$\langle BER_{total} \rangle = \int_0^\infty \int_0^\infty \int_0^\infty f(X_1, X_2, X_3) BER_{total}(X_1^2, X_2^2, X_3^2) dX_1 dX_2 dX_3 \tag{3.35}$$

where $f(X_1, X_2, X_3)$ denotes the PDF of turbulence model. The result shows that ternary reception link performance outperforms dual and single reception cases. For instance, considering the electrical SNR=15dB, the average BER increases from

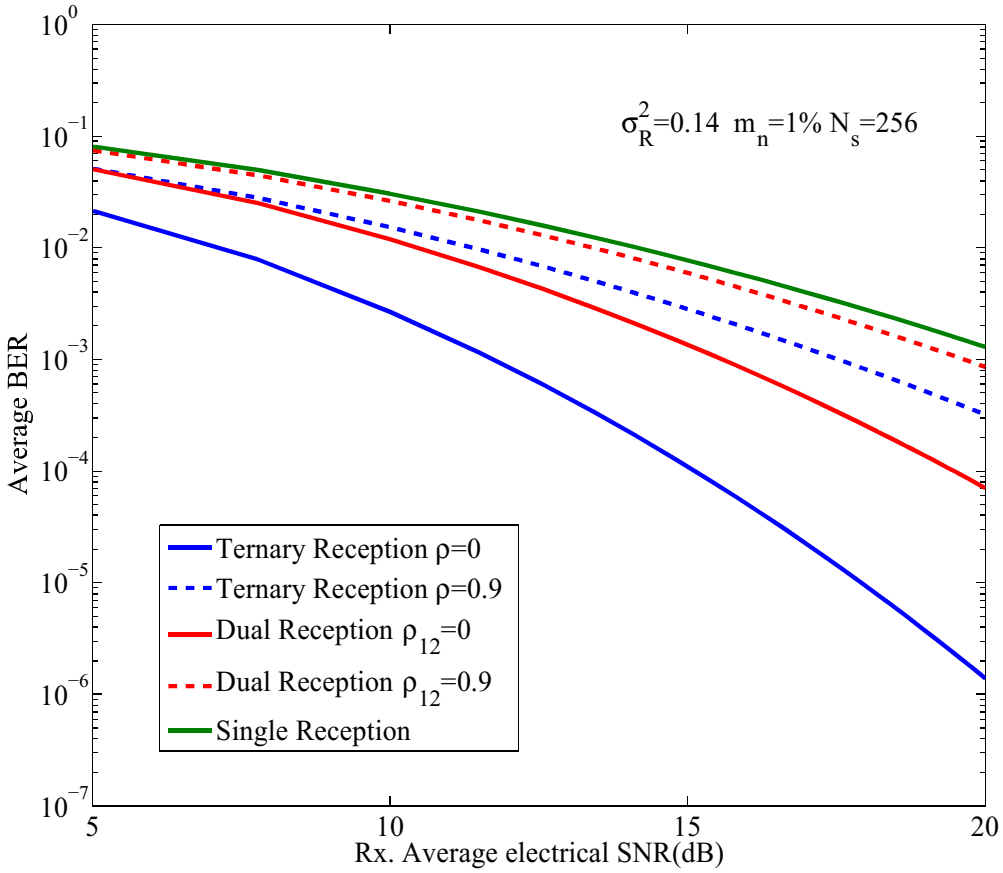

FIGURE 3.8: Link performance comparison of a turbulent OFDM-based FSO link under ternary reception, dual diversity reception and single reception conditions. *by F.BAI, performance analysis of RoFSO lnks with diversity reception for transmission of OFDM signals under correlated log-normal fading channels. Journal of ICT standardization [25,75].*

10^{-4} for ternary reception, 10^{-3} for dual reception to 10^{-2} for single reception with AA under same channel correlation coefficient $\rho_{12} = 0$, respectively. These results determine that selecting diversity reception may increase the overall link performance, and diversity techniques can be obtained in practice through aperture averaging effect. Furthermore, I determined that there is a 5dB difference at BER=10^{-4} for the ternary reception with channel correlation parameter $\rho_{12} = 0$ and $\rho_{12} = 0.9$, respectively. As pointed out above, the result indicates that increased channel correlation coefficient leads to the link performance degradation.

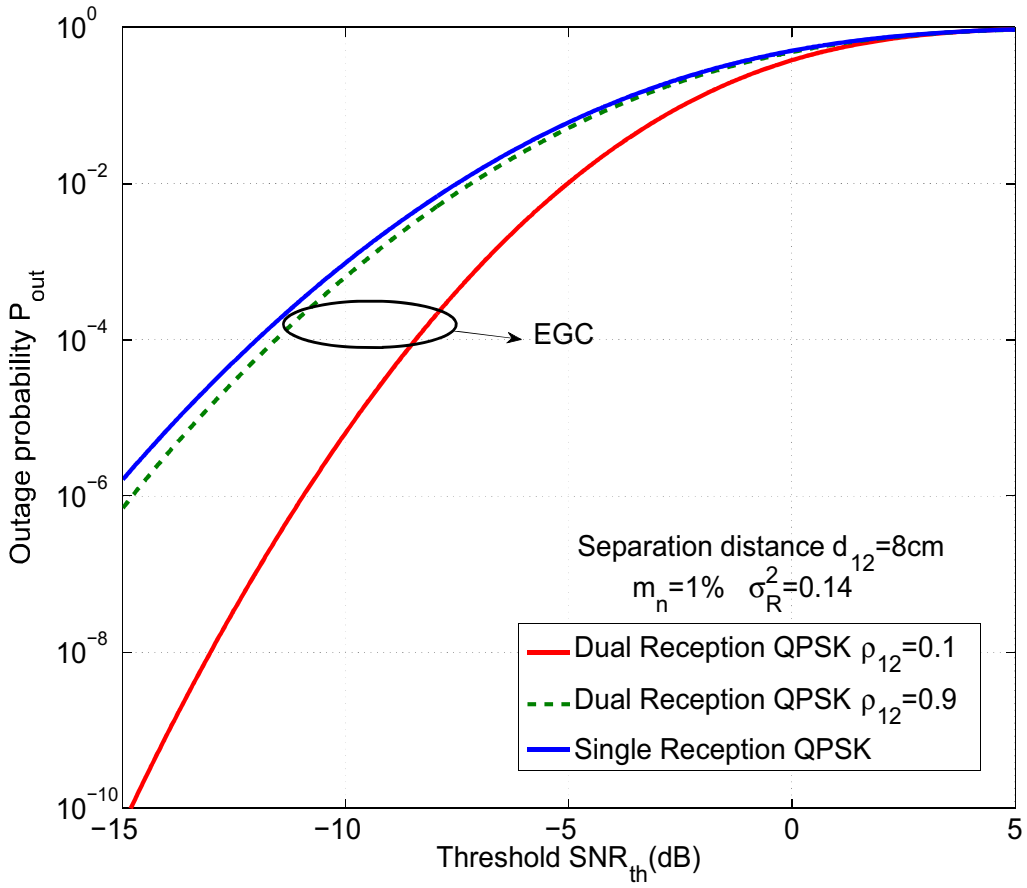

FIGURE 3.9: Performance of dual diversity reception with MRC combining scheme in term of outage probability. *by F.BAI, performance analysis of RoFSO lnks with diversity reception for transmission of OFDM signals under correlated log-normal fading channels. Journal of ICT standardization [25,75].*

The system's outage probability P_{out} is analyzed using Eq.(3.33). Figure 3.9 shows P_{out} for single and dual reception with QPSK under the weak turbulence effect, and optical modulation index $m_n = 0.01$. Two cases of channel correlation coefficient have been considered, $\rho_{12} = (0.1, 0.9)$, respectively [25],[75]. It is observed that the use of a dual reception leads to better P_{out}, which outlines its contribution to mitigating the turbulence-induced fading. For instance, for a SNR_{th}=-15dB, P_{out} decreases from 10^{-10} to 10^{-6} for a dual reception with $\rho_{12} = 0.1$ and single reception, respectively. Now, considering the case of the channel correlation, $\rho_{12} = (0.1, 0.9)$

at the same outage probability $P_{out} = 10^{-6}$, I obtained a 4dB different for threshold SNR_{th} between $\rho_{12} = 0.1$ and $\rho_{12} = 0.9$ with a dual reception, respectively. The proposed system performance with channel correlation increasing leads to the performance degradation as the case of two channels are overlapped.

3.5 Conclusion

In this chapter, I provide a theoretical study of the channel correlation effect on the diversity reception OFDM-FSO system over turbulence channel. In our study, a novel transceiver architecture for turbulent OFDM-FSO system with diversity reception over correlated fading channel has been considered. I analyze and evaluate the channel correlation effects on the transmission performance of system over correlated log-normal turbulence channel in terms of SNR, BER and outage probability by different combining schemes and in the case of plane-wave model. The analysis results determined that spatial diversity -based OFDM-FSO system performance is related to the variation of channel correlation, modulation formats, receiver aperture size and scintillation, respectively. The numerical results also represented that spatial diversity can be seem as a helpful solution to compensate the turbulence-induced signal fading as well as reduction of data errors. The evaluation of the proposed system behaviors confirm that the use of the diversity reception with OFDM scheme lead to a potential ability on link performance improvement, especially in high demand on transmission capacity becomes more important in access networks.

Chapter 4

PolSK-Based Direct Detection OCDMA Systems Through Turbulent FSO Links

4.1 Introduction

Generally, different modulation types, in particular based on intensity modulation/direction detection (IM/DD), for FSO systems have been wildly reported, such as on-off keying (OOK), *etc.* However, the performance of this modulation scheme is readily affected by the turbulence fluctuation and optical modulation index; thus, this mean the requirement of the knowledge of the channel characteristic, and an optimal adaptive detection is required at the receiver to improve the link performance, which brings to the system complexity in the real case [64],[69].

Different from IM-based modulation schemes, polarization shift keying (PolSK) technology was proposed as an alternative modulation technique to both envelop- and phase-based modulation schemes [78]. By this way of modulating, data information is encoded by different states of polarization (SOPs) of the optical source

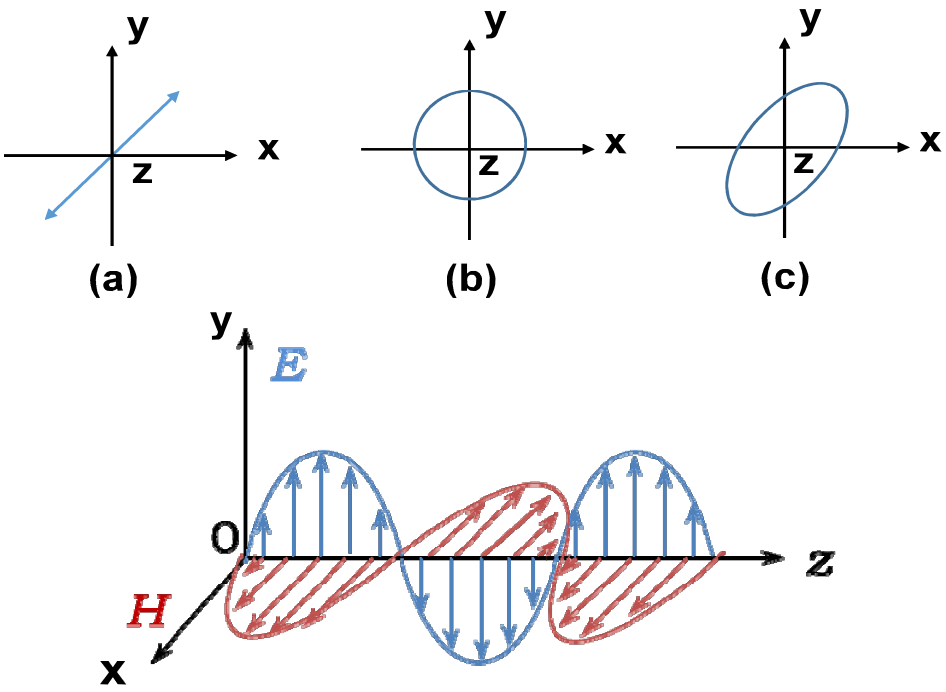

FIGURE 4.1: The electrical field vector of linear polarization light (a), circle polarization light (b) and elliptical polarization light (c). E: electric field, H: magnetic field

by using an external modulator (*i.e.*, a Mach–Zehnder interferometer) [78]. In the general of polarization light, the field amplitudes can be seen as along the horizontal axis E_x and vertical axis E_y, and can be described by following equations

$$E_x = A_x exp[j(\omega t + \varphi_x)] \cdot \hat{x} \tag{4.1}$$

$$E_y = A_y exp[j(\omega t + \varphi_y)] \cdot \hat{y} \tag{4.2}$$

where A_x and A_y denote the amplitude of the electrical field, respectively, and φ_x and φ_y denote the phase of the x-component and y-component, respectively, and ω being with the optical frequency. Then, assuming that laser beam is set to three polarization categories including the linear, circle and elliptical, respectively. The

functions are given as [78]:

$$\Delta\varphi_{linear} = m\pi(m = 0, \pm1, \pm2, ...) \tag{4.3}$$

$$\Delta\varphi_{circle} = m\pi/2(m = 0, \pm3, \pm5, ...) \tag{4.4}$$

$$\Delta\varphi_{elliptical} \neq 0, \pi or \pi/2, A_x \neq A_y \tag{4.5}$$

where $\Delta\varphi = \varphi_y - \varphi_x$ denotes the phase difference between the two components.

For inherent property of light wave, polarization states are the most stable properties compared with the amplitude and phase when propagating though a turbulent channel. Various PolSK modulation types have been proposed in FSO transmission systems [79]. In [68], it demonstrated that the binary PolSK (BPolSK) modulation offers an enhanced link performance in terms of the peak optical power by about 3 dB compared to the ASK scheme. For this reason, a novel transceiver architecture based on the PolSK scheme with multiplexing transmission technique has been proposed to mitigate the channel fading, as well as to enhance the system capacity in FSO communication systems in this chapter [69].

Optical code division multiplexing access (OCDMA) acts an useful solution to support multiplexing transmission and multiple users access, which supports high-speed and large capacity communication in optical fiber networks. At the same time, the OCDMA technique has also drawn a lot of attention in optical wireless communications. The use of OCDMA schemes as a countermeasure for improving link performance has been considered in [36],[80],[81], where the propagation signal influenced by turbulence effect and multiple-access interference (MAI) was exhaustively discussed. Fig.4.2 shows the system configuration of CDMA signal transmitted through a RoFSO link [36].

Basically, for the case of the received CDMA signal S_{CDMA} at the receiver end from the K users is described as:

$$S_{CDMA}(t) = \sum_{k=1}^{K} S_k(t - \tau_k) = \sum_{k=1}^{K} d_k(t - \tau_k)c_k(t - \tau_k) \tag{4.6}$$

and

$$d_k(t) = \sum_{i=0}^{M-1} d_{k,i} P_T(t - iT_s) \tag{4.7}$$

and

$$c_k(t) = \sum_{i=0}^{N-1} d_{k,i} P_T(t - iT_c) \tag{4.8}$$

where the τ_k, $0 \leq \tau_k \leq T_s$ is the time delay of the k-th user, and $d_k(t)$ and $c_k(t)$ are the intended user data signal with M bits and spreading code for k th user, respectively. The code sequence signal has N chips and $d_k(t)$, $c_k(t) \in \{0, 1\}$, where P_T denotes a unity rectangular pulse of width T, and T_s and T_c are the symbol duration and chip duration.

However, in the most of previous literatures such as discussed in [36], FSO links only can be used to transmit the CDMA signal based on intensity modulation as well as coding/decoding in the RF domain as shown in figure 4.2 . There is no systematic study of a cost-effective all-optical OCDMA-FSO system with external modulation has been carried out. Therefore, such a study will be important in designing and optimizing methods to enhance the performance of the OCDMA FSO systems in operation environments, combining the multiplexing transmission technologies and an optimum robust modulation scheme for the mitigation of signal fading [69].

The advantages of combining PolSK and OCDMA in optical fiber networks were already reported in [82], where the fiber dispersion and noise are the important impairment factors. However, no complete study providing an analytical model for PolSK-modulated OCDMA systems over an FSO link has been proposed so far

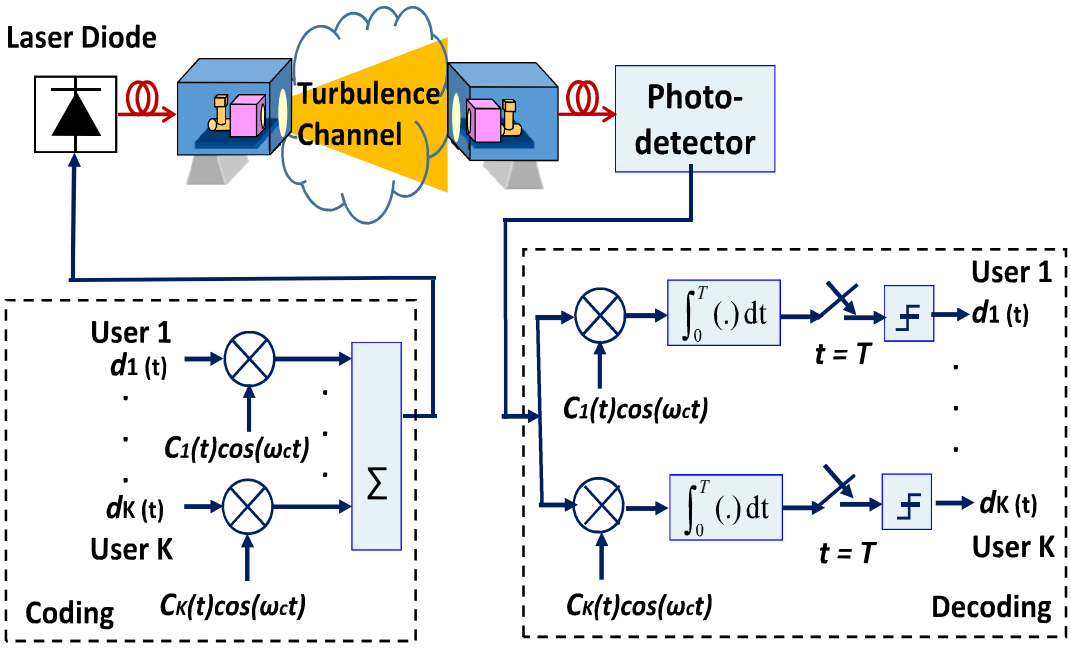

FIGURE 4.2: Conventional CDMA signals over turbulent RoFSO link.

to our knowledge. Therefore, the goal of this chapter is to analyze and explore the potential of proposed system on high speed optical wireless transmission, and the main contribution of this work is based on my previous results [69]. Firstly, I proposed a novel PolSK-modulated OCDMA systems over turbulent FSO link with IM/DD. Then, I developed a closed-form mathematical modeling for describing and evaluating the impact of scintillation and MAI on the link performance, in terms of the BER as well as the outage probability in the case of Gamma-Gamma turbulence model. Finally, the numerical results show that the transmission performance of the proposed system is highly sensitive to atmospheric turbulence and MAI. For comparison, the OOK and PolSK for the OCDMA-FSO link performance have also been presented. This theoretical study provides an all-optical CDMA-FSO system structure based on the PolSK modulation scheme, which takes into consideration the significant influence and limitation factors. I should mentioned that the work of this chapter is reference to my previous paper, which published on [69].

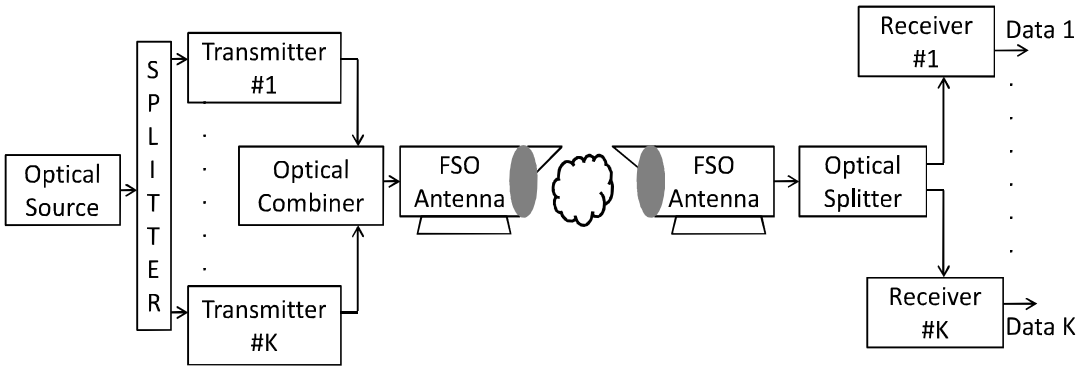

FIGURE 4.3: PolSK modulated OCDMA systems over turbulent FSO links. *by F.BAI, performance analysis of polarization modulated direct-detection optical CDMA systems over turbulent FSO links modeled by the gamma-gamma distribution, MDPI, Photonics [69].*

4.2 Analysis of PolSK Modulated OCDMA Systems Over Turbulent FSO Links

4.2.1 System Model

The focus of this subsection is to establish an analytical model that is able to characterize the polarization-modulated optical CDMA signal propagation through turbulent FSO links. Considering the main effect of atmospheric turbulence is irradiance fluctuations, known as scintillation. For covering a wildly range of turbulence strength, the Gamma-Gamma distribution has been adopted in this analysis. It should note that the modified prime codes (MPCs) with the auto-correlation and cross-correlation value bounded by one as serving for spreading code in this analysis. The modified prime code is characterized by its code length $F = p^2$; the code weight $W = p$. The cardinality of MPC is defined p^2, and the p is a prime number [83]. The configuration of proposed system is shown in Figure 4.3 [69].

Next, a detailed theoretical model for describing the OCDMA signals transmission processing by PolSK modulation will be provided. Since a laser beam with a fully polarized SOP generated by a laser diode and propagating along the z-axis can

be described as equation 4.1 and 4.2. In this work, assuming for simplicity that the laser beam is set to be linearly polarized at an angle of $\pi/4$ ($\theta = 45^0$) with respect to the transmitter reference axis. The linearly polarized beam is divided into horizontal and vertical SOPs with equal amplitude ($A_x = A_y$) and zero phase difference ($\Delta\varphi = \varphi_y - \varphi_x = 0$) at the output of the polarization beam splitter (PBS). Then, the SOP of the input beam is switched between two orthogonal states by the optical phase modulator, which refer to 0^0 to 180^0 ($\Delta\varphi = 0 or \Delta\varphi = \pi$). The N times per bit is according to the modified prime code mapping the optical signal into CDMA format. Then, the emitted PolSK-modulated electrical field vector at the polarization beam combiner (PBC) output is given as [69]:

$$E_{T.k}(t) = \sqrt{\frac{P_t}{2}} exp\left[j\left(\omega_s t + \varphi_s\right)\right]\left\{\hat{x} + exp\left(j\Delta\varphi S_k(t)\right)\hat{y}\right\} \tag{4.9}$$

where $S_k(t)$ denotes the CDMA signal, and P_t with being the transmitted optical power. Moreover, the use of Jones notation for representing the electrical field vector can be defined as [84]

$$J = \begin{bmatrix} E_x & E_y \end{bmatrix}^T \tag{4.10}$$

where J is Jones matrix, and in the case of two SOPs ("1" or "0") can be express by J_H and J_Y are orthogonal if their inner product is zero as mentioned in [84]. For the binary PolSK modulation scheme, the data bits mpped into the Jones vectors when the angle of one polarization component is switched relative the other between two angles. Therefore, the k-th user SOP-encoded OCDMA signal with the first user as the desired one, defined as [69]:

$$J_k(t) = \begin{cases} J^0 & \text{if } d_k(t) XOR c_k(t) = 0 (\Delta\varphi = 0) symbol"0" \\ J^1 & \text{if } d_k(t) XOR c_k(t) = 1 (\Delta\varphi = \pi) symbol"1" \end{cases} \tag{4.11}$$

where XOR represented the exclusive disjunction operation. Thus, the emitted optical signal represented by the Jones vector for "0" and "1", are given as:

$$J^0 = \frac{1}{\sqrt{2}}[11]^T \tag{4.12}$$

$$J^1 = \frac{1}{\sqrt{2}}[-11]^T \tag{4.13}$$

Hence, complex Jones matrix with unit determinant is derived as:

$$Q = \begin{bmatrix} J^0 & J^1 \end{bmatrix} \tag{4.14}$$

Finally, each user modulated signal is combined together by the optical combiner. Consequently, the received optical signal suffers from several impairments, including the channel attenuation, such as beam divergence and turbulence-induced scintillation. Thus, the received composite signal at the output of splitter by the Jones vector notation can be described as [69]:

$$J_r(t, X) = \begin{bmatrix} E_{r.x} & E_{r.y} \end{bmatrix}^T = J_1(t, X) + \sum_{k=2}^{K} J_k(t, X) + J_{FSO}(t) \tag{4.15}$$

where the first and second elements are represented the data from the intended user and interference by other users, and $J_{FSO}(t)$ denotes the Jones vector of AWGN. The X quantifies the variation of signal fading, as mentioned earlier, and its PDF is defined by Equation 2.13. As shown in Figure 4.4, the changing of SOP due to the turbulence effect is compensated by the polarization controller, whose function is to ensure that the received signal at the receiver side has the same SOP reference axis as reported in [85]. Then, the received composite signal passes through the PBS and divided into upper and lower branches. In the case of signal processing, the received signal of each branch is correlated through the optical correlator device. This processing can be described as, considering the if a coded signal with the correct codeword arrives, the optical correlator is tuned to the intended user's assigned spreading code to de-spreading the CDMA format signals, and thus the

auto-correlation function achieves a high peak value. However, conversely, for an incorrect codeword, a cross-correlation is generated with increased the MAI as mentioned in [86]. Hence, the polarizer acts a polarization filter which produces only corresponding to the desired part of polarization components. The the function of each polarizer output is given as [85], [84]:

$$J_P^z(t,X) = \begin{bmatrix} E_{RX}^z & 0 \end{bmatrix}^T = \frac{1}{\sqrt{2}} \left\{ E_{r.x}^z + E_{r.y}^z \right\} \tag{4.16}$$

Next, a mathematical modeling for describing the PolSK modulated optical CDMA signal processing has been established. Firstly, the received signal for a single receiver in the presence of turbulence effect, is given as [69]:

$$E_R(t,X) = Re\left\{ E_0(t) e^{j(\omega_s t + \varphi_r)} \sum_{k=1}^{K} Q \begin{bmatrix} d_k(t) \\ 1 - d_k(t) \end{bmatrix} P_T(t - kT_S) c_k(t) \right\} \tag{4.17}$$

where $E_R(t,X)$ is proportional to variable X and has the same statistical model, $Re(.)$ denotes the real part, and φ_r with being the phase of the received optical field. The each orthogonal component (x-, y-component) are assumed as being equally amplitude and channel attenuated without the losses of turbulence-induced depolarized. Then, the received signal at the output of polarizer for the upper branch is derived as follow [69],[85]:

$$\begin{aligned} E_{R.x.k}^0(t,X) = \Bigg[& \frac{E_{x.k} + E_{y.k}}{2} + \sum_{k=1}^{K} d_k(t) c_k(t) \\ & \times \frac{E_{x.k} - E_{y.k}}{2} P_T(t - kT_S) \Bigg] cos\left(\omega_s t + \varphi_{x.k}\right) \end{aligned} \tag{4.18}$$

and similarly, the lower branch is given as:

$$\begin{aligned} E_{R.y.k}^1(t,X) = \Bigg[& \frac{E_{x.k} - E_{y.k}}{2} + \sum_{k=1}^{K} d_k(t) c_k(t) \\ & \times \frac{E_{x.k} + E_{y.k}}{2} P_T(t - kT_S) \Bigg] cos\left(\omega_s t + \varphi_{y.k}\right) \end{aligned} \tag{4.19}$$

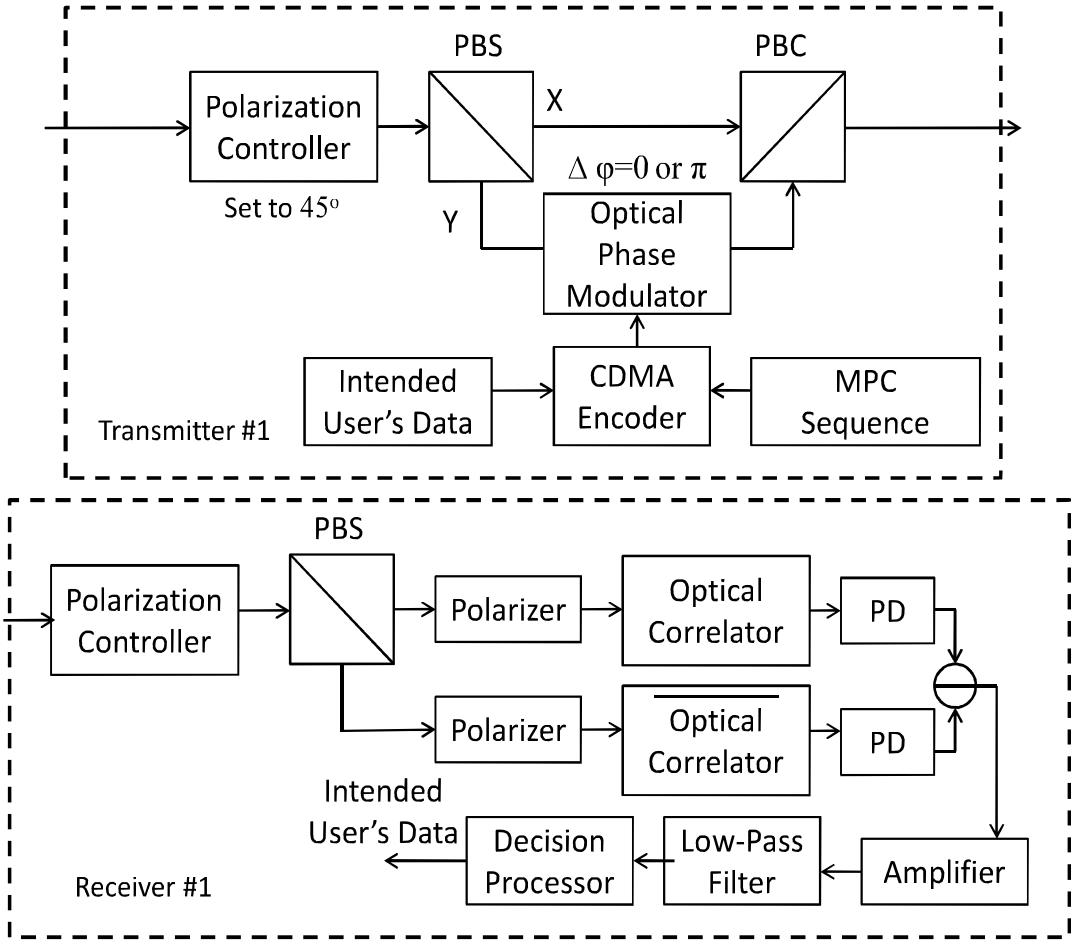

FIGURE 4.4: Block diagram of the proposed system transceiver structure. *by F.BAI, performance analysis of polarization modulated direct-detection optical CDMA systems over turbulent FSO links modeled by the gamma-gamma distribution MDPI, Photonics [69].*

Here, orthogonal components of k-th user based on the equation 4.14, are given as

$$E_{x.k} = J^0 d_k(t) c_k(t) E_0(t) \tag{4.20}$$

and

$$E_{y.k} = J^1 (1 - d_k(t)) c_k(t) E_0(t) \tag{4.21}$$

where $\varphi_{x.k}$ and $\varphi_{y.k}$ represented the phase of the received optical field for each component, respectively. Further, as previous mentioned on optical correlator that spreads the encoded signals by pre-reserving the intended user's assigned spreading code. In the same time, it should note that correlator is set up with the complement of the code (phase shift in π) in the lower branch. With that, the received signals are detected by the balanced detector to generate the different photo currents, and ready for extraction in the following decision processing. Thus, the photo current at a certain symbol duration T_s at the upper branch can be described as [69]:

$$I^0_{R.x} = \Re \int_{t=0}^{T_s} \sum_{n=1}^{N} \frac{c(nT_c)+1}{2} \left(E^0_{R.x.k}(t,X)\right)^2 dt \tag{4.22}$$

and lower branch [69]

$$I^0_{R.y} = \Re \int_{t=0}^{T_s} \sum_{n=1}^{N} \frac{1-c(nT_c)}{2} \left(E^0_{R.y.k}(t,X)\right)^2 dt \tag{4.23}$$

where $\Re$ and $c_k(t-nT_c)$ denote the responsivity of photo detector and n-th chip of the assigned spreading code of the kth user, respectively. Note, the sum term of the functions can be solved as:

$$\left(\sum_{k=1}^{K} a_k\right)^2 = \sum_{k=1}^{K} a_k^2 + \sum_{k=1}^{K} \sum_{j=1, j\neq k}^{K} a_k a_j \tag{4.24}$$

Since the second-order terms in the functions can be filtered out cause of beyond the photo detector frequency range. Then, equation 4.22 and 4.23 based on equation 4.24 can be modified as follow [69],[85]:

$$\begin{aligned} I^0_{R.x} =& \frac{\Re X}{4} \sum_{n=1}^{N} \left\{ \frac{c(nT_c)+1}{2} \left[\sum_{k=1}^{K} \left(E^2_{x.k} + E^2_{y.k}\right.\right.\right. \\ &+ \left.\left.\left. d_k(t)c_k(t-nT_c)(E^2_{x.k} - E^2_{y.k})\right)\right] \right\} + n_0(t) \end{aligned} \tag{4.25}$$

Similarly, the lower branch is given as [69],[85]:

$$\begin{aligned} I^0_{R.y} =& \frac{\Re X}{4} \sum_{n=1}^{N} \left\{ \frac{1 - c(nT_c)}{2} \left[\sum_{k=1}^{K} \left(E^2_{x.k} + E^2_{y.k} \right. \right. \right. \\ & \left. \left. \left. + \; d_k(t) c_k(t - nT_c)(E^2_{x.k} - E^2_{y.k}) \right) \right] \right\} + n_1(t) \end{aligned} \tag{4.26}$$

where the $n_0(t)$ and $n_1(t)$ represent the filtered Gaussian noise. In the following processing at the output of balanced detector, the differential photo current is derived as [69]:

$$\begin{aligned} I_{diff}(t, X) =& I^0_{R.x} - I^1_{R.y} \\ =& \frac{\Re X}{4} \sum_{n=1}^{N} c(nT_c) \sum_{k=1}^{K} \left(E^2_{x.k} + E^2_{y.k} \right. \\ & \left. + \, d_k(t) c_k(t - nT_c)(E^2_{x.k} - E^2_{y.k}) \right) + n_{opt}(t) \end{aligned} \tag{4.27}$$

where total noise $n_{opt}(t)$ includes the thermal noise, shot noise and relative intensity noise (RIN) processes. I assume that first user as the intended user with interference by other users, thus, the equation 4.27 can be modified as:

$$\begin{aligned} I_{diff}(t, X) = & \underbrace{\left[\frac{\Re X}{4} \sum_{n=1}^{N} c(nT_c) \left(E^2_{x.k} + E^2_{y.k} \right) \right.}_{\text{DC current}} \\ & + \underbrace{\frac{\Re X}{4} \sum_{n=1}^{N} c(nT_c) d_1(t) c_1(t - nT_c)(E^2_{x.1} - E^2_{y.1})}_{\text{desired user}} \\ & + \underbrace{\left. \frac{\Re X}{4} \sum_{n=1}^{N} \sum_{k=2}^{K} c(nT_c) d_k(t) c_k(t - nT_c)(E^2_{x.k} - E^2_{y.k}) \right]}_{\text{interference}} + n_{opt}(t) \end{aligned} \tag{4.28}$$

where DC photo current can be filtered in the balanced detector, and second term and third term denote the desired user data with auto-correlation and interference with cross-correlation, respectively.

4.2.2 Signal-to-Noise-Ratio and Bit-Error Ratio Analysis

Now, I derive the expressions of proposed system performance in terms of SNR and BER, which considers the scintillaiton effect and multiple-access interference (MAI) within CDMA users. In the case of IM/DD based FSO link, at the input of single receiver for kth user, the received optical power is written as [69]:

$$P_{r.FSO}(t) = X \cdot P_{r.0}(t) L_{FSO} + n_{FSO}(t) \tag{4.29}$$

where $P_{r.0}(t)$ is the received optical power in the absence turbulence, and $n_{FSO}(t)$ and L_{FSO} denote the AWGN and FSO link losses, respectively, and FSO losses can be expressed as [69]

$$L_{FSO}(dB) = L_{Geo} + L_{point} + L_{vis}, \tag{4.30}$$

where L_{Geo} is geometrical loss, and L_{vis} is channel scattering with low-visibility caused by channel attenuation, L_{point} is the pointing error between the transmitter and receiver antennas. Hence, considering the $\tau_k = 0$, and background light interference can be filtered in bandpass filter (BPF). Generally, the detected photo current at the output of matched filter is given as [69]:

$$\begin{aligned} Z(t, X) = & \int_{t=0}^{T_s} i(t, X) \sum_{n=1}^{N} c\left(nT_c\right) dt \\ = & D(t, X) + I_{MAI}(t, X) + n_{opt}(t) \end{aligned} \tag{4.31}$$

where output photo current of PDs with the noise component is given as [69]

$$i(t, X) = \Re P_{RX} \sum_{k=1}^{K} S_k(t) + n_{opt}(t) \tag{4.32}$$

where $P_{RX} = P_{r.0} X$ denotes the received optical power over the scintillation, $D(t, X)$ and $I_{MAI}(t, X)$ denote the signal from the desired user and the interference component, respectively.

Moreover, I should mentioned that the desired signal as well as interference contribute the average power (K-1 users) to the each PD in the same time. Thus, the AWGN with a double-sided power spectral density of $N_0/2$, and is derived as [69]:

$$\begin{aligned} N_0 =& N_{shot} + N_{th} + N_{RIN} \\ =& 2q\left(P_{RX}\Re\right) + \frac{4K_B T_{abs} F_e}{R_L} + \left(RIN\right)\left(P_{RX}\Re\right)^2 \end{aligned} \tag{4.33}$$

where q and K_B are the electron charge and Boltzmann's constant, respectively, F_e denotes the noise factor, and T_{abs} with being the absolute temperature and R_L denotes the PD load resistance. Here, the proposed FSO link performance in the term of SNR in the presence of turbulence can be expressed as [69]:

$$\begin{aligned} SNR(K, X^2) =& \frac{D\left(t, X\right)^2}{\sigma^2_{I_{MAI}} + \sigma^2_{n_{opt}}} \\ =& \frac{\left[\frac{\Re X}{4}\sum_{n=1}^{N} c(nT_c) d_1(t) c_1(t - nT_c)(E^2_{x.1} - E^2_{y.1})\right]^2}{\left[\frac{\Re X}{4}\sum_{n=1}^{N}\sum_{k=2}^{K} c(nT_c) d_k(t) c_k(t - nT_c)(E^2_{x.k} - E^2_{y.k})\right]^2 + N_0 B} \end{aligned} \tag{4.34}$$

where bandwidth is given as $B = 1/T_s$ and required to pass the signal without distortion.

Then, for the following analysis, I focus on the MPC properties, the auto-correlation denoted by using the $\sum_{n=1}^{N} c(nT_c)c_1(t - nT_c) = p$ in the equation 4.34. In the meantime, the term $\sum_{n=1}^{N} c(nT_c)c_k(t - nT_c) = \lambda_c$ represents the cross-correlation value. As we known, the cross-correlation value is either *zero* or *one*, depending on whether the codes are in the same group or different groups, while only the *one* can cause the interference, which is among the intended user and $(p^2 - p)$ users from the different groups (whole sequences p^2, sequences from the same group of the intend user p) [69],[83].

Further, defining the cross-correlation values as uniformly distributed among interfering users, the PDF of variable λ_c is defined as $P(\lambda_c) = k/p^2 - p$ [69],[85], and k is the number of actively involved multiple users. Therefore, the SNR function is

modified as follow [69]:

$$SNR(K,X^2)=\left(\frac{1}{\left(\frac{K(K-1)}{(p^2-p)p}\right)^2+\frac{16N_0B}{\left(\Re\cdot X\cdot p\cdot d_1(t)(E_{x.1}^2-E_{y.1}^2)\right)^2}}\right) \tag{4.35}$$

In this work, it is important to determine the scintillation effect on the proposed link performance, thus, a averaging error probability for binary PoLSK modulation within turbulence modeled by Gamma-Gamma distribution can be expressed as:

$$\left\langle P_e^{BPolSK}(K)\right\rangle=\int_0^\infty P_e^{BPolSK}(K)P(X)_{G-G}dX \tag{4.36}$$

where condition error probability in the presence of turbulence is given as [79]:

$$P_e^{BPolSK}(K)=\frac{1}{2}exp(\frac{-SNR(K,X^2)}{2}) \tag{4.37}$$

In order to simplify the integral of equation 4.37, a well-known solution in terms of Meijer's G-function $G_{p,q}^{m,n}(.)$ [87], has been proposed. Assuming the $SNR(K,X^2)$ can be approximated by averaging the noises and interference power over scintillation, is derived as [42],[75]:

$$SNR(K,X^2)\approx\frac{\langle S(t,X)^2\rangle X^2}{\left\langle\sigma_{I_{MAI}}^2\right\rangle+\left\langle\sigma_{n_{opt}}^2\right\rangle}\approx\left\langle SNR(K,X^2)\right\rangle X^2 \tag{4.38}$$

Thus, a closed-form error probability for the proposed link becomes [69],[87]:

$$\begin{aligned}\left\langle P_e^{BPolSK}(K)\right\rangle=&\frac{2^{\alpha+\beta-1}}{8\pi\Gamma(\alpha)\Gamma(\beta)}\\&\times G_{4,1}^{1,4}\left(\frac{8\left\langle SNR(K,X^2)\right\rangle}{(\alpha\beta)^2}\Big|\begin{matrix}\frac{1-\alpha}{2},&\frac{2-\alpha}{2},&\frac{1-\beta}{2},&\frac{2-\beta}{2}\\&&0&\end{matrix}\right)\end{aligned} \tag{4.39}$$

Here, the expressions in terms of Meijer's G-function are used following transforms [87]:

$$erfc(\sqrt{x}) = \frac{1}{\sqrt{x}} G_{1,2}^{2,0}\left[x|_{0,1/2}^{1}\right] \tag{4.40}$$

and

$$K_n(x) = \frac{1}{2} G_{0,2}^{2,0}\left[\frac{x^2}{4}|_{n/2,-n/2}^{--}\right] \tag{4.41}$$

4.2.3 Outage Probability Analysis

The outage probability is an useful way to determine the degradation of link performance in the presence of atmospheric turbulence. Defining as the probability that the instantaneous SNR falls below a special threshold value of SNR, which represented a specified value of the SNR above which the quality of the FSO link is satisfactory. The outage probability for a given threshold SNR_{th} is defined as [69]:

$$\begin{aligned} P_{out}(SNR_{th}) &= P_r(SNR(K, X^2) < SNR_{th}) \\ &= P_r\left(X^2 \langle SNR(K, X^2) \rangle < SNR_{th}\right) \end{aligned} \tag{4.42}$$

I assume a constant C_{th} can be expressed as [69]:

$$C_{th} = \left(SNR_{th} / \langle SNR(K, X^2) \rangle\right)^{1/2} \tag{4.43}$$

Thus, the outage probability is derived as [69]:

$$\begin{aligned} P_{out}(SNR_{th}) &= \int_0^{C_{th}} P_X(X)_{G-G} dX \\ &= \int_0^{C_{th}} \frac{2(\alpha\beta)^{\frac{\alpha+\beta}{2}}}{\Gamma(\alpha)\Gamma(\beta)} X^{\frac{\alpha+\beta}{2}-1} K_{\alpha-\beta}(2\sqrt{\alpha\beta X}) dX \end{aligned} \tag{4.44}$$

TABLE 4.1: Numerical parameters. *by F.BAI, performance analysis of polarization modulated direct-detection optical CDMA systems over turbulent FSO links modeled by the gamma-gamma distribution, MDPI, Photonics [69].*

Parameters	**Value**
Link distance L	1000 m
Channel bandwidth B	2 GHz
Operating wavelength λ	1550 nm
Aperture diameter D	100 mm
Coupling losses L_{point}	3 dB
Beam divergence Θ	$\pm$0.75 rmad
Relative intensity noise RIN	$-$130 dB/Hz
Absolute temperature T_{abs}	300 k
PD responsivity ρ	0.9 A/W
Electron charge q	1.602×10^{19} C
Noise figure F_e	2 dB
PBS/PBC loss	2 dB
Atmospheric attenuation L_{vis}	1 dB
Geometrical loss L_{Geo}	1 dB

Similar to the above solution by closed-form in term of Meijer's G-function, thus, the equation 4.44 becomes:

$$P_{out}(SNR_{th}) = \frac{(\alpha\beta)^{\frac{\alpha+\beta}{2}}}{\Gamma(\alpha)\Gamma(\beta)} C_{th} G_{1,3}^{2,1}\left(\alpha\beta C_{th}\Big|_{\frac{\alpha-\beta}{2},}^{1-\frac{\alpha-\beta}{2}}{}_{\frac{\beta-\alpha}{2},}^{\ }{}_{\frac{\alpha+\beta}{2}}\right) \tag{4.45}$$

4.3 Numerical Results and Discussions

In this section, I focus on evaluating the overall proposed system performance in terms of BER and outage probability, taking into consideration the turbulence-induced scintillation and MAI effects. The main numerical parameters in following calculation are shown in Table 4.1 [69].

Since the behavior of the OOK-modulated OCDMA FSO system has already been investigated in several works [88], I prefer to give a performance comparison between the proposed system and OOK-based system under the same link conditions. Hence, it should note that OOK-based OCDMA FSO system employing a fixed threshold

in this analysis. Figure 4.5 plots the error probability versus the electric SNR for both of PolSK- and OOK- (fixed threshold of 0.5) OCDMA systems over turbulent FSO links when the number of active users $K = 1$ (no interference) and $K = 30$, respectively, and prime code parameter $p = 13$ [69]. It is observed that the BER performance degradation within the variation of turbulence levels, and OOK displaying the worst case scenario. For a BER of 10^{-6} and scintillation parameters $\alpha = 11.6, \beta = 10.1$ as a weak turbulent regime, the SNR for PolSK and OOK are about 24.5 dB and 33 dB, respectively. When the scintillation parameters are changed to $\alpha = 2.1, \beta = 1.3$ as a strong turbulent regime, a lower SNR is required for PolSK compared with OOK at the same BER level. Thus, based on these numerical results illustrated in this plot, it determined that the information encoded in the intensity of the carrier signal is much more prone to turbulence-induced fluctuation. In other words, PolSK scheme offers an improved link performance compared to OOK across the whole turbulence regimes [69].

To give an insight in efficiency of the proposed technique in this analysis, Figure 4.6 shows the variation of BER performance against the received optical power P_r [69]. In this case, the number of active users is $p^2 - p$ which defined the total of the interfering users when the prime number is given a fixed value $p = 13$. The effect of the turbulence on the average BER is obvious, as the scintillation index increases. For instance, a single active user system with average $BER = 10^{-3}$, $P_r = -30$ dBm, without turbulence outperforms the weak turbulence $(\alpha, \beta) = (11.6, 10.1)$ and strong turbulence $(\alpha, \beta) = (2.1, 1.3)$ by approximately 4 dBm and 20 dBm, respectively. Hence, three cases of the number of simultaneous active users have been considered, represented by $K = 1$, $K = 25$ and $K = 45$, as the single user, 15% and 30% of the full-load in the proposed scheme, respectively. As it apparent from the graph, the result determines that the proposed system able to support 15% of the active users to provide a high transmission performance, *i.e.*, $BER = 10^{-8}$ with received optical power $P_r = -18$ dBm in the weak turbulence. However, when the system accommodates 30% of all users, the system is unable to

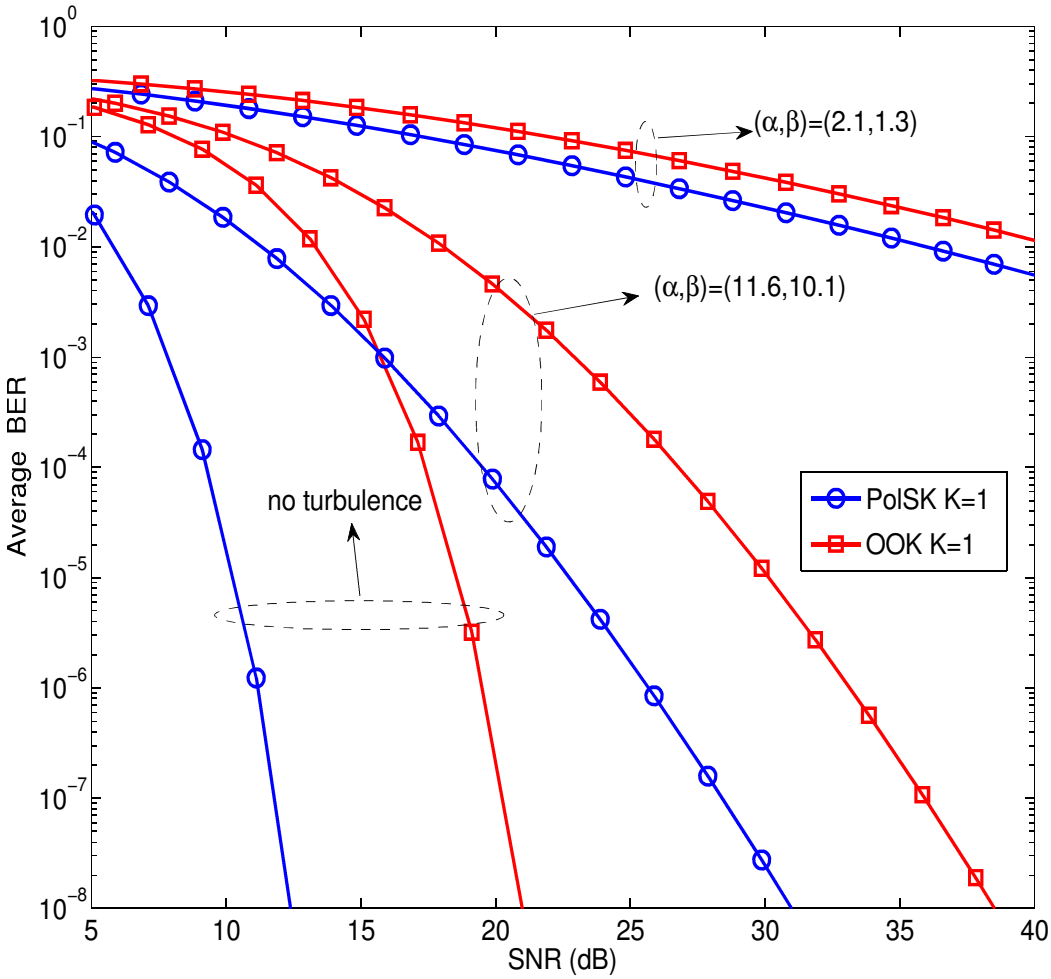

FIGURE 4.5: Performance comparison between the PolSK- and OOK-based OCDMA systems over turbulence channel. *by F.BAI, performance analysis of polarization modulated direct-detection optical CDMA systems over turbulent FSO links modeled by the gamma-gamma distribution, MDPI, Photonics [69].*

guarantee a reliable communication service in the whole of the turbulence regime due to MAI as a dominate noise under this condition. These results indicate that the system performance is highly sensitive to the atmospheric turbulence and also requires higher received optical power to overcome the BER degradation caused by MAI at the same time.

To highlight the impact of MAI on the overall system load performance, further, I conduct a study on the capacity performance when the large number of active users shared in the same channel, as shown in Figure 4.7. In this analysis, in the case of received optical power $P_r = -20$ dBm, the system accommodates the variation

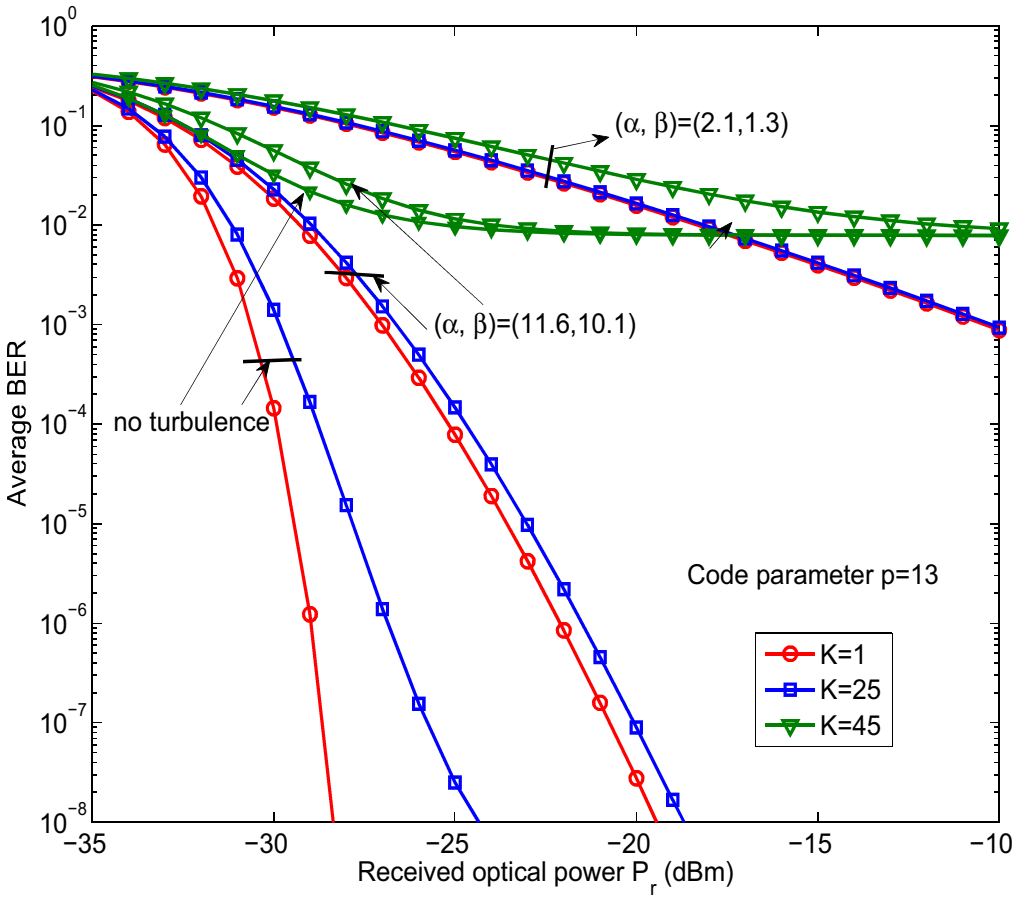

FIGURE 4.6: BER performance against received optical cross the whole turbulence regimes, $K = 1$, $K = 25$ and $K = 45$. *by F.BAI, performance analysis of polarization modulated direct-detection optical CDMA systems over turbulent FSO links modeled by the gamma-gamma distribution, MDPI, Photonics[69].*

number of active users, with prime number parameters $p = 5$, $p = 11$, $p = 13$, $p = 17$. In fact, the prime code corresponding to the code-set cardinality p^2 is the main limiting factor of the number of supporting active users. From the graph, the BER performance improved by p increases due to heavier code weight p and longer code length p^2. Furhter, the larger of the p is closely related to the higher auto-correlation peaks or lower hit probabilities [83]. The BER performance gets worse as K increases with respect to the strong mutual interference and, therefore, is unable to guarantee a reliable communication performance for larger active users, as the previous analysis in Figure 4.6 [69]. Under the different turbulence strength regimes,

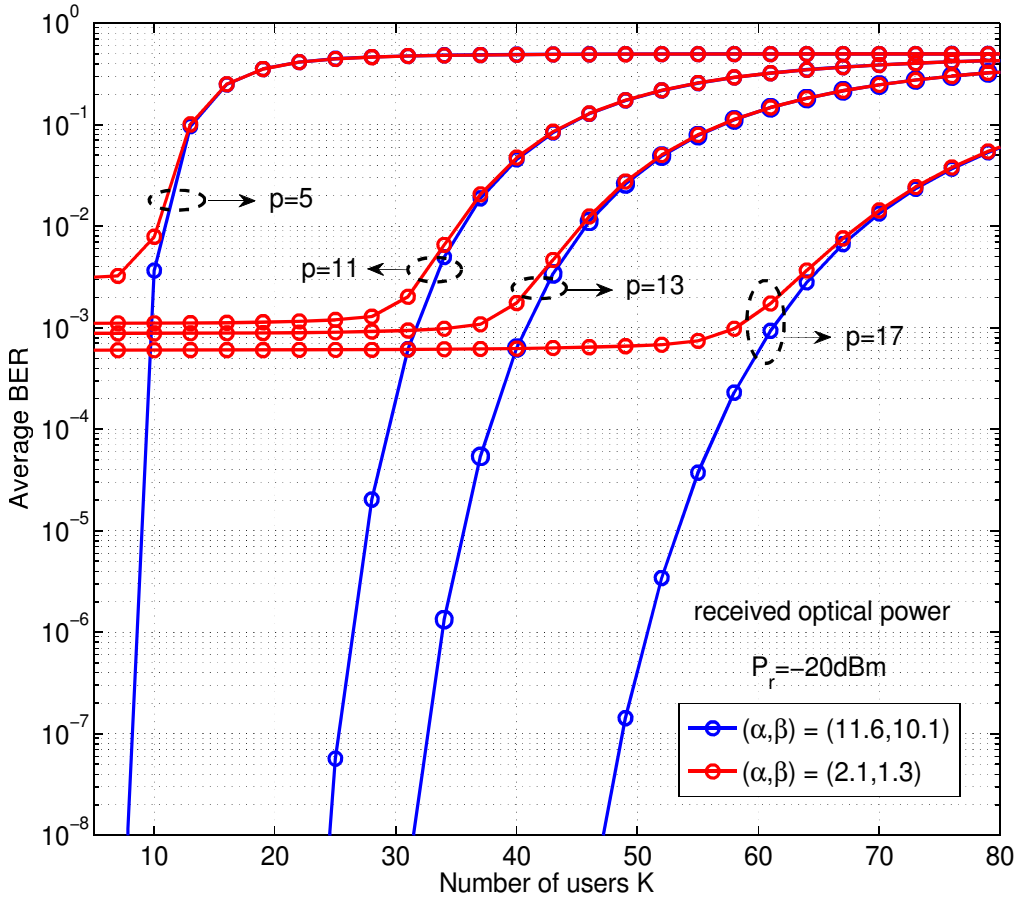

FIGURE 4.7: Average BER performance versus the number of active users K with different prime number p in the presence of turbulence. *by F.BAI, performance analysis of polarization modulated direct-detection optical CDMA systems over turbulent FSO links modeled by the gamma-gamma distribution, MDPI, Photonics[69].*

the impact of optical scintillation on the system BER performance is observed, especially when the signal propagates through the strong turbulent channel: $(\alpha, \beta) = (2.1, 1.3)$. These results indicate that the system employed a greater number of users, leading to growing interference, however, a larger prime number p can be adopted to guarantee a reliable link performance when the system accommodates a large number of users.

Next, an analysis of system outage probability P_{out} by using Equation 4.45 has been provided. Figure 4.8 shows the variation of the outage probability P_{out} versus a single user with different SNR thresholds (SNR_{th}) in both the weak and strong

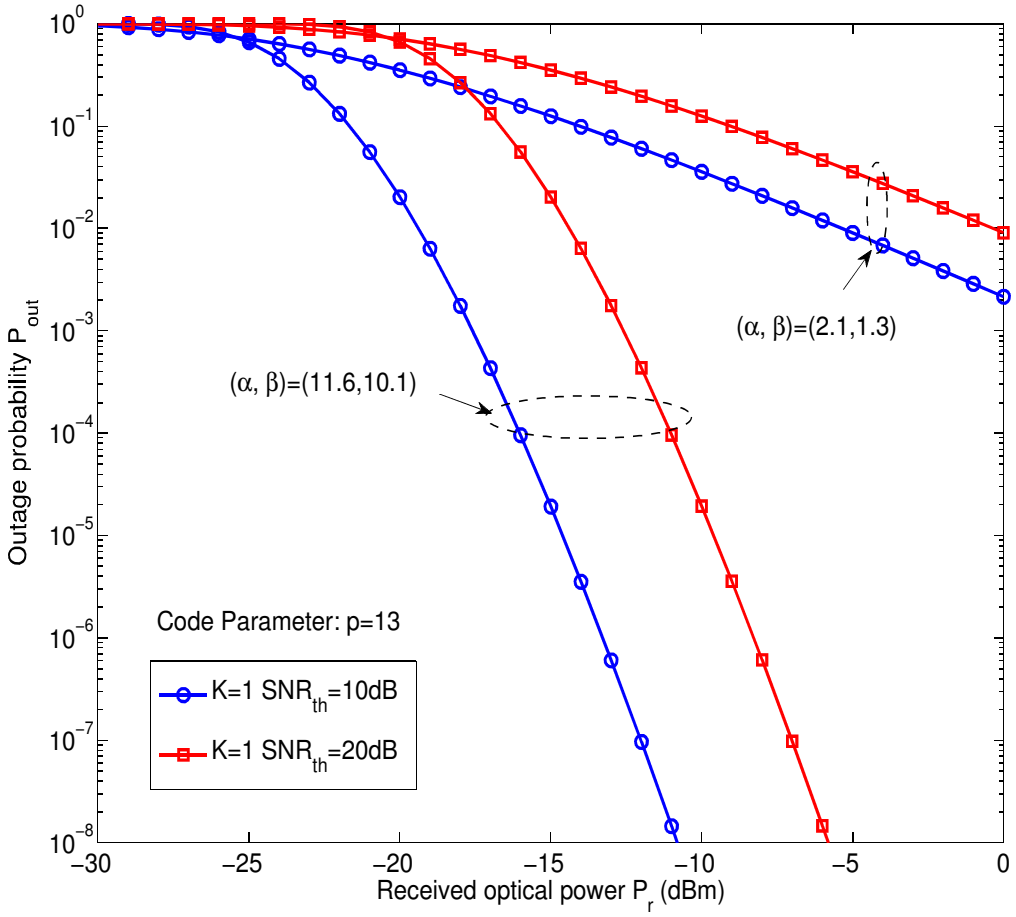

FIGURE 4.8: Outage probability P_{out} against received optical power, when SNR_{th} = (10 dB, 20 dB), $K = 1$ in the presence of turbulence. *by F.BAI, performance analysis of polarization modulated direct-detection optical CDMA systems over turbulent FSO links modeled by the gamma-gamma distribution, MDPI, Photonics [69].*

turbulence regimes, the prime number is $p = 13$ [69]. Two cases of the SNR threshold level have been considered, SNR_{th} = (10 dB, 20 dB), respectively. Obviously, the outage probability is similar to the BER performance under the turbulence fluctuation. We can see clearly that the outage probability is affected by the atmospheric turbulence and required more received optical power to achieve a better link performance. For instance, when the system $P_{out} = 10^{-2}$ and $SNR_{th} = 10$ dB, the received optical power is close to -19 dBm in weak turbulence compared to -5 dBm in strong turbulence. In fact, system outage probability is also highly dependent on the effect of turbulence fluctuation. Besides, for the received optical power

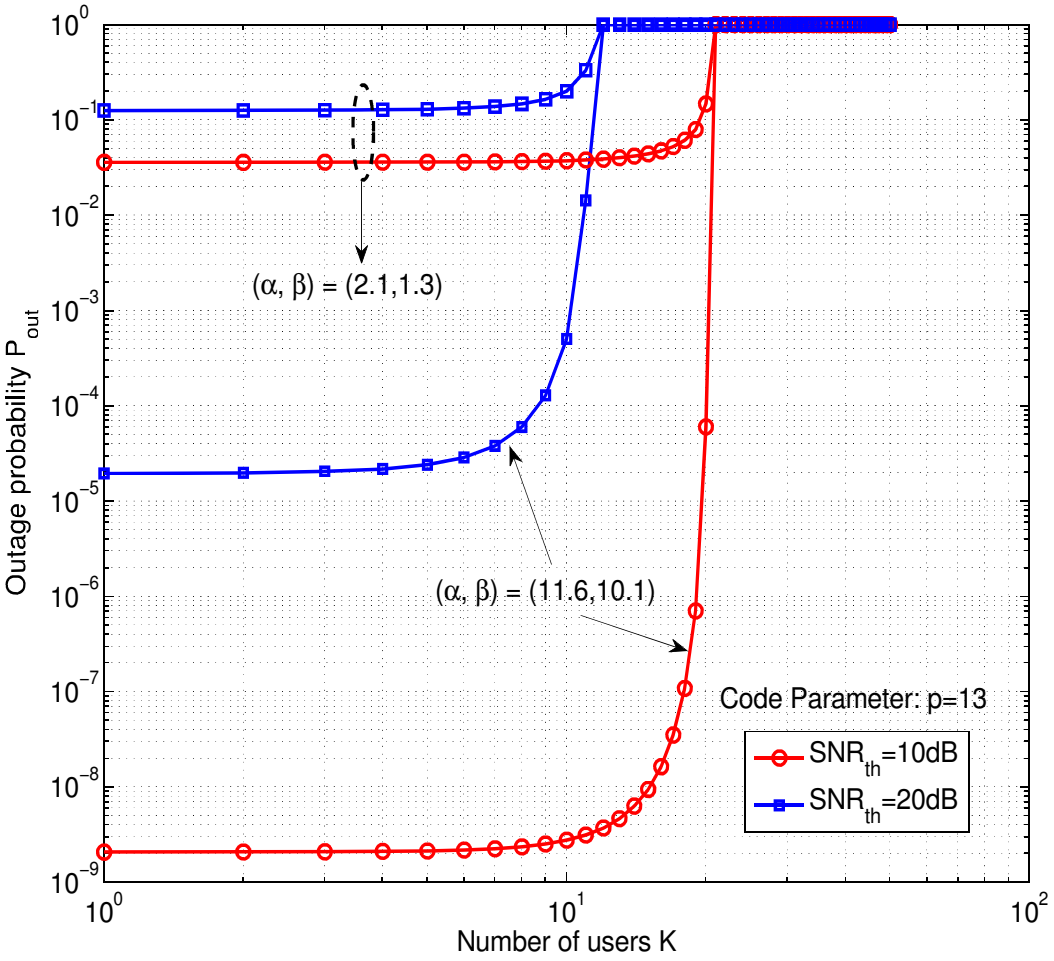

FIGURE 4.9: Average BER performance versus the number of active users K with different prime number p in the presence of turbulence. *by F.BAI, performance analysis of polarization modulated direct-detection optical CDMA systems over turbulent FSO links modeled by the gamma-gamma distribution, MDPI, Photonics [69].*

$P_r = -15$ dBm, the outage probability is close to 10^{-5} and 10^{-2} for $SNR_{th} = 10$ dB and $SNR_{th} = 20$ dB, respectively. Note the number of active users $K = 1$ in this analysis, which means that the system only suffered from the impact of turbulence fluctuation without MAI.

Finally, Figure 4.9 shows the variation of the outage probability as a function of the number of users K with the SNR threshold level at $SNR_{th} = (10$ dB, 20 dB), a fixed prime parameter $p = 13$ in both the weak and strong turbulence regimes [69]. It can be observed that the outage probability gets worse with increasing the number

of active users, due to the increase of MAI effect. In order to tolerate the large number of active users and provide reliable communication service, a longer code is necessary. Hence, the graph also shows the impact of atmospheric turbulence on the outage probability performance. For the number of active users $K = 20$, the outage probability increases from $P_{out} = 10^{-3}$ $P_{out} = 10^{-1}$ for the weak turbulence and strong turbulence regime with the same SNR threshold, $SNR_{th} = 20$ dB, respectively.

4.4 Conclusion

In this chapter, a theoretical model based on polarization modulated OCDMA systems over an atmospheric FSO link, considering the MAI and scintillation effects, have been discussed. A mathematical model for characterizing the PolSK-OCDMA signal processing, in term of Meijer's function is presented. Different from the optical fiber medium, this analysis results demonstrated that the PolSK-OCDMA FSO system transmission performance is sensitive to the optical scintillation caused by atmospheric turbulence. Moreover, important performance metric parameter, such as the prime number p, have been measured and analyzed to evaluate and quantify the influence of MAI effects on the proposed system. The obtained results indicate that a large number of active users can degrade the system performance due to the effect of MAI, while a larger prime number can potentially improve the overall system performance. Finally, I also conclude that the choice of PolSK modulation for the design of the FSO system is an optimum method for the mitigation of channel fading, which obtained from a comparison with internal modulation (i.e., OOK) based FSO Link.

Chapter 5

PolSK-Based OCDMA Systems with Heterodyne Detection over Turbulent FSO Links

5.1 Introduction

Recently, various PoLSK schemes-based FSO link have been adopted in [79],[65], depending on its stable properties compared to the amplitude and phase when the light beam propagating under turbulence. Several results show that PolSK modulation offers an effective method for reduction of turbulence effect, especially in the strong turbulence regime.

Immediately following the above discussed in Chapter 4, alternatively, a heterodyne detection (coherent detection) technique has been proposed in OCDMA-FSO link in the presence of turbulence. The reason for this proposal is to cover the shortage of directly-detected FSO systems in overcoming the impact of turbulence, enhance the power efficiency, thus, the use of heterodyne detection as a countermeasure has been reported in [79], [89], which has been demonstrated that heterodyne detection can

TABLE 5.1: Comparison between homodyne detection and heterodyne detection.

	Homodyne detection	Heterodyne detection
Detection method	Directly by modulating the optical signal to baseband	Optical signal is converted to an electrical signal with IF
Challenges	Unstable, Costly	Phase compensation
Minimum PD bandwidth	BW	$BW + \omega_{IF} \approx 2BW$

offer a better background noise rejection and increased detector sensitivity compared to direct detection, leading to a potential for channel fading reduction, especially at the high value of turbulence strength [89].

Hence, a conclusion on comparison between the coherent detection and direct detection schemes is given as follow: a coherent detection by using the local oscillator within a sufficient power achieves the shot-limited receiver sensitivity and provides a signal gain; Compared with direct detection system, the receiver sensitivity can be improved by using the phase detection (polarization states), a coherent receiver only selects the polarization components of the received optical signal that match the polarization of the LO and rejects the others.

Back to the theory of coherent FSO communications. I should noted that the "coherent" used in this work as a FSO system where a local oscillator light beam is combined with the incoming the received optical signal, then, produce an AC photo current signal. Different from the direct detection, this AC term is proportional to the received optical signal electric field [90]. On the contrary way, the AC part is proportional to the optical power in the direct detection scheme. In general, coherent detection can be divided into two categories, homodyne detection and heterodyne detection, respectively. The use of homodyne detection for converting the received optical signal where demodulated signal is directly to the baseband, LO frequency is synchronized to the optical signal carrier frequency [91]. Hence, a simplify coherent detection known as heterodyne detection which combined optical signal is converted to an electrical signal with intermediate frequency (IF). The Table 5.1 shows the comparison between the homodyne and heterodyne detection.

For the motivation given above, such a study to combine the PolSK-modulated OCDMA systems and heterodyne detection is important in optimizing the solution to enhance the FSO link performance in the terms of high transmission capacity and compensation for turbulence mitigation. This chapter aims at demonstrating the potential of the proposed system in overcoming the degradation of signal quality, taking into consideration the turbulence-induced signal fading and interference noise. Moreover, a performance comparison between heterodyne detection and direct detection applied on OCDMA-FSO link has been also discussed. I should mentioned that the work of this chapter is reference to my previous paper, which published on [91].

5.2 Performance Analysis of Heterodyne Detection PolSK-OCDMA FSO Systems

5.2.1 System Model

In this subsection, a novel receiver configuration deploying the heterodyne detection has been proposed. The focus of this section is to establish an analytical model that is able to characterize the polarization-modulated optical CDMA signal through heterodyne detection FSO link, taking into account the turbulence-induced scintillation and MAI. Additionally, a closed-form expression in terms of BER and outage probability by Meijer's-G function have been provided. A wildly accepted turbulence model, Gamma-Gamma distribution which provides a accurately description for variation of irradiance intensity over weak to strong turbulence regime. I noted that this turbulence model is defined spherical wave model with aperture averaging (AA). The modified prime code used in this work, and characterized by its code length $F = p^2$; the code weight $W = p$. The cardinality of MPC is defined p^2, and the p is a prime number.

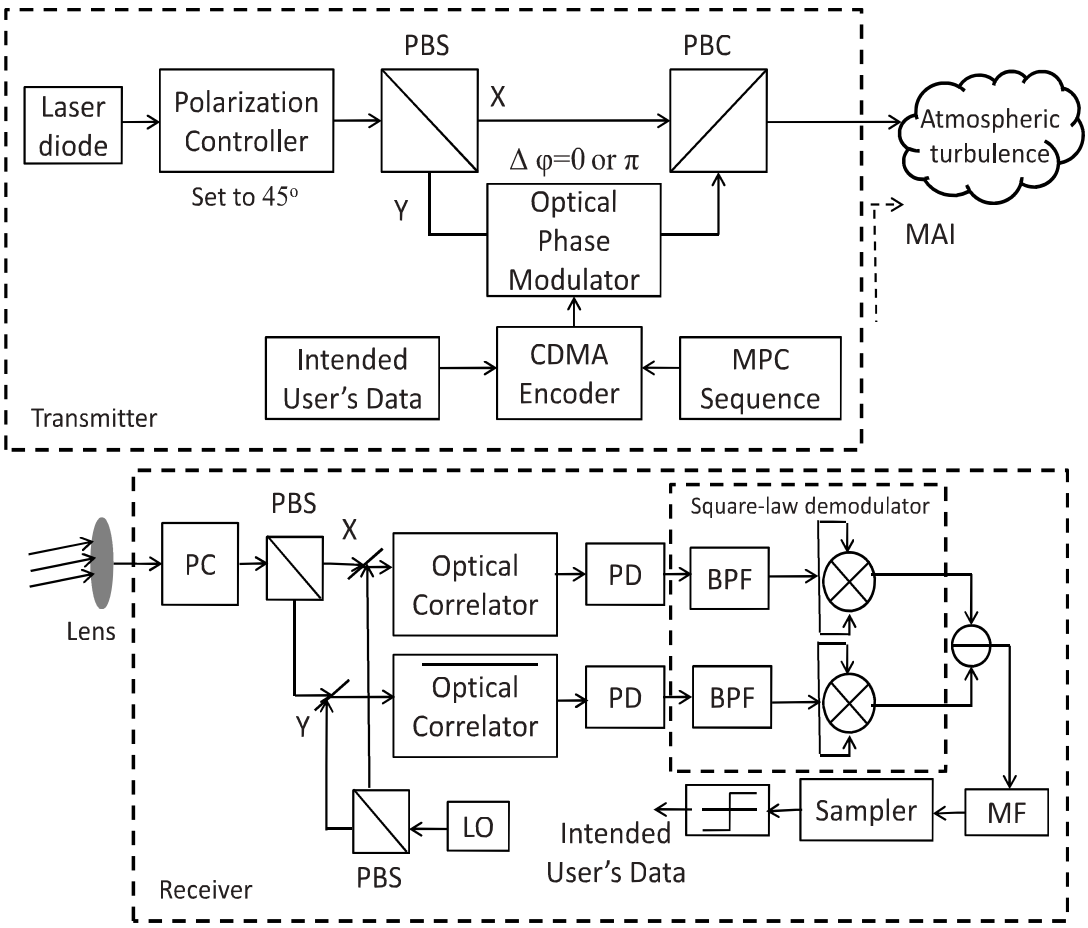

FIGURE 5.1: Heterodyne detection PolSK-OCDMA FSO link. *by F.BAI, performance analysis of heterodyne-detected OCDMA systems using PolSK modulation over a free-space optical turbulence channel, MDPI, Electronics[91].*

The proposed configuration is illustrated in Figure 5.1 [91]. At the transmitter side, the transmitted laser beam is set to be linearly polarized at an angel of $\pi/4$ as a transmitter reference axis by using a polarization controller (PC) and then is fed into the polarization beam splitter (PBS) and split into two equal beams with $\hat{x}$ and $\hat{y}$ polarization components, respectively, while only the $\hat{y}$-component is phase modulated by using a optical phase modulator between zero and π depending on the input data stream as mentioned in chapter 4. Hence, under this assumption, each incoming user's data are encoded by means of an MPC signature sequence and then alternatively mapped into two linear orthogonal states of polarization (SOPs) of the laser beam with a constant envelop.

The propagation signal suffers from the combined effects of the channel fading and interference noise over the atmosphere. The received signal that propagates from the channel can be expressed as $\sum_{k=1}^{K} S_k(t-\tau_k)$, where τ_k, $0 \leq \tau_k \leq T_s$ is the time delay between the desired user and k-th user. Thus, the overall field vectors in the channel is given [91]:

$$E_{channel}(t) = \sum_{k=1}^{K} E_{T.k}(t) \cdot h + E_{FSO}(t) \tag{5.1}$$

where h denotes the channel fading of the propagation path, and can be expressed as [91]:

$$h = L_a L_p X(t) \tag{5.2}$$

where L_a is the atmospheric attenuation, including the rain and visibility losses, L_r and L_v, respectively; L_p denotes the geometric spread and pointing error losses, and $X(t)$ the quantifies variation of the channel fading in terms of optical scintillation due to the turbulence effects and is satisfied with the gamma-gamma turbulence model, as mentioned earlier. $E_{FSO}(t)$ denotes the field vector of additive Gaussian white noise (AWGN), including the background radiation, thermal noise and shot noise. In the analysis to follow, the mathematical modeling for PolSK-OCDMA signal processing based on heterodyne detection is presented. The received composite signal outputs from the $1 \times K$ optical splitter (OS) for a single receiver are expressed as follows [91]

$$\begin{aligned} E_R(t,X) = Re\Big\{ & E_0(t) exp\left[j(\omega_s t + \varphi_r(t))\right] \\ & \times \sum_{k=1}^{K} Q \begin{bmatrix} d_k(t) \\ 1-d_k(t) \end{bmatrix} c_k(t) P_T(t-kT_S) \Big\} \end{aligned} \tag{5.3}$$

In the formula, $Re\{.\}$ represents the real part of $E_R(t, X)$; the electromagnetic filed vector of the k-th user before the external modulation is defined as:

$$E_0(t) = [E_x(t), E_y(t)]^T \tag{5.4}$$

where the overall phase noise is given as [91]:

$$\varphi_r(t) = \varphi_s(t) + \varphi_c(t) \tag{5.5}$$

where $\varphi_c(t)$ representing the phase noise induced from a turbulent channel, $\varphi_s(t)$ denotes the phase information from the transmitter. The turbulence-induced SOP fluctuation is compensated by using the polarization controller (PC), whose function is to ensure that the received optical beam has the same SOP reference axis as the transmitter side. Thus, both of the received orthogonal components are assumed as being equally amplitude and turbulence fluctuated without the loss of orthogonality between the two orthogonal polarizations.

The power of the local oscillator laser source is equally split by the PBS between the x and y component, linearly polarized at $\pi/4$, and thus, the local oscillator (LO) signal $E_{LO}(t)$ of the desired user (e.g., the first user) is given by:

$$E_{LO}(t) = \sqrt{\frac{P_{LO}}{2}} exp\left[j(\omega_{LO}t + \varphi_{LO}(t))\right]\{\hat{x} + \hat{y}\} \tag{5.6}$$

where parameters P_{LO}, ω_{LO} and $\varphi_{LO}(t)$ denote the power, angular frequency and local oscillator phase noise generated from the heterodyne receiver, respectively. The received composite signals in both the upper branch (x-component) and lower branch (y-component) are then coherently combined with the local optical field of $E_{LO}(t)$ in using the 3-dB balanced directional coupler within a balanced intensity coupling ratio; thus, the mixed electric field consequently can be written as:

$$E_{upper}(t, X) = \{E_{R.x}(t, X) + E_{LO.x}(t)\}\hat{x} \tag{5.7}$$

and

$$E_{lower}(t, X) = \{E_{R.y}(t, X) + E_{LO.y}(t)\}\,\hat{y} \tag{5.8}$$

Hence, the received signal at the upper branch after combining with LO can be expressed as:

$$E_{R.x}(t, X) = \left(\frac{E_{x.k} + E_{y.k}}{2} + \sum_{k=1}^{K} d_k(t)c_k(t)\frac{E_{x.k} - E_{y.k}}{2}P_T(t - kT_S)\right) \tag{5.9}$$

and lower branch is given as:

$$E_{R.y}(t, X) = \left(\frac{E_{x.k} - E_{y.k}}{2} + \sum_{k=1}^{K} d_k(t)c_k(t)\frac{E_{x.k} + E_{y.k}}{2}P_T(t - kT_S)\right) \tag{5.10}$$

The orthogonal components of the kth user for the x-component as:

$$E_{x.k} = J^0 d_k(t)c_k(t)E_0(t) \tag{5.11}$$

and y-component as:

$$E_{y.k} = J^1(1 - d_k(t))c_k(t)E_0(t) \tag{5.12}$$

In the regard to the OCDMA signal de-spreading in this proposed system, a simplify device known as optical correlator has been adopted, which correlates the incoming signals in terms of desired user with auto-correlation and interference with cross-correlation as earlier mentioned in chapter 4.

The optical fields are detected by the dual detectors with unit area to generate differential current ready for extraction in the following processing. The outputs of identical dual detectors are passed through electric bandpass filters (BPFs) with a one-sideband bandwidth B_0. Assuming that the BPF bandwidth is larger than the IF line-width to avoid the phase noise to amplitude noise conversion [91],[89], and FSO noise, such as background light interference, can be considered negligible in

this analysis. The photocurrent after removing the direct-current (DC) and high frequency components in the upper branch can be described as [91]:

$$\begin{aligned} I^0_{R.x}(t,X) =& \Re X \sum_{n=1}^{N} \left\{ \frac{c(nT_c)+1}{2} \left[\sum_{k=1}^{K} \sqrt{2P_{LO}} \left(\frac{E_{x.k}+E_{y.k}}{2} \right.\right.\right. \\ &+ \left.\left.\left. d_k(t)c_k(t-nT_c)\frac{E_{x.k}-E_{y.k}}{2} \right) cos(\omega_{IF}t+\varphi_{IF}(t)) \right] \right\} + n_x(t) \end{aligned} \tag{5.13}$$

and the lower branch is similarly as:

$$\begin{aligned} I^1_{R.y}(t,X) =& \Re X \sum_{n=1}^{N} \left\{ \frac{1-c(nT_c)}{2} \left[\sum_{k=1}^{K} \sqrt{2P_{LO}} \left(\frac{E_{x.k}-E_{y.k}}{2} \right.\right.\right. \\ &+ \left.\left.\left. d_k(t)c_k(t-nT_c)\frac{E_{x.k}+E_{y.k}}{2} \right) cos(\omega_{IF}t+\varphi_{IF}(t)) \right] \right\} + n_y(t) \end{aligned} \tag{5.14}$$

where $\Re$ denotes the responsivity of the detector, and frequency of IF signal is given as:

$$\omega_{IF} = \omega_s - \omega_{LO} \tag{5.15}$$

and the phase of IF signal as follow

$$\varphi_{IF}(t) = \varphi_r(t) - \varphi_{LO}(t) \tag{5.16}$$

Then, a square-law demodulator is used to process the photo current $I^0_{R.x}$ and $I^1_{R.y}$, and then the IF noise can be removed, and signal information is recovered [91]. Finally, the differential output between the upper and lower branch over a symbol duration T_s is given by:

$$C_d(t,X) = \int_{t=0}^{T_s} \left(I^0_{R.X}(t,X)\right)^2 - \left(I^1_{R.y}(t,X)\right)^2 dt \tag{5.17}$$

Hence, it noted that the decision signal is sampled at the $t = T_s$ to obtain the variable decision C_d, the decision rule of the final bit d is defined as [91]:

$$d = \begin{cases} 0 & if \quad C_d < 0 \\ 1 & if \quad C_d \geq 0 \end{cases} \tag{5.18}$$

5.2.2 Signal-to-Noise-Ratio and Bit-Error Ratio Analysis

In this subsection, the closed-form expressions for investigating the degree to which proposed system may be expected to be degraded due to the irradiance fluctuation and multiple users interference. Assuming the time delay $\tau_k = 0$ as a synchronized case. Thus, the electric signal in equation 5.17 can be modified as [91]:

$$\begin{aligned} C_d(t, X) \propto & \frac{(\Re X)^2 P_{LO}}{2} \sum_{n=1}^{N} c(nT_c) \\ & \times \sum_{k=1}^{K} \left(d_k(t) c_k(t - nT_c)(E_{x.k}^2 - E_{y.k}^2) \right) + n_{opt}(t) \end{aligned} \tag{5.19}$$

Further, considering the signal components by desired signal and interference, thus, equation 5.18 becomes [91]:

$$\begin{aligned} C_d(t, X) \propto & \underbrace{\frac{(\Re X)^2 P_{LO}}{2} \sum_{n=1}^{N} c(nT_c) d_1(t) c_1(t - nT_c)(E_{x.k}^2 - E_{y.k}^2)}_{\text{desired user data}} \\ & + \underbrace{\frac{(\Re X)^2 P_{LO}}{2} \sum_{n=1}^{N} \sum_{k=2}^{K} c(nT_c) d_k(t) c_k(t - nT_c)(E_{x.k}^2 - E_{y.k}^2)}_{\text{MAI}} + n_{opt}(t) \end{aligned} \tag{5.20}$$

In this expression, the link noise process n_{opt} which includes the shot noise and thermal noise, is given by:

$$\begin{aligned} \sigma_{opt}^2 =& \sigma_{shot}^2 + \sigma_{th}^2 \\ =& 2q\Re(P_{LO} + P_R)B_0 + \frac{4K_B T_{abs} F_e B_0}{R_L} \end{aligned} \tag{5.21}$$

where q and K_B are the electron charge and Boltzmann's constant, respectively, T_{abs} denotes the absolute temperature and F_e and R_L represent the noise factor and load resistance, respectively. Particularly, the power of LO is assumed to be sufficiently high compared to the received signal power, $P_{LO} \gg P_R$, where P_R is characterized by the received optical power. The shot noise can then be calculated as

$$\sigma_{shot}^2 \approx 2q\Re P_{LO} B_0 \tag{5.22}$$

Finally, the signal-to-noise ratio (SNR) is derived as:

$$\begin{aligned} SNR(K,X) &= \frac{P_d(t,X)}{\sigma_{MAI}^2 + \sigma_{opt}^2} \\ &= \frac{\frac{(\Re X)^2}{2} P_{LO} \sum_{n=1}^{N} c(nT_c) d_1(t) c_1(t-nT_c)(E_{x.1}^2 - E_{y.1}^2)}{\frac{(\Re X)^2}{2} P_{LO} \sum_{n=1}^{N} \sum_{k=2}^{K} c(nT_c) d_k(t) c_k(t-nT_c)(E_{x.k}^2 - E_{y.k}^2) + \sigma_{opt}^2} \end{aligned} \tag{5.23}$$

where $P_d(t,X)$ is the expected desired signal power in the presence of turbulence.

Similarly, the MPC as the signature code used to determine the auto-correlation and cross-correlation. Thus, same as the previous work results, the equation 5.23 can be modified as [91]:

$$SNR(K,X) = \frac{1}{\left(\frac{K(K-1)}{p(p^2-p)}\right)^2 + \frac{2\sigma_{opt}^2}{(\Re X)^2 \cdot P_{LO} \cdot d_1(t) \cdot (E_{x.1}^2 - E_{y.1}^2)}} \tag{5.24}$$

Next, a closed-form expression for the average bit error probability by the Meijer's-G function, thus, is derived as [87]:

$$\langle P_e \rangle = \frac{2^{(\alpha+\beta)}}{8\pi\Gamma(\alpha)\Gamma(\beta)} G_{4,1}^{1,4}\left(\frac{8\langle SNR(K,X)\rangle}{(\alpha\beta)^2} \middle| \begin{matrix} \frac{1-\alpha}{2}, & \frac{2-\alpha}{2}, & \frac{1-\beta}{2}, & \frac{2-\beta}{2} \\ & 0 & & \end{matrix} \right) \tag{5.25}$$

TABLE 5.2: Numerical parameters. *by F.BAI, performance analysis of heterodyne-detected OCDMA systems using PolSK modulation over a free-space optical turbulence channel, MDPI, Electronics [91].*

Parameters	**Value**
Transmission distance L	1 km
Wavelength λ	1550 nm
Aperture diameter D	150 mm
bandwidth B_0	2 GHz
Absolute temperature T_{abs}	300 k
Detector responsivity $\Re$	0.9 A/W
Electron charge q	1.602×10^{19} C
Noise figure F_e	2 dB
LO optical power P_{LO}	0 dBm
Pointing error loss L_p	1 dB
Visibility loss L_v	0.4 dB [92],[93]

5.2.3 Outage Probability Analysis

Same as the last chapter mentioned, the outage probability as an evaluation method, in term of Meijer's-G function is obtained as [91]:

$$\begin{aligned} P_{out}(SNR_{th}) =& \int_0^{C_{th}} \frac{2(\alpha\beta)^{\frac{\alpha+\beta}{2}}}{\Gamma(\alpha)\Gamma(\beta)} X^{\frac{\alpha+\beta}{2}-1} K_{\alpha-\beta}(2\sqrt{\alpha\beta X})dX \\ =& \frac{(\alpha\beta)^{\frac{\alpha+\beta}{2}}}{\Gamma(\alpha)\Gamma(\beta)} C_{th} G_{1,3}^{2,1}\left(\alpha\beta C_{th}\Big|_{\frac{\alpha-\beta}{2},}^{1-\frac{\alpha-\beta}{2}}{}_{\frac{\beta-\alpha}{2},}^{\ }{}_{\frac{\alpha+\beta}{2}}\right) \end{aligned} \tag{5.26}$$

5.3 Numerical Results and Discussions

The main simulation parameters are shown in Table 5.2 [91]. In this section, I use simulation and numerical analysis to verify the overall performance of the proposed system, taking into account the error probability and outage probability. This analysis uses weak and strong turbulence intensity levels at different Rytov variance values $\sigma = 0.2$ and $\sigma = 5$. The scintillation parameters are $\{\alpha = 11.6, \beta = 10.1\}$, $\{\alpha = 2.6, \beta = 1.3\}$, respectively.

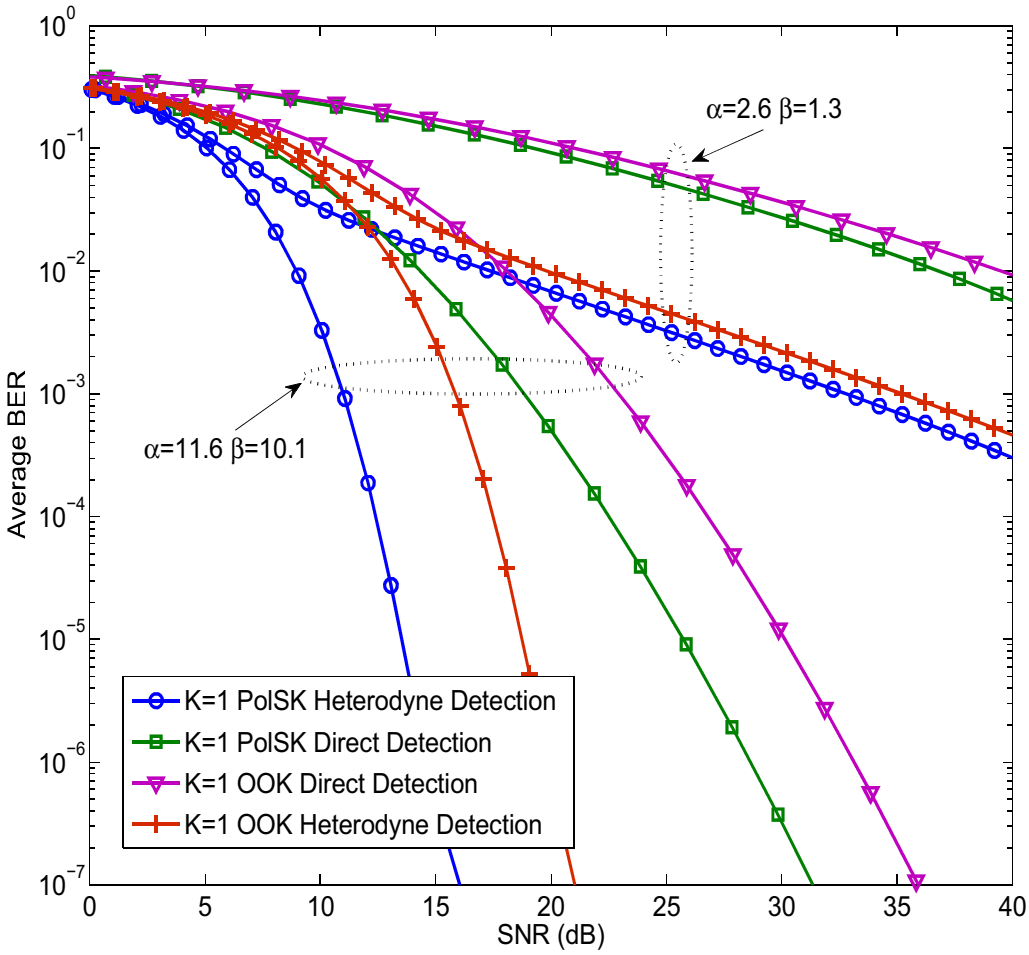

FIGURE 5.2: Average BER versus SNR in both of OOK- and PolSK-based OCDMA-FSO link, when $K = 1$. *by F.BAI, performance analysis of heterodyne-detected OCDMA systems using PolSK modulation over a free-space optical turbulence channel, MDPI, Electronics [91].*

As the performance of OOK-based OCDMA FSO system with and without heterodyne detection has been well studied in several literature, I first prefer to give a comparison between OOK with a fixed threshold detection and PolSK modulation under the same link conditions. Figure 5.2 shows the numerical results of the relationship between the electrical SNR and BER when the single OCDMA user with modified prime code parameter $p = 13$ and without MAI noise [91]. It is seen that the system average error probability increases as the turbulence strength increases, with link performance under strong turbulence showing the worst case scenario. For

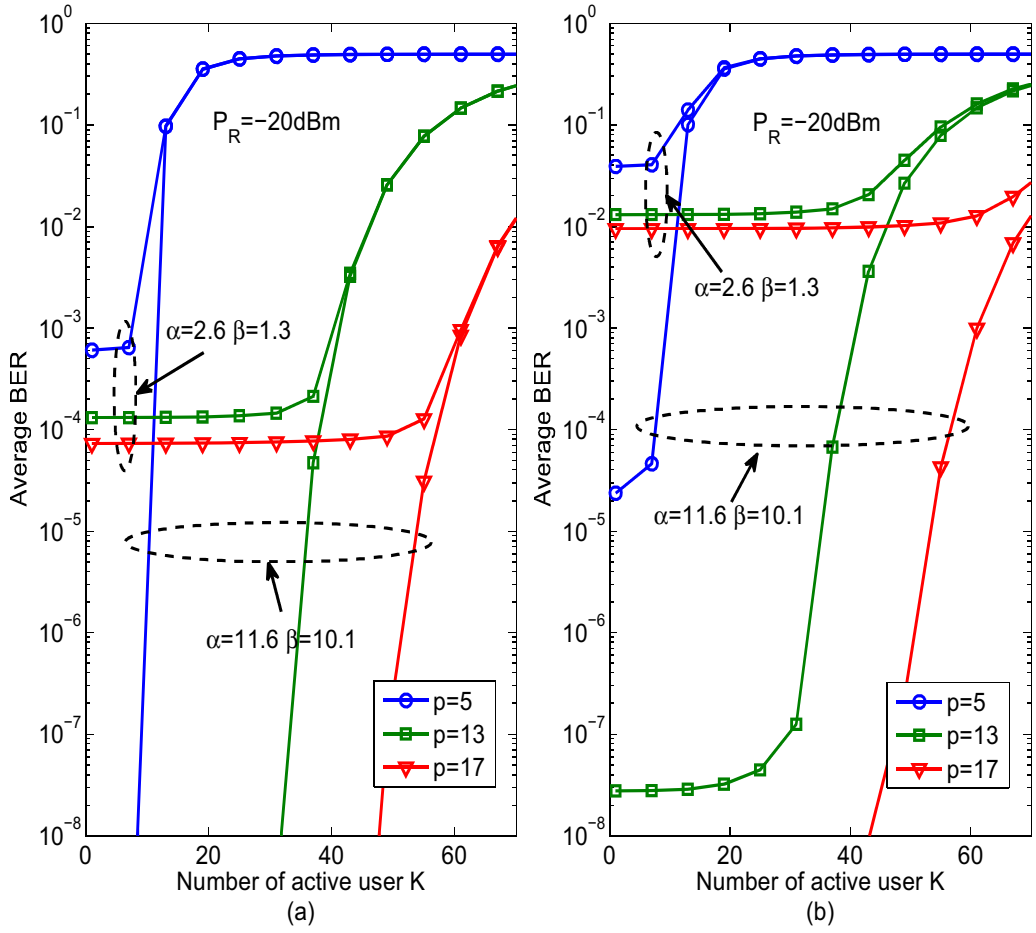

FIGURE 5.3: Average BER versus variation of number of users when $P_R = -20$ dBm in the presence of turbulence, (**a**) Heterodyne detection; (**b**) direct detection. *by F.BAI, performance analysis of heterodyne-detected OCDMA systems using PolSK modulation over a free-space optical turbulence channel, MDPI, Electronics [91].*

instance, when $SNR = 16$ dB for the proposed system, the average BER performance is 1×10^{-7}, 2×10^{-2} under weak and strong turbulence regimes, respectively. At the same time, it is recognized that the proposed system offers the optimum performance compared to that of the conventional cases. In addition, the system error probability using the heterodyne detection is significantly improved compared to the direct detection mode, especially considered in the case of turbulence conditions. The average BER of both modulation schemes with heterodyne detection can be lower by one order of magnitude than the case of the direct detection in

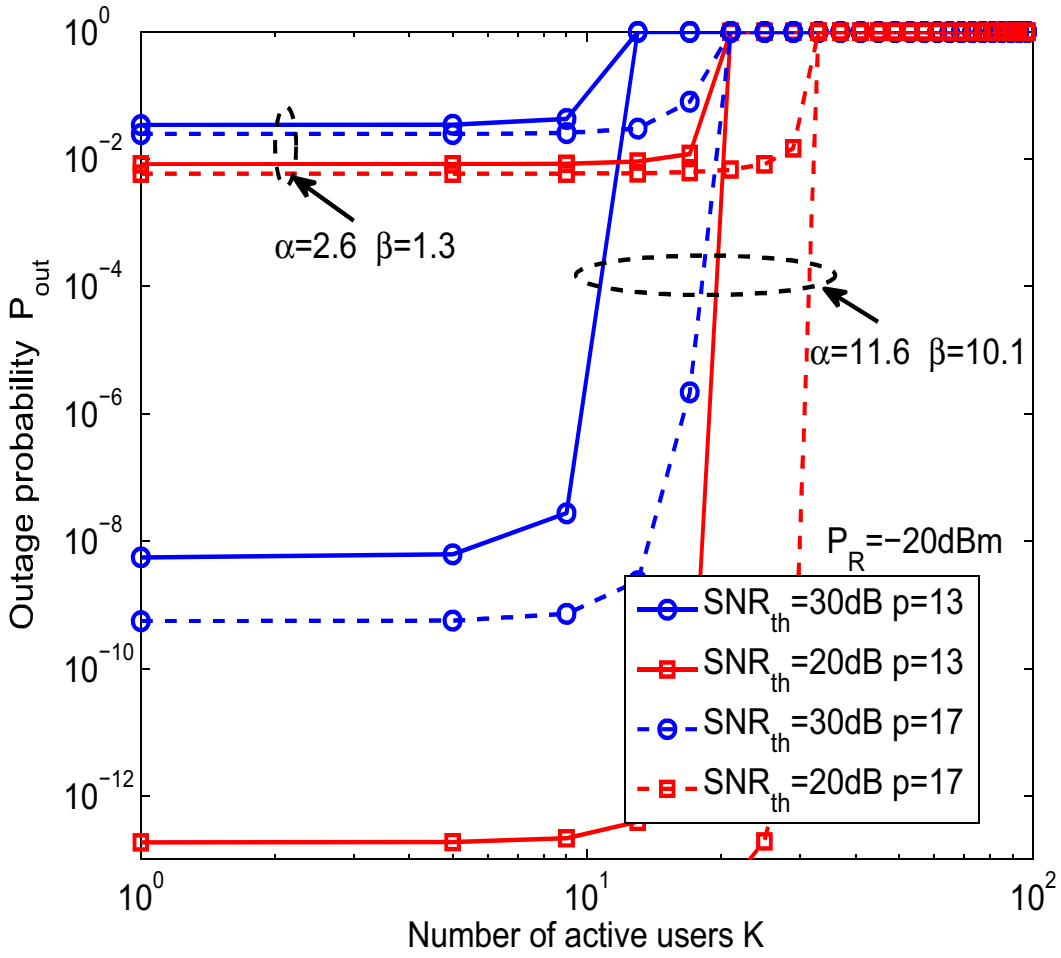

FIGURE 5.4: Variation of the outage probability against number of users, when P_R=-20dBm under turbulence channel. *by F.BAI, performance analysis of heterodyne-detected OCDMA systems using PolSK modulation over a free-space optical turbulence channel, MDPI, Electronics [91].*

the strong turbulence for the same SNR. Furthermore, using the PolSK modulation scheme also displays a better system performance than OOK with a fixed threshold detection. This result can be explained as it was previously studied that polarization states can maintain much more stable properties when propagating through the turbulence channel. The above-mentioned results indicate that combining the PolSK modulation and coherent detection can be used as an efficient method of turbulence mitigation to overcome the link performance degradation.

Next, I present the results that aim at highlighting the limit of MAI noise to the

system load-ability under turbulence effects. The average BER performance against the variation of number of active users with MPC parameters, $p = 5$, $p = 13$ and $p = 17$, respectively, in the different turbulence regimes is shown in Figure 5.3 9 (a) [91]. For the received optical power $P_R = -20$ dBm, the average BER is decreased when the number of active users increases with respect to the strong interference caused by multiple users. In fact, the conventional CDMA system is able to maintain a credible quality of communication when multiple users share the same link, which mainly depends on the code parameter corresponding to the code-set cardinality p^2 [83]. The average bit error probability improved by the larger of the MPC parameters p, which is related to the higher auto-correlation peaks as discussed in [84].

To continue the performance comparison, both the heterodyne detection and direct detection are under the same link conditions, as shown in Figure 5.3 a,b [91]. It is noted that the performance of heterodyne detection outperforms that of direct detection under the same link conditions, especially in the strong turbulence regimes, where the heterodyne detection can be lower by nearly two orders of magnitude than the case of direct detection in terms of the average BER for the same number of active users. Therefore, based on the results illustrated in this plot, we can determine that coherent detection is an attractive alternative to-the direct detection, which offers an efficient way to compensate the turbulence induced channel fading.

Finally, it can be observed that outage probability increases as the number of active users increases, as shown in the Figure 5.4 [91], this is explained as above as being due to the increase of the MAI noise. Two cases of SNR_{th} and prime code parameter p have been considered, $SNR_{th} = (20\text{ dB}, 30\text{ dB})$, $p = (13, 17)$, respectively. For instance, for $SNR_{th} = 20$ dB and $P_{out} = 1 \times 10^{-2}$ with $p = 13$, the number of active users decreases from value $K = 20$ to $K = 12$ across the weak and strong turbulence regimes.

5.4 Conclusion

This work combines the advantages of PolSK modulation and heterodyne detection and proposes an analytical model to characterize the performance of PolSK-based OCDMA systems with heterodyne detection over a turbulent FSO link. I derived the closed-form expressions of the system error probability and outage probability over the gamma-gamma turbulence channel. The MPC parameter as a performance metric has been also considered and quantifies the impact of interference noise on the system load-ability. The conclusions obtained through numerical simulation indicate that the performance of the propose system is highly sensitive to turbulence-induced irradiance fluctuation and the MAI effect; the choice of heterodyne detection receiver offers an improved FSO link performance compared to the conventional cases and provides an effective and promising method for turbulence mitigation in the field of FSO communications.

Chapter 6

Conclusion

6.1 Summary of Thesis

Advanced FSO technologies, has been considered as a promising solution to connect the construction and end user. It offers a number of potential on future high-speed, large capacity applications in both of indoor and outdoor. In this thesis, the work was aimed at analysis the transmission performance of FSO system by advanced turbulence mitigation methods in an atmospheric turbulence channel, taking into consideration the its characteristics and limitations. The goal of this work was also provided comparison with previous proposed systems.

Firstly, giving a brief overview of FSO communications from its fundamentals, features and limitations in chapter 1. Then, the major influence factors known as channel attenuation as well as turbulence-induced scintillation were introduced. Hence, various turbulence mitigation methods were also discussed in chapter 2, such as the internal modulation and external modulation, direct detection and coherent detection. This discussion covered the existing solutions for overcoming the turbulence-induced channel fading, especially in improving the reliability of FSO link operating in the practical environment.

Further, I presented a theoretical study and numerical results for the OFDM-based RoFSO systems with spatial diversity technology over correlated log-normal turbulence distribution. The performance of proposed link in terms of BER and outage probability expressions have been derived. Important performance metric for investigating the proposed link have been analyzed and discussed under the channel correlation effect and different combining schemes. Moreover, a comparison between the aperture averaging and diversity reception has been also carried out. The analysis results demonstrate that the proposed system is sensitivity to the variation of channel correlation. The comparison of aperture averaging in a turbulent FSO link that determined the efficient in selection of diversity reception, in terms of reduction of turbulence and power efficient.

This work focused on PolSK modulated scheme in OCDMA-FSO link to investigate the transmission performance, both of direct detection and coherent detection. Firstly, a novel system configuration and analytical modeling across the weak-strong turbulence regime has been provided and discussed. The advantages of combining the PolSK scheme and OCDMA technique in the field of optical fiber communications has been reported, especially in large capacity and number of active users. The performed analysis outlines the main influence factors for investigating the proposed link performance, considering on turbulence-induced scintillation and multiple-access interference (MAI). For giving a highlight on this work, further, a comparison with OOK modulation obtained form a evaluation under the same environment conditions. The numerical results can be seen as an useful method for designing the advanced FSO system over a actual environment, which can supporting the multiple users shared the channel.

Moreover, a coherent detection technology has been carried out in this work, which acts an efficient compensation for my previous work depending its potential on combating the turbulence-induced fading. Hence, an analytical modeling is provided to characterize the performance of PolSK-OCDMA systems with heterodyne detection over turbulent FSO link across the whole turbulence regimes. The obtained results

demonstrate that coherent detection offers an improved receiver sensitivity, leading to potential ability on turbulence mitigation in the presence of turbulence.

6.2 Future Works

This work covers several issues that has been considered in turbulence mitigation as discussion in chapter 3, chapter 4 and chapter 5. However, I will focus on an extensive measurements of proposed system by real experiment in the next step. This further work will providing a more deeper understanding of these proposals on the practical environment.

Hence, coherent detection based FSO link under the phase fluctuation effect have not been considered in analytical modeling. Thus, I will pay attention on further investigation for accurate describing the system modeling. In the case of turbulence model, several statistic models have been proposed in recent years, such as double-weibull distribution and generalized gamma distribution. A more accurately link performance analytical model based on these turbulence model will be considered and discussed in the next step. For the applications of FSO communication system, such as under water and multi-path diversity which is as an alternative solution in the future applications. Investigation of theses novel applications performance is important, especially in connection the existing network construction.

Bibliography

[1] A.G. Siamarou. "broadband wireless local-area networks at millimeter waves around 60 ghz". *Antennas and Propagation Magazine, IEEE*, 45(1):177–181, Feb 2003.

[2] R.J. Honer and A.M. Mahdy. "emerging urban applications of broadband optical wireless networking". In *Emerging Network Intelligence, 2009 First International Conference on*, pages 39–42, Oct 2009.

[3] G.D. Peng, Y.H. Luo, J.X. Zhang, J.H.and Wen, Yan B.B., and J. Canning. "recent development of new active optical fibres for broadband photonic applications". pages 5–9, Oct 2013.

[4] E. Leitgeb and T. Plank. "combination of free space optics (fso) and rf for different wireless application scenarios". pages 1–4, April 2015.

[5] J. Schuster S. Bloom, E. Korevaar and H. Willebrand. "understanding the performance of free-space optics". pages 178–200, April 2003.

[6] S. Hranilovic. "wireless optical communication system". 2004.

[7] M. Toyoshima, T. Sasaki, H. Takenaka, Y. Shoji, Yoshihisa Takayama, Y. Koyama, H. Kunimori, M. Akioka, M. Fujiwara, and M. Sasaki. "research and development of free-space laser communications and quantum key distribution technologies at nict". In *Space Optical Systems and Applications (ICSOS), 2011 International Conference on*, pages 1–7, May 2011.

[8] J. Lesh. "free space laser communications". In *Lasers and Electro-Optics, 1999. CLEO '99. Summaries of Papers Presented at the Conference on*, pages 316–, May 1999.

[9] A.C. Boucouvalas. "reliability of indoor and short range fso - paper not available at publishing time". In *Transparent Optical Networks, 2005, Proceedings of 2005 7th International Conference*, volume 1, pages 402–402, July 2005.

[10] H. Hemmati. "laser communications: From terrestrial broadband to deep-space". In *Transparent Optical Networks (ICTON), 2014 16th International Conference on*, pages 1–3, July 2014.

[11] R.K. Sharma, H. Kaushal, and P.K. Sharma. "analysis of indoor fso link under diffused channel topology". In *2015 International Conference on Computing, Communication Automation (ICCCA)*, pages 1268–1272, May 2015.

[12] J. Vitasek, P. Siska, J. Latal, S. Hejduk, A. Liner, and V. Vasinek. "the transmitter for indoor free space optic networks". In *2013 36th International Conference on Telecommunications and Signal Processing (TSP)*, pages 290–293, July 2013.

[13] N.A.M. Nor, E. Fabiyi, M.M. Abadi, Xuan Tang, Z. Ghassemlooy, and A. Burton. "a laboratory demonstration investigation of moderate-to-strong turbulence effects on free space optics". In *2015 13th International Conference on Telecommunications (ConTEL)*, pages 1–5, July 2015.

[14] D. Kedar and S. Arnon. "urban optical wireless communication networks: the main challenges and possible solutions". *Communications Magazine, IEEE*, 42 (5):S2–S7, May 2004.

[15] S. Arnon. "optimization of urban optical wireless communication systems". *IEEE Transactions on Wireless Communications*, 2(4):626–629, July 2003.

[16] S.S. Muhammad, P. Kohldorfer, and E. Leitgeb. "channel modeling for terrestrial free space optical links". In *Proceedings of 2005 7th International Conference on Transparent Optical Networks*, volume 1, pages 407–410 Vol. 1, July 2005.

[17] M.C.R. Cordeiro, C.P. Colvero, and J.P. von der Weid. "experimental comparison of scintillation effects in far and near infrared wavelengths in fso systems". In *2005 SBMO/IEEE MTT-S International Conference on Microwave and Optoelectronics*, pages 393–395, July 2005.

[18] H. E. Nistazakis, E.A. Karagianni, A.D. Tsigopoulos, M.E. Fafalios, and G.S. Tombras. "average capacity of optical wireless communication systems over atmospheric turbulence channels". *Journal of Lightwave Technology*, 27(8): 974–979, April 2009.

[19] T. Singh. "calculations of the impact on atmospheric turbulence conditions on free space optical communication links using gamma-gamma model". In *2013 Fourth International Conference on Computing, Communications and Networking Technologies (ICCCNT)*, pages 1–5, July 2013.

[20] T. Joseph, H. Kaushal, V.K. Jain, and S. Kar. "performance analysis of ook modulation scheme with spatial diversity in atmospheric turbulence". In *2014 23rd Wireless and Optical Communication Conference (WOCC)*, pages 1–3, May 2014.

[21] A.A. Johnsi and V. Saminadan. "performance of diversity combining techniques for fso-mimo system". In *2013 International Conference on Communications and Signal Processing (ICCSP)*, pages 479–483, April 2013.

[22] A. Viswanath, V.K. Jain, and S. Kar. "experimental evaluation of the effect of aperture averaging technique on the performance of free space optical communication link for different intensity modulation schemes". In *2015 7th International Conference on Communication Systems and Networks (COMSNETS)*, pages 1–5, Jan 2015.

[23] M. Khalighi, N. Schwartz, N. Aitamer, and S. Bourennane. "fading reduction by aperture averaging and spatial diversity in optical wireless systems". *IEEE/OSA Journal of Optical Communications and Networking*, 1(6):580–593, November 2009.

[24] S.M. Navidpour, M. Uysal, and M. Kavehrad. "ber performance of free-space optical transmission with spatial diversity". *IEEE Transactions on Wireless Communications*, 6(8):2813–2819, August 2007.

[25] F. Bai, Y.W. Su, and T. Sato. "performance evaluation of a dual diversity reception base on ofdm rofso systems over correlated log-normal fading channel. In *ITU Kaleidoscope Academic Conference: Living in a converged world - Impossible without standards?, Proceedings of the 2014*, pages 263–268, June 2014.

[26] C.Y. Chen, Yang H.M., J.T. Fan, X. Feng, C. Han, and Y. Ding. "model for outage probability of free-space optical links with spatial diversity through atmospheric turbulence". In *ICIC '09 Second International Conference on Information and Computing Science*, volume 4, pages 209–211, May 2009.

[27] M. Abaza, R. Mesleh, A. Mansour, and E. H.M. Aggoune. "spatial diversity for fso communication systems over atmospheric turbulence channels". In *2014 IEEE Wireless Communications and Networking Conference (WCNC)*, pages 382–387, April 2014.

[28] W. Gappmair, S. Hranilovic, and E. Leitgeb. "ook performance for terrestrial fso links in turbulent atmosphere with pointing errors modeled by hoyt distributions". *IEEE Communications Letters*, 15(8):875–877, August 2011.

[29] Z.X. Wang and C.Y. Zhong, W.D.and Yu. "dynamic decision threshold and adaptive coherent detection in fso communication system". In *2011 8th International Conference on Information, Communications and Signal Processing (ICICS)*, pages 1–5, Dec 2011.

[30] X. Tang, Z. Ghassemlooy, S. Rajbhandari, W.O. Popoola, C.G. Lee, E. Leitgeb, and V. Ahmadi. "free-space optical communication employing polarization shift keying coherent modulation in atmospheric turbulence channel". *2010 7th International Symposium on Communication Systems Networks and Digital Signal Processing (CSNDSP)*, pages 615–620, July 2010.

[31] J.W. Strohbehn and S. Clifford. "polarization and angle-of-arrival fluctuations for a plane wave propagated through a turbulent medium". *IEEE Transactions on Antennas and Propagation*, 15(3):416–421, May 1967.

[32] S.A.J. Florez. "circular polarization and availability in free space optics (f-so) communication systems". In *2010 IEEE Latin-American Conference on Communications*, pages 1–6, Sept 2010.

[33] X.H. Zhao, Y. Yao, Y.X. Sun, X.C. Xu, and C. Tian, J.J.and Liu. "condition of keeping polarization property unchanged in the circle polarization shift keying system". *Journal of Optical Communications and Networking, IEEE/OSA,*, 2 (8):570–575, August 2010.

[34] Y. Zhao, X.H. andYao, Yunxu Sun, and C. Liu. "circle polarization shift keying with direct detection for free-space optical communication". *J. Opt. Commun. Netw.,*, 1(4):307–312, Sep 2009.

[35] K. Sasaki, N. Minato, T. Ushikubo, and Y. Arimoto. First ocdma experimental demonstration over free space and optical fiber link. *"Conference on Optical Fiber communication/National Fiber Optic Engineers Conference"*, pages 1–3, Feb 2008.

[36] N. C. Ben, A. Bekkali, K. Wakamori, and M. Matsumoto. "performance analysis of cdma-based wireless services transmission over a turbulent rf-on-fso channel". pages 475–486, May 2011.

[37] W.D.and Yu C.Y. Wang, Z.X.and Zhong. "dynamic decision threshold and adaptive coherent detection in fso communication system". In *2011 8th International Conference on Information, Communications and Signal Processing (ICICS)*, pages 1–5, Dec 2011.

[38] D. Ly-Gagnon, S. Tsukamoto, K. Katoh, and K. Kikuchi. "coherent detection of optical quadrature phase-shift keying signals with carrier phase estimation". *Journal of Lightwave Technology*, 24(1):12–21, Jan 2006.

[39] K.P. Peppas and P.T. Mathiopoulos. "free-space optical communication with spatial modulation and coherent detection over h-k atmospheric turbulence channels". *Journal of Lightwave Technology*, 33(20):4221–4232, Oct 2015.

[40] P. Kumar. "comparative analysis of ber performance for direct detection and coherent detection fso communication systems". pages 369–374, April 2015.

[41] Z.X. Wang and C.Y. Zhong, W.D.and Yu. "dynamic decision threshold and adaptive coherent detection in fso communication system". In *2011 8th International Conference on Information, Communications and Signal Processing (ICICS)*, pages 1–5, Dec 2011.

[42] A. Bekkali, C. Ben Naila, K. Kazaura, K. Wakamori, and M. Matsumoto. "transmission analysis of ofdm-based wireless services over turbulent radio-on-fso links modeled by gamma-gamma distribution". volume 2, pages 510–520, June 2010.

[43] https://en.wikipedia.org/wiki/Photophone.

[44] C.C. Fan. "engineering innovation: Prof. charles k. kao's nobel prize". In *2010 19th Annual Wireless and Optical Communications Conference (WOCC)*, pages 1–4, May 2010.

[45] http://opticalcomm.jpl.nasa.gov/PAGES/flight.html.

[46] http://global.jaxa.jp/.

[47] L. Hutcheson. "fttx: Current status and the future". *IEEE Communications Magazine*, 46(7):90–95, July 2008.

[48] A. Ghosh, D.R. Wolter, J.G. Andrews, and R.H. Chen. "broadband wireless access with wimax/802.16: current performance benchmarks and future potential". *IEEE Communications Magazine*, 43(2):129–136, Feb 2005.

[49] E. Leitgeb, T. Plank, M. Loschnigg, and P. Mandl. "free space optics in different (civil and military) application scenarios in combination with other wireless technologies". In *2014 16th International Telecommunications Network Strategy and Planning Symposium (Networks)*, pages 1–7, Sept 2014.

[50] R. Paudel, Z. Ghassemlooy, L.M. Hoa, S. Rajbhandari, and B. Livingstone. "investigation of fso ground-to-train communications in a laboratory environment". In *2011 Second Asian Himalayas International Conference on Internet (AH-ICI)*, Nov 2011.

[51] E. Zedini and M.S. Alouini. "multihop relaying over im/dd fso systems with pointing errors". *Journal of Lightwave Technology*, PP(99):1–1, 2015.

[52] K. Prabu, S. Bose, and D.S. Kumar. "analysis of optical modulators for radio over free space optical communication systems and radio over fiber systems". In *2012 Annual IEEE India Conference (INDICON)*, pages 1176–1179, Dec 2012.

[53] C.S. Mary. "signaling safety [electrical safety]". *Industry Applications Magazine, IEEE*, 17(1):6–6, Jan 2011.

[54] http://esc.gsfc.nasa.gov/267/271/335.html.

[55] N. Agrawal, C.C. Davis, and S.D. Milner. "free space optical sensor networking for underwater sensing applications". In *2009 5th International Conference on Intelligent Sensors, Sensor Networks and Information Processing (ISSNIP)*, pages 475–480, Dec 2009.

[56] Z. Ghassemlooy, S. Arnon, M. Uysal, and J.L. Xu, Z.Y.and Chen. "emerging optical wireless communications-advances and challenges". *IEEE Journal on Selected Areas in Communications*, 33(9):1738–1749, Sept 2015.

[57] Larry C. Andrews and Ronald L. Phillips. *Laser Beam Propagation through Random Media*. SPIE, Washington, USA, 2nd edition edition, 2005.

[58] V.N.H. Silva, A.P.L. Barbero, and R.M. Ribeiro. "a new triangulation-like technique for the evaluation of the refractive index structure constant (c_n^2) in free-space optical links". *Journal of Lightwave Technology*, 29(24):3603–3610, Dec 2011.

[59] Larry C. Andrews and Ronald L. Phillips. *Laser Beam Scintillation with Applications*. SPIE, Washington, USA, 2001.

[60] M. Abaza, R. Mesleh, A. Mansour, and E.H.M. Aggoune. "spatial diversity for fso communication systems over atmospheric turbulence channels". In *2014 IEEE Wireless Communications and Networking Conference (WCNC)*, pages 382–387, April 2014.

[61] A. Malpani and A. Malpani. "performance analysis of fso communication with aperture averaging under varying atmospheric turbulence regimes". In *2012 Ninth International Conference on Wireless and Optical Communications Networks (WOCN)*, pages 1–6, Sept 2012.

[62] T.A. Tsiftsis, H.G. Sandalidis, G.K. Karagiannidis, and M. Uysal. "fso links with spatial diversity over strong atmospheric turbulence channels". In *IEEE International Conference on Communications*, pages 5379–5384, May 2008.

[63] X.M. Zhu and J.M. Kahn. "performance bounds for coded free-space optical communications through atmospheric turbulence channels". volume 51, pages 1233–1239, Aug 2003.

[64] H. Samimi and P. Azmi. "performance analysis of adaptive subcarrier intensity-modulated free-space optical systems - retracted". *Optoelectronics, IET*, 5(4): 168–174, August 2011.

[65] X. Tang, S. Rajbhandari, W.O. Popoola, Z. Ghassemlooy, E. Leitgeb, S.S. Muhammad, and G. Kandus. "performance of bpsk subcarrier intensity modulation free-space optical communications using a log-normal atmospheric turbulence model". In *2010 Symposium on Photonics and Optoelectronic (SOPO)*, pages 1–4, June 2010.

[66] W.O. Popoola and Z. Ghassemlooy. "bpsk subcarrier intensity modulated free-space optical communications in atmospheric turbulence". *Journal of Lightwave Technology*, 27(8):967–973, April 2009.

[67] X.H. Zhao, Y.X. Yao, Y.and Sun, J.J. Xu, X.C.and Tian, and C. Liu. "condition of keeping polarization property unchanged in the circle polarization shift keying system". *Journal of Optical Communications and Networking, IEEE/OSA,*, 2(8):570–575, August 2010.

[68] Z. Ghassemlooy, X. Tang, and S. Rajbhandari. "experimental investigation of polarisation modulated free space optical communication with direct detection in a turbulence channel". *Communications, IET,*, 6(11):1489–1494, July 2012.

[69] F. Bai, Y.W. Su, and T. Sato. "performance analysis of polarization modulated directdetection optical cdma systems over turbulent fso linksmodeled by the gamma-gamma distribution". *Photonics,*, 2(1):139, 2015. ISSN 2304-6732.

[70] X. Tang, Z. Ghassemlooy, S. Rajbhandari, W.O. Popoola, and C.G. Lee. "differential circular polarization shift keying with heterodyne detection for free space optical links with turbulence channel. *2011 16th European Conference on Networks and Optical Communications (NOC).*

[71] Hamed Al-Raweshidy and Shozo Komaki. *Radio Over Fiber Technologies for Mobile Communications*. Artech, 2002.

[72] https://www.itu.int/rec/T REC-G.640-200603-I/en.

[73] D. Skraparlis, M. Sandell, V.K. Sakarellos, A.D. Panagopoulos, and J.D. Kanellopoulos. "on the effect of correlation on the performance of dual diversity receivers in lognormal fading. *Communications Letters, IEEE.*

[74] A. Scott and R. Frobenius. *OFDM, OFDMA, AND WiMAX*, pages 431–437. Wiley-IEEE Press, 2008.

[75] Y.W. Su F. Bai and T. Sato. "performance analysis of rofso lnks with diversity reception for transmission of ofdm signals under correlated log-normal fading channels". *Journal of ICT standardization*, pages 129–150, 2014.

[76] Z.X. Chen, S. Yu, T.Y. Wang, G.H. Wu, and W.Y. Wang, S.L.and Gu. "channel correlation in aperture receiver diversity systems for free-space optical communication". *Journal of Optics*, 2012.

[77] M. Khalighi, N. Schwartz, N. Aitamer, and S. Bourennane. "fading reduction by aperture averaging and spatial diversity in optical wireless systems". *IEEE/OSA Journal of Optical Communications and Networking*, 1(6):580–593, November 2009.

[78] G.S. Hooshang and M. Massoud Karbassian. In *"Optical CDMA Networks: Principles, Analysis and Applications"*. Wiley-IEEE Press, 2012.

[79] X. Tang, Z. Ghassemlooy, S. Rajbhandari, W.O. Popoola, and C.G. Lee. "differential circular polarization shift keying with heterodyne detection for free space optical links with turbulence channel". In *2011 16th European Conference on Networks and Optical Communications (NOC)*, July 2011.

[80] K. Wakafuji and T. Ohtsuki. "performance analysis of atmospheric optical subcarrier multiplexing systems and atmospheric optical code division multiplexing systems". In *2004 IEEE International Conference on Communications*, volume 6, pages 3336–3340, June 2004.

[81] P. Liu, P.T. Dat, K. Wakamori, and M. Matsumoto. "a new scheme on time-diversity atmospheric ocdma system over atmospheric turbulence channels". In *2010 IEEE GLOBECOM Workshops (GC Wkshps)*, pages 1020–1025, Dec 2010.

[82] K. Iversen, J. Muechenhein, and D. Junghanns. "performance evaluation of optical cdma using polsk-dd to improve bipolar capacity". pages 319–329, 1995.

[83] G.C. Yang and W.C. Kwong. *"Prime Codes with Applications to CDMA Optical and Wireless Networks"*. Artech House, 2002.

[84] M.M. Karbassian and H. Ghafouri-Shiraz. "transceiver architecture for incoherent optical cdma networks based on polarization modulation". *Journal of Lightwave Technology*, 26(24):3820–3828, Dec 2008.

[85] K. Iversen, J. Muechenhein, and D. Junghanns. "on the combination of optical cdma and polsk". *J. Opt.Commun.*, pages 126–130, 1994.

[86] T. OFarrell and S. Lochmann. "performance analysis of an optical correlator receiver for sik ds-cdma communication systems". *Electronics Letters*, 30(1): 63–65, Jan 1994.

[87] O.I. Adamchik, V.S.; Marichev. "the algorithm for calculating integrals of hypergeometric type functions and its realization in reduce system". *In Proceedings of the International Conference Symbolic Algebraic,*, pages 212–224, Augest 1990.

[88] M. Jazayerifar and J.A. Salehi. "atmospheric optical cdma communication systems via optical orthogonal codes". *IEEE Transactions on Communications*, 54(9):1614–1623, Sept 2006.

[89] X. Tang, Z. Ghassemlooy, S. Rajbhandari, W.O. Popoola, and C.G. Lee. "coherent heterodyne multilevel polarization shift keying with spatial diversity in

a free-space optical turbulence channel". *Journal of Lightwave Technology,*, 30 (16):2689–2695, Aug 2012.

[90] L. J.A. LopeZ and C.E. Rodriguez Hidalgp. "interconnecting university networks using a full-duplex fso system using coherent detection and polarization-division multiplexing: Design and simulation". In *2015 IEEE Optical Interconnects Conference (OI)*, pages 106–107, April 2015.

[91] F. Bai. Y.W. Su, T. Sato. "performance analysis of heterodyne-detected ocdma systems using polsk modulation over a free-space optical turbulence channel. 4:785–798, Oct 2015.

[92] I.I. Kim and E.J. Korevaar B. McArthur. "comparison of laser beam propagation at 785 nm and 1550 nm in fog and haze for optical wireless communications". *Proceeding of SPIE*, 4214:26–37, February 2001.

[93] N. Wang and J.L. Cheng. "moment-based estimation for the shape parameters of the gamma-gamma atmospheric turbulence model". *Opt. Express,*, 18(12): 12824–12831, Jun 2010.

List of academic achievements

Category		
Articles in refereed journals	○ **Fan Bai**, Yuwei Su and Takuro Sato, "Performance Analysis of Heterodyne-Detected OCDMA Systems Using PolSK Modulation over a Free-Space Optical Turbulence Channel", *MDPI*, *Electronics*, 4(4), *pp* .785-798, 16 October, 2015	Chapter 5
	○ **Fan Bai**, Yuwei Su and Takuro Sato, "Performance Analysis of Polarization Modulated Direct Detection Optical CDMA Systems over Turbulent FSO Links Modeled by the Gamma-Gamma Distribution", *MDPI*, *Photonics*, 2(1), *pp*.139-155, 29 January, 2015	Chapter 4
	○ **Fan Bai**, Yuwei Su and Takuro Sato, "Performance Analysis of RoFSO Links with Diversity Reception for Transmission of OFDM Signals under Correlated Log-normal Fading Channels", *Journal of ICT standardization*, 2(2), *pp* .129-150, 10 November, 2014	Chapter 3
Presentations at International conferences	○ **Fan Bai**, Yuwei Su and Takuro Sato, "Performance Evaluation of a Dual Diversity Reception Base on OFDM RoFSO Systems over Correlated Log-normal Fading Channel", *ITU Kaleidoscope Academic Conference: Living in a converged world - Impossible without standards*, 263-268, Russia, June, 2014	Chapter 3
Presentations at Domestic conferences	**Fan Bai**, Yuwei Su and Takuro Sato, "Advanced Free-space Optical communication: Challenges and Mitigation techniques", IET Japan network workshop, Tokyo, December, 2015	
	Fan Bai, Yuwei Su and Mitsuji Matsumoto, "Transmission Analysis of OFDM Combine with Spatial Diversity Techniques Based-on Free Space Optics over Gamma-Gamma Turbulent Channel", *IEICE general conference*, Gifu, Japan, March, 2013	
	Fan Bai, Yuwei Su and Mitsuji Matsumoto, "Study on Digital TV Broadcasting Signals Transmission over OFDM(A) PON System Supporting Radio-over-Fiber", *IIEEJ general conference*, Tokyo, Japan, 2012	
	Fan Bai, Takuro Sato, "Network evolution in coming 10 years: what is the future of network?-Toward optical wireless communications", GITS/GITI research festival, Ph.D academy, Waseda university, 2014	
	Fan Bai, Yuwei Su and Mitsuji Matsumoto, "Transmission Analysis of Optical OFDMA-Based Passive Optical Network Architecture Supporting Heterogeneous Services", *Progress in Electromagnetics Research Symposium* (*PIERS*), Kuala Lumpur, Malaysia, March, 2012	

Others achievements	Yuwei Su, **Fan Bai** and Mitsuji Matsumoto, "Transmission Analysis of a Ternary Diversity Reception Based on OFDM FSO System over Correlated Log-normal Fading Channel", *Progress in Electromagnetics Research Symposium*, Guangzhou, China, August, 2014 Kou Dayong, **Bai Fan**, Su Yuwei and Mitsuji Matsumoto, "Performance Analysis of DC-biased Optical OFDM for Indoor Visible Light Wireless Communication System Based on White LEDs" IEICE general conference, Niigata, March 2014	
Awards	ITU-T Kaleidoscope Young Student Research Award, June 2014	